# Parametric comparison of stability systems

## Development of a parametric tool for the comparison and optimisation of four concrete stability systems for high-rise buildings between 100 m and 250 m in an early design phase

TU Delft

J.A.C. Jongenotter

# Parametric comparison of stability systems

Development of a parametric tool for the comparison
and optimisation of four concrete stability systems for high-rise
buildings between 100 $m$ and 250 $m$ in an early design phase

By

J.A.C. Jongenotter

to obtain the degree of Master of Science at the Delft University of Technology,
to be defended on Friday February 26, 2021 at 10:00 AM.

| | | |
|---|---|---|
| Student number: | 4382307 | |
| Project duration: | March, 2020 - Februari, 2021 | |
| Thesis committee: | Dr. Ir. K.C. Terwel, | TU Delft, chair |
| | Ir. C. Noteboom, | TU Delft |
| | Ir. P. Eigenraam, | TU Delft |
| | Ir. A.R. Van Eerden, | IMd Raadgevende Ingenieurs |

An electronic version of this thesis is available at http://repository.tudelft.nl/.

# ABSTRACT

At the moment, there is a high demand for residential buildings in The Netherlands. High-rise can be part of the solution for this. This thesis tries to improve the early design process of high-rise buildings.. This will be done by using a parametric model. Literature study shows that parametric tools are not widely used nowadays in this field. Applying them could make the design process more efficient.

First, the scope of the research has been determined. It has been decided to focus on high-rise between 100 and 250 $m$, executed in concrete cast-in-situ. This, because concrete is an extensively used building material for high-rise, in particular for residential buildings. The project is divided into five phases as can be seen in figure 1. First the theoretical background is given, then the model is set up, followed by some parametric studies and user interaction and lastly the final remarks are presented. This methodology finally leads to an answer on the main question of this thesis:

*What is the optimal stability system for a concrete high-rise building based on input parameters and optimisation goal for the early design stage?*

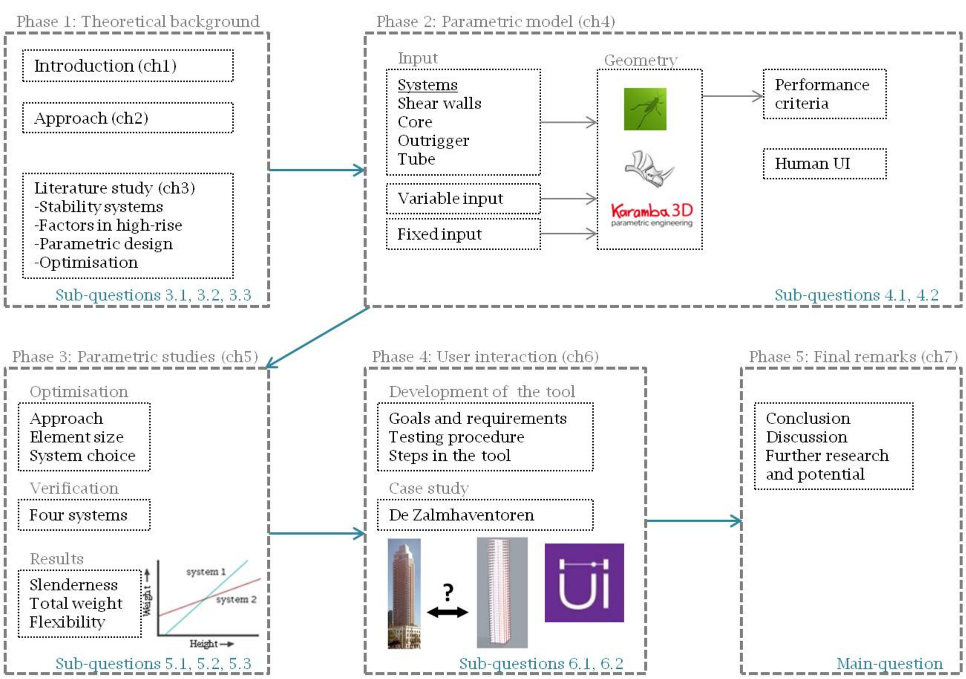


**Figure 1** Workflow of the project

From literature study can be concluded that four systems are interesting to take into account during the project. These are the shear wall system, core, outrigger and tube. Factors in high-rise that have to be taken into account are: material choice, reinforcement design, floor design, loads, foundation design, second order effects, comfort and influence of perforations.

Research showed that Grasshopper in combination with Karamba and Human UI can be used for the parametric model. Total weight and embodied carbon, element slenderness and flexibility are appointed as optimisation goals. Flexibility is defined as the effective floor area and ratio facade openings.

The model development starts with determining the input. Input is divided into variable and fixed input. Variable input contains dimensions of the building and core. Fixed input contains material choice, load, building and column shape, floor type and schematising of connections. The four systems are implemented in one model. In this model, four performance criteria are checked. These are strength of the elements, building stiffness, foundation stiffness and maximum allowable accelerations in the building. The modelling method described above is implemented in a Human UI panel, in which the different steps can be followed.

The parametric model can be used to compare the four systems. For this, an optimisation procedure is implemented. First the global dimensions of the building are determined manually (shape optimisation), then element sizes are optimised in the parametric model (size optimisation) and based on these results, the optimal system can be chosen by the user (topology optimisation). The validity of the model and the optimisation have been checked by comparing the expected output with the model output. The optimisation results are plotted in graphs for the three optimisation goals. Also unity checks for stiffness and strength are given. Optimisation is executed on a building of 36 x 36 $m$ with core of 14.4 x 14.4 $m$ and a variable height. The results show that a core is the most optimal system for a building height between 100 and 150 $m$. The outrigger and shear walls are the best option between 150 and 200 $m$. The tube is most favourable between 200 and 250 $m$.

The steps in the model are processed in a tool in Grasshopper. This tool is meant as user-friendly interface to control the model and compare the four systems. The tool exists of five steps. First the input parameters can be manually inserted by sliders in step 0. These parameters are divided into building dimensions, core dimensions and other parameters. In step 1, a size optimisation is executed for each system individually. This leads to the choice for one system. For this system, the deflection and strength of wall and column elements are checked in step 2. In the third step, a first assumption is made for the pile diameter in the foundation, based on pile configuration and length. In the final step, step 4, the maximum acceleration in the building is checked. To fully prove the validity of the model and tool, De Zalmhaventoren has been rebuilt. Although some simplifications are made in Grasshopper, results are similar. Applied wall sizes are in the range 300 to 600 $mm$, where 350 to 600 $mm$ is advised by the tool. The difference in deflection is around 3%. Applying more piles with smaller diameter leads to a similar foundation stiffness and the maximum acceleration is calculated as 0.116 $m/s^2$, where 0.112 was calculated by the model.

The optimisation results and tool have led to a comparison of four concrete stability systems. It can be concluded that more insight is obtained in the applicability per system based on input parameters. This resulted in a more transparent, flexible and quick early design process.

## PREFACE

This rapport includes my master thesis as final part of the master Building Engineering, specialisation Structural Design, at Delft University of Technology. The research was performed in cooperation with IMd Raadgevende Ingenieurs in Rotterdam and covers the topics parametric design and high-rise.

I am grateful to IMd Raadgevende Ingenieurs for the possibility of graduating at their company. The graduation period was not as expected. In the first weeks of the graduation, the COVID-19 pandemic came up. This forced me to work from home. Despite this, I always felt involved in the company and I enjoyed my period of graduation.

I would like to thank my committee members for their support during the thesis. First I want to thank Karel Terwel for chairing the committee. He helped me setting up the report and always kept an eye on the progress of the research. Chris Noteboom gave me useful feedback and came up with creative solutions when I was stuck. Peter Eigenraam helped me with parametric modelling. He learned me how to formalise and improve my model. Sander van Eerden, my supervisor from IMd, gave me insight in the design of high-rise buildings in practice. I learned many things from him concerning the execution of a high-rise project and accessory challenges. I want to thank Ikram Talib from IMd for her ideas and feedback during the project.

Special thanks to my family for supporting me during the graduation period. I have always felt supported during my studies and during the decisions I had to make. Due to these pleasant circumstances, I was always enable to fully focus on my studies to get the best out of it.

I want to end with a quote from my first report card from kindergarden: *'Jesse gaat z'n gangetje, bouwen en constructie hebben zijn voorkeur.'* 20 years ago, I have taken the first steps towards completing my studies. This final thesis makes the circle complete.

Jesse Jongenotter
Zuid-Beijerland, January 2021

# Table of Contents

# List of Figures

# List of Tables

# Chapter 1

# Introduction

This chapter gives an introduction to the research. First the problem will be introduced, followed by a primary literature research and problem description and finally the research goal will be stated.

## 1.1 Problem statement

At the moment, there is a high demand for residential buildings in The Netherlands (Paling, 2020). The housing shortage at this moment is around 315.000 residences. This is as many as the total city of Rotterdam. Within three years, this shortage will increase to 625.000. This is because of urbanisation in combination with the daily increasing population in The Netherlands, but also in the rest of the world. The problem here is the demand of people to live as close as possible to the center of a city, while space is lacking in these densely populated areas. As a consequence of this problem, a big gap between demand and supply arises. Rents are increasing and in particular for starters on the housing market, it is difficult to get a dwelling.

As a result of the problem stated above, there is a need for high-rise residential buildings in The Netherlands, for now and in the near future. The last decades, this process has already been started. In particular in Rotterdam, many high-rise projects have been executed recently. Montevideo (152 $m$) in 2005 and New Orleans (158 $m$) in 2010 are two examples of this. At the moment the Zalmhaventoren is being built, with 215 $m$ the first tower in The Netherlands which will break down the barrier of 200 $m$. Also in other Dutch cities high-rise buildings are more and more conventional.

As stated above, there will be a high demand for high-rise buildings in The Netherlands, now and in the near future. A question for the engineer here is how to contribute to this process and how to work in a more efficient way by saving time and money. This is the starting point of this thesis.

## 1.2 Literature research

Literature research in this thesis is in the first place executed to primary sources as research theses and academic refereed journals. These sources are used to map recently executed research. This leads to insight in the gaps in this current state of knowledge. Afterwards it can be determined how this thesis can benefit to this. Secondary sources are (educative) books and professional journals. This kind of sources are used to find the theoretical background of the topics.

### Primary literature research

This part of the literature research contains master theses. Reports are considered in the area of high-rise, stability systems, influencing parameters and parametric design. The most important reports covering these areas are mentioned below. The complete study can be found in appendix A.

Lankhorst (2018) compares five different kind of stability systems and three floor types on their environmental impact. Buildings with a height of 150 $m$, 200 $m$ and 250 $m$ in The Netherlands are compared, making use of the materials precast concrete, in-situ concrete and steel and all with a concrete core. The environmental impact was calculated by a life-cycle analysis. It is found that both concrete has a low impact and that the outrigger and diagrid are the most effective systems. Potential further research can cover influence of the foundation, use of internal columns or lighter floor systems.

StructuralComponents 2 (Rolvink, 2010) focuses on high-rise and stability systems. A toolbox is developed with components which can be used for parametric modelling of structures. The toolbox consists of a framework, which comprises the core layers and libraries and a representation layer, with a user interface. The first design method applied here is top-down design. This means that distinction is made between different structural typologies. The second method is the bottom-up design. Here a model is assembled existing of different structural elements. This should give insight in the structural performance of the building. Future extensions of the tool can cover multi-disciplinary design with other disciplines integrated, multi-criteria optimisation, tests on real design projects and integrating of building costs.

In StructuralComponents 6 (Viik, 2019) a tool has been developed, based on previous version StructuralComponents 5, that provides early-stage structural validation for concrete mid-rise buildings made of shear walls, cores and floors. First the requirements of such a tool are investigated. A flexible calculation method was developed to determine the forces and deflections. This was implemented in a tool with user-interface included and examined to a real building design.

### Secondary literature research

Secondary literature study contains books and professional journals. This is used for the theoretical part of this thesis, which is elaborated in chapter 3. Sources that give an overview of stability systems for high-rise buildings are Draagconstructies II (Nijsse, 2012), Structural Developments in Tall Buildings (Ali and Moon, 2007), Tall Building Structures (Smith and Coull, 1991) and Building Structures Illustrated (Ching, Onouye, and Zuberbuhler, 2014). These sources are used to appoint the considered systems, explain their structural behaviour and to point out parameters that influence this.

## 1.3 Problem description and relevance

### Relevance from practice

In early design stages, it is important to have insight in the consequences of design decisions that are made (Rolvink, Coenders, and Breider, 2011). Changes in design can easily be made, while limited information is available. In addition, the impact of these changes is high. Having insight in this process by using a parametric model can ease decision making. Initially, setting up a parametric model will lead to a higher amount of effort compared with a non-parametric way, but when the model is used for more projects, this time can be earned back (Van Der Linden, 2018).

Part of this is the choice for stability system for high-rise buildings. In this early phase usually experience with reference projects and rules of thumb are used for first dimensions (Ham and Terwel, 2017). The choice for a system and the way of execution depends on multiple parameters of which height and slenderness are the most important. Design decisions made by the architect also influence this choice. This can both cover exterior and interior elements of the structural design.

During the early design phases freedom is required to make quick changes and adaptation (Rolvink, 2010). Manually changing the design involves extra time, money and effort. A parametric model can offer a solution for this. This model is meant for structural engineers. It can individually be applied for exploration of the design options, but also in meetings with other members of a multi-disciplinary design team or architect.

The project is about the choice of different stability systems for high-rise buildings. It will be researched what the influence is of different parameters on the choice of a stability system. When having a clear overview of this in early stages of a project, decision making will become easier. This will be done with the help of a parametric model.

**Relevance from literature review**

Literature research shows that recently a number of projects have been executed concerning high-rise or stability systems in combination with parametric design. From these projects, a number of conclusions can be drawn:

- All previous models make assumptions for the influence of the foundation.
- Parametric models are used to draw a conclusion and are focused on one specific aspect of high-rise. This means that these models are not suitable to use as user-friendly tool.
- As a consequence of this, the output of these models is limited.
- The only model that can be used as a tool for high-rise for engineers is described in Structural Components 2 (Rolvink, 2010). However, from interviews with developers Anke Rolvink and Jeroen Coenders can be concluded that the tool originates from 2010. It is developed for Rhino 4 and Grasshopper version 0.6.0046 and not compatible with current versions and accessory components. The tool has not been updated to these current versions, so it is no longer usable.
- None of the considered models take wall cutouts into account and their consequence on the stiffness of the core or wall.

## 1.4 Research goal

From literature research is concluded that current parametric models focus on one aspect of high-rise. This leads to limited output that does not fit to the wishes of the engineer. That is why parametric tools are not widely used nowadays in this design phase. Aim of the project is to make the early design process more efficient by use of a parametric model.

The model must be able to visualise design options and optimise structural elements. This means use of the least amount of material while meeting the performance criteria. This to find the appropriateness of different stability systems based on the input. The model should give insight in this process and help to understand the phenomena of the observed stability systems. An additional requirement is creating a user friendly tool for the design of buildings between 100 and 250 $m$.

# Chapter 2

# Approach

This chapter gives the approach of the project. It starts with defining the project boundaries. Afterwards the methodology is explained as well as the research questions. Finally this is summarised in a flow scheme.

## 2.1 Boundaries and scope

The list below shows the boundaries of the model. Chapter 3 gives the theoretical background of these items and chapter 4 explains how they are taken into account during model development. Factors that play a role in the design of high-rise are described by Dijkstra (2008). His list of fourteen challenges has been used as basis for the list below.

- Project phase: The early design phase. Conventionally, the phases sketch design, preliminary design, final design and detailed design can be distinguished. This project aims to support during the first two of these phases.
- Location: The tool will be developed for projects located in The Netherlands. When using the tool abroad, different design codes, soil conditions and earth quake conditions have to be considered.
- Height range: 100 $m$ - 250 $m$. This range is based on the current high-rise buildings in The Netherlands. The highest building under construction in the Netherlands at the moment is 215 $m$ (De Zalmhaventoren). This height is increased with 35 $m$ for possibly higher buildings in future.
- Building and element shape: A rectangular building and square columns are considered.
- Building length and width: The tool will be suitable for buildings between 18 $m$ and 40 $m$ for both length and width, with a maximum length over width range of two.
- Material: The material used is concrete cast-in-situ with reinforcement. The theoretical background of the reinforcement will be explained in this report, but will not be processed in the model.
- Foundation: Based on three pile configurations and accessory number of piles, an estimation of the pile diameter is done, with pile length as input.
- Perforations: Possible perforations in wall elements are taken into account by a reduction factor.
- Comfort: The acceleration in the building will be compared with the maximal allowed acceleration according to Eurocode 1 (2002)
- Load: Horizontal, vertical and gravity load from Eurocode 1 (2002) are applied.

The items on the list below are out of scope. This because they are too specific or not of interest for a model within this design stage.

- Building physical aspects and services
- Building costs
- Installations
- Environmental analyses
- Earthquake design
- Vertical transportation
- Fire safety
- Aesthetics
- Organisation of the building site

## 2.2 Methodology

The project consists of five steps. These steps are mentioned now.

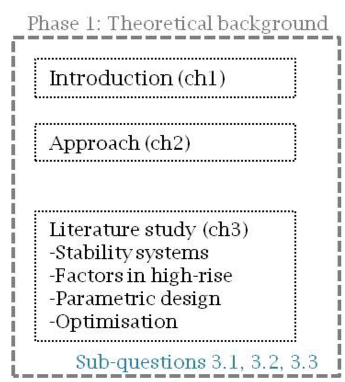


1. **Theoretical background: (Chapter 1,2 and 3)**
   The first three chapters form the theoretical background of the report. In chapter three will be determined which stability systems are considered and what the elementary properties of these systems are. Parameters that play a role here are worked out. Part of this is looking to the added value that parametric tools can have to the development of the model. This means that research will be executed on which tools can be useful for modeling, visualising and optimising.

2. **Parametric model: (Chapter 4)**
   The second step is developing the model in Grasshopper, making use of the plugin Karamba, which is used for structural analysis. Goal of the model is to get insight in the choice between four stability systems. Geometry is created based on the defined input parameters. The model is used to check a number of performance criteria and to make an user interface in Human UI.

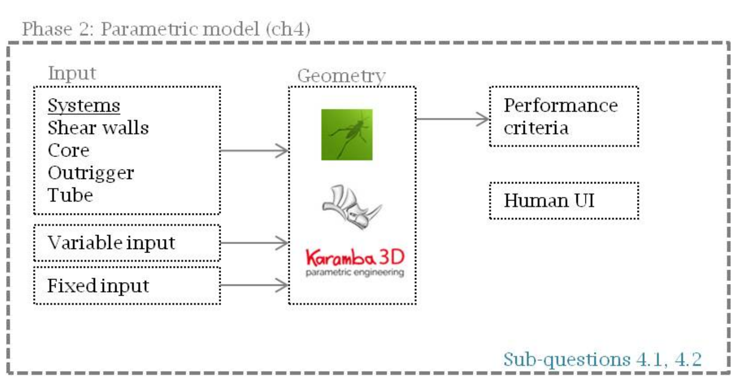

3. **Parametric results: (Chapter 5)**
   In the third step of the process, the parametric model is used to extract the required output. First, the optimisation procedure is explained. Second, a comparison has been made between the optimisation results and the predicted results and after this, three optimisation goals are defined which are plotted as function of the height. Finally, De Zalmhaventoren is inserted into the model and the results are compared.

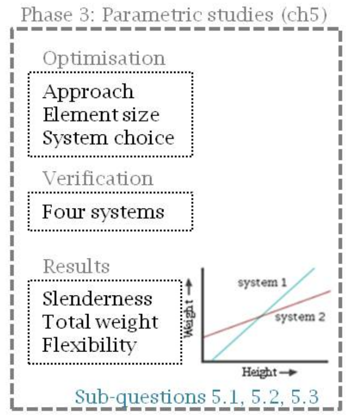


4. **User interaction: (Chapter 6)**
   The next step is to describe the tool and the interaction with the user. First, the goals and requirements are formulated. The tool is tested by professionals, based on a list of criteria. Finally, all steps are described when using the tool.


5. **Final remarks: (Chapter 7)**
   In the last part of the thesis, the obtained results will be discussed. The validity and reliability of the model will be checked. A conclusion will be drawn and a recommendation is given based on the outcomes of the project.


## 2.3 Research questions

The goal of the research and the accessory methodology have lead to the following research questions. The first research question which can be formulated as:

*Which research has been executed concerning parametric modelling for stability systems and what can this thesis add to that?*

is already answered in chapter 1. The other sub-questions and finally the main question of the research are listed below.

**Sub-questions**

Chapter 3 Theory

1. *Which stability systems are most likely to consider for concrete high-rise between 100 m and 250 m?*
2. *Which parameters play a role in the design of a high-rise structure?*
3. *Which parametric tools are available for the structural design, optimisation and visualisation of a high-rise structure?*

Chapter 4 Parametric model

1. *Which building parameters are assumed to be variable and which are fixed?*
2. *Which performance criteria have to be taken into account in the model?*

Chapter 5 Parametric results

1. *What is the most optimal system based on input parameters and slenderness?*
2. *What is the most optimal system based on input parameters and total weight?*
3. *What is the most optimal system based on input parameters and flexibility?*

Chapter 6 User interaction

1. *Which steps must be present in the Human UI tool to run through the early design process?*
2. *How can the tool influence the current design process?*

**Main question**

*What is the optimal stability system for a concrete high-rise building based on input parameters and optimisation goal for the early design stage?*

## 2.4 Summary

The scheme presented below summarises the steps involved in the research.

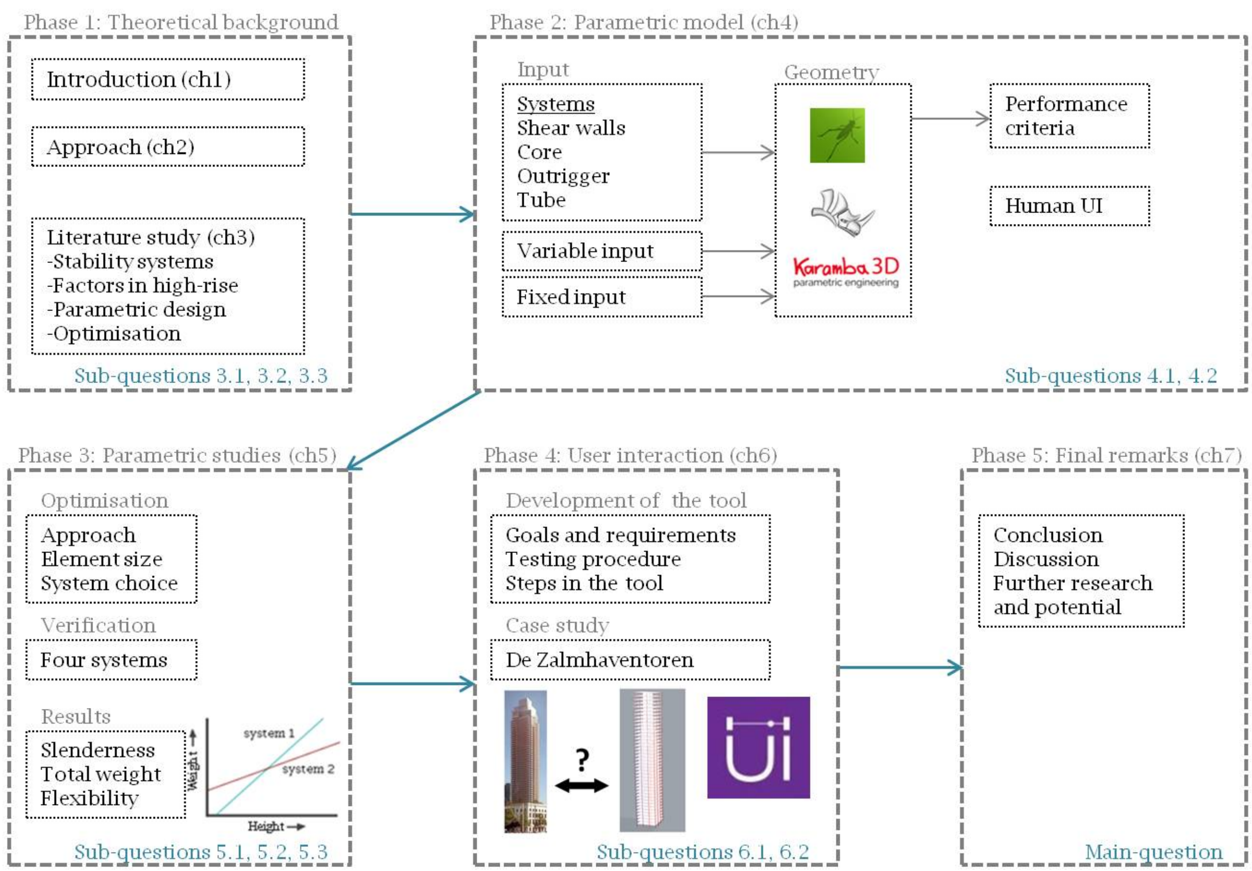


**Figure 2.1** Workflow of the project

# Chapter 3

# Theory

In this chapter, the theoretical background of the topics of this thesis will be explained. The research is divided into four parts: Stability systems, parameters in high-rise, parametric design and optimisation. The state-of-the art status of these topics will be explained, to obtain insight in them.

## 3.1 Stability systems

Tall buildings have to handle own weight and live loads, which can be separated into horizontal and vertical load. This means that enough stiffness is required. To ensure this, a stability system has to be applied. It is important to have a clear overview of the stability systems that are used for this. There are several sources available, which all show a different distribution of systems. These will be listed and out of these, four systems are chosen to work out further during the research. This is done based on material and applied height boundaries.

### 3.1.1 Division of systems

The following sources give an overview of different divisions of stability systems.

#### Draagsystemen II

A straightforward distribution of systems is given in the reader Draagsystemen II (Nijsse, 2012). The systems frame, core, outrigger, tube and mega frame are explained with an estimation of the maximum applicable height as shown in figure 3.1.

#### Structural Developments in Tall Buildings

In Structural Developments in Tall Buildings, Ali and Moon (2007) make distinction between exterior and interior systems. When the main part of the stability system is at the perimeter of the building, it is an exterior structure and when the main part is inside the building, it is called an interior structure. It should be noticed that every interior structure also has some exterior components and vice-versa. The separation gives a guideline about how to visualise the different systems. The exterior and interior systems can be seen in figure 3.2. The dashed line indicates the height range that will be applied in the rest of the rapport. The numbers correspond to the following structural systems: 1: shear walls 2: core 3: outrigger 4: tube.

### Tall Building Structures

A third division is described in Tall Building Structures (Smith and Coull, 1991). Here is stated that choice of structural form is not only an arrangement of structural elements. Material choice, construction method, the architects requirements and location also play a role in this process. The more tall and slender the building becomes, the more important it is to choose an adequate structural form. The following systems are distinguished:

- Frame structure
- Wall structure
- Tube
- Outrigger
- Suspended structure (variant of an outrigger)
- Core
- Space structure
- Hybrid structure

### Building Structures Illustrated

Ching, Onouye, and Zuberbuhler (2014) make a separation between exterior and interior systems, in a similar way as Ali and Moon (2007) did. This can be seen in figure 3.3.

### Designing tall buildings

Sarkisian (2016) makes distinction between steel systems, reinforced concrete systems and composite systems. The concrete systems can be seen in figure 3.4.

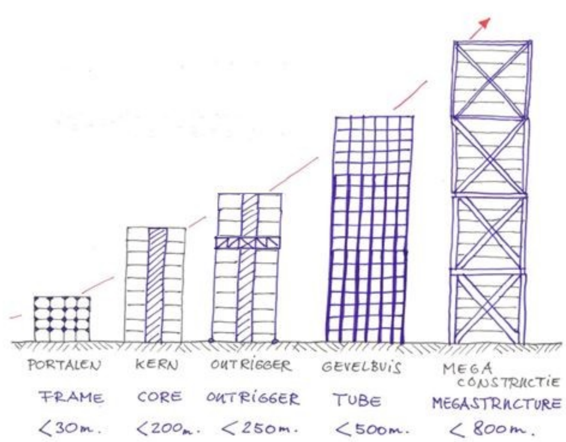


**Figure 3.1** Overview of stability systems by Nijsse (2012).

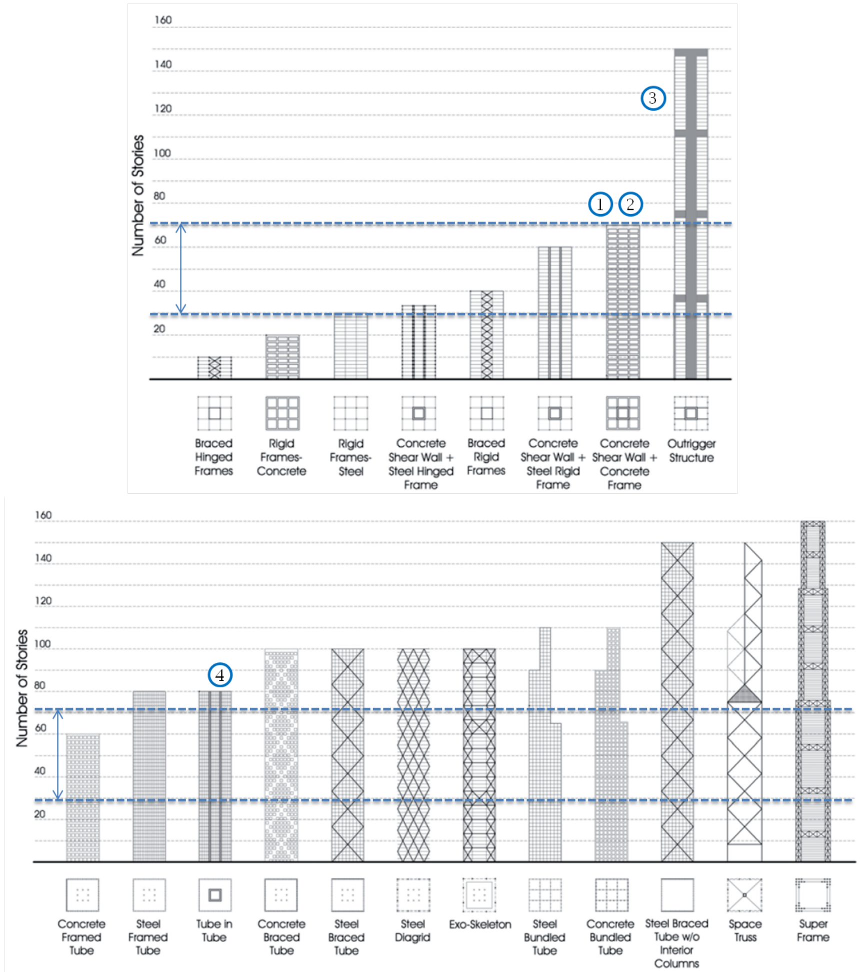


**Figure 3.2** Interior (top) and exterior systems (bottom) by Ali and Moon (2007). The dashed lines and numbers indicate the height range and applied system.

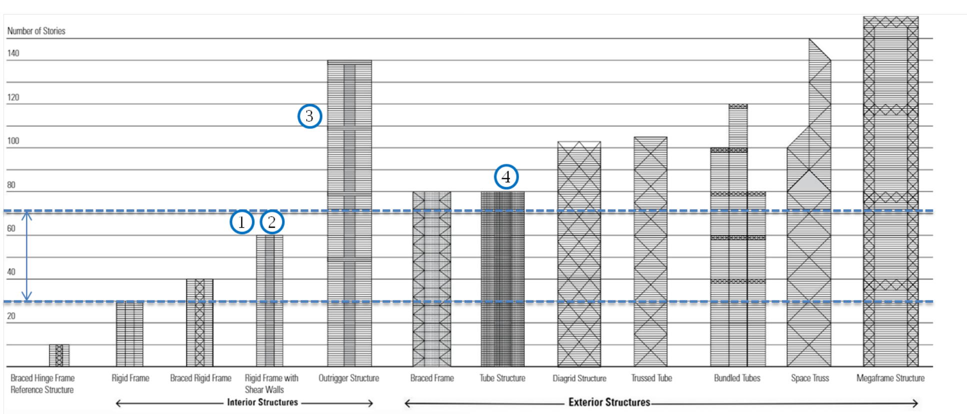


**Figure 3.3** Overview of interior and exterior systems by Ching, Onouye, and Zuberbuhler (2014)

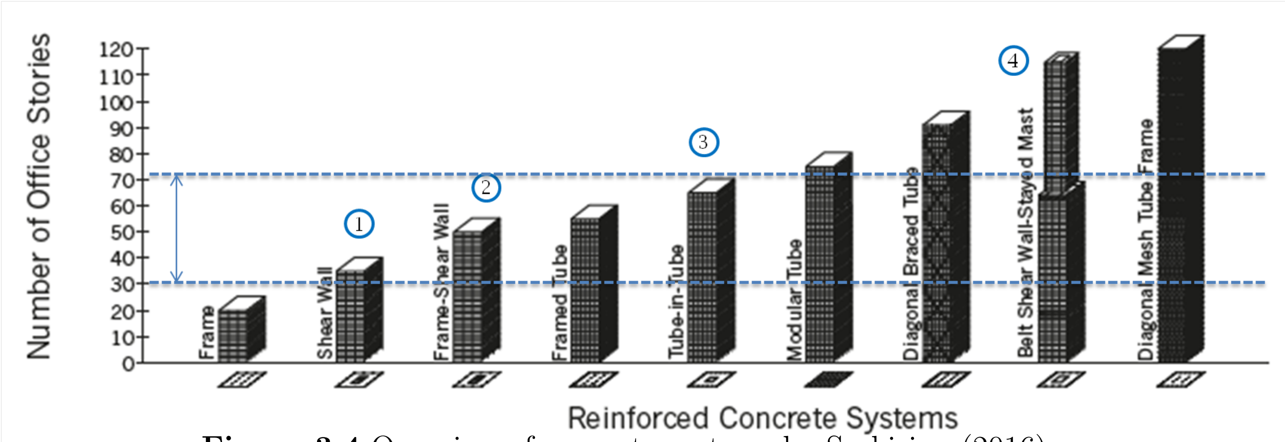


**Figure 3.4** Overview of concrete systems by Sarkisian (2016)

### Conclusion

The overviews of stability systems are used to decide which systems need to be considered in this thesis. This is done based on elementary properties, material choice, reference buildings and the applied height range. Only systems that can be executed in concrete are considered. The system has to be applicable to high-rise buildings in The Netherlands. A minimum of 100 meters and a maximum of 250 meters is taken as height range. This leads to four systems that will be considered. These are a shear wall system (1), core (2), outrigger (3) and tube (4). The numbers between brackets correspond to the systems as depicted in figure 3.2, 3.3 and 3.4. The four systems are now explained, as well as their theoretical background and a reference building. Based on the figures, a first prediction can be done for the maximum number of stories that can be applied in the system to work in an efficient way. For shear walls this is 60, for a core 40, for an outrigger 140 and for a tube 80 floors. However, the maximum reachable height for an outrigger depends strongly on the number of outriggers. For a building with only one outrigger, the maximum number of storeys will be around 70 or 252 $m$, in line with figure 3.1. The predicted values will be compared with the results of the parametric model in chapter 5.

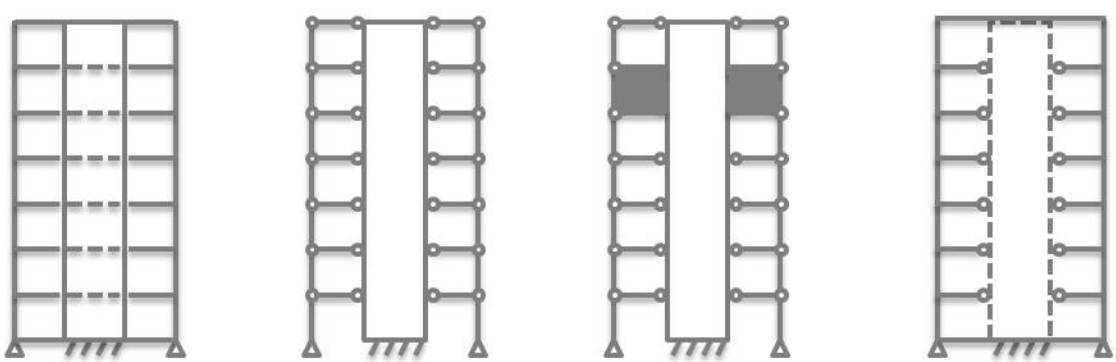

**Figure 3.5** Schematisation of the four systems that will be researched. From left to right: Shear walls, core, outrigger and tube

### 3.1.2 Shear walls

Shear walls are walls with both an architecturally function as partition elements and structural function by resisting gravity and lateral loads. They act as thin, deep cantilever beams, transferring lateral loads to the ground foundation (Ching, Onouye, and Zuberbuhler, 2014). They resist the concentrated shear load from the floor or roof diaphragm. If two or more shear walls are rigidly connected, they can be seen as coupled shear walls. Shear walls can be placed both in the facade and in the floor plan. For residential use, shear walls are more distributed throughout the floor plan (Sarkisian, 2016). Their solid form serves simultaneously as acoustic and fire insulator. The advantage of this system is that many configurations are possible. The number of wall elements can be minimized by tactically locating the shear walls to minimize tension forces and foundation uplift in the wall elements.

In contrast to what the name shear wall says, it mainly behaves as a bending element (Rolvink, 2010). For buildings with bigger floor space, also shear deformation has to be included. In this case a shear wall is schematized by an Euler-Bernoulli beam. This is a beam subjected to bending. The fourth order differential equation of this beam is derived below, with help of the kinematic, constitutive and equilibrium relation.

$$\phi = -\frac{\mathrm{d}w}{\mathrm{d}x} \qquad \kappa = \frac{\mathrm{d}\phi}{\mathrm{d}x} \qquad M = EI * \kappa \qquad \frac{\mathrm{d}V}{\mathrm{d}x} = -q \qquad \frac{\mathrm{d}M}{\mathrm{d}x} = V \qquad EI\frac{\mathrm{d}^4 w}{\mathrm{d}x^4} = q \tag{3.1}$$

This equation can be used to find the deflection of the building over the height. For this, the equation $EI\frac{d^4w}{dx^4} = q$ has to be integrated four times. The integration constants can be found by filling in the boundary conditions. For a cantilever beam subjected to bending, these boundary conditions are:

$for\ \ x = 0 : w = 0\ \ and\ \ \phi = 0, \quad for\ \ x = l : V = 0\ \ and\ \ M = 0$

Solving the four integration constants with the four boundary conditions leads to the following expression for the deflection at the top of the building:

$$w = \frac{ql^4}{8EI} \tag{3.2}$$

When placing shear walls in a floor plan, rotation can occur due to asymmetric positioning and different rigidities of the walls. This is a result of a different positioning of the origin of the cross section and the center of rigidity. If this is the case, the horizontal deflection is a summation of the displacement due to translation and the displacement due to twist (Hoenderkamp, 2002):

$$w(z)_{x;total} = w(z)_x + y\theta(z)_x \tag{3.3}$$

The twist ($\theta$) along the elements can be found here by solving the differential equation $EI\frac{\mathrm{d}^4\theta}{\mathrm{d}x^4} = q(z) * e$, with $EI$ representing the warping stiffness and $e$ the eccentricity of the load. To prevent this torsion, the rotation point has to be aligned with the equivalent load, both in x and y direction.

| | |
|---|---|
| Reference | |
| Name | De Zalmhaventoren |
| Location | Rotterdam (The Netherlands) |
| Year | 2022 (expected) |
| Height | 215 m |
| Source | Hoogtepunt voor binnenstedelijke woningbouw (Van Eerden, 2017) |

### 3.1.3 Core

A core is a stiff element in the center of the building, which is clamped in the foundation (Nijsse, 2012). A reason for the placement in the center is to minimize the possibility of torsion due to lateral loads and to put as much as possible vertical load here as possible (Sarkisian, 2016). Usually, stairs, elevators and installations are located in the building core. The walls of a core are normally made of concrete. In this situation, the core is combined with columns in the facade. Main function of the columns is to restrain vertical loads. Due to the high spacing between the columns or the low stiffness, columns cannot fully take horizontal loads. These are fully taken by the core. A core can be schematized by an Euler-Bernoulli beam and can be derived as in equation 3.1 (Simone, 2011). The effectiveness of the core depends on the cutouts in the wall, which influence the stiffness. Dependent on the location and size of these cutouts, the wall elements can be schematised either as one wall or as two coupled elements.

When designing a construction with a core, research showed that a minimum net floor area of 75% is needed to make a tall building profitable (Sarkisian, 2016). Recently, developers of high-rise aim to increase this value up to 80% or even 90%. For buildings below 200 m this can be seen as realistic. The ineffective area in a floor plan is on average around 23%, consisting mainly out of the core program (12%), structural area (5%) and elevator shaft area (4%). When building height increases, the percentages presented above increase as well. These values should be kept in mind when determining the core size.

| | |
|---|---|
| Reference | |
| Name | Rembrandt tower |
| Location | Amsterdam (The Netherlands) |
| Year | 1995 |
| Height | 135 m |
| Source | Building Structures 2 Steel (Abspoel, 2013) |

### 3.1.4 Outrigger

An outrigger system is a core system, complemented with one or more stiff frames or walls (Smith and Coull, 1991). These frames are structurally connected to the facade elements. When one outrigger is applied, it is commonly placed around two-thirds of the building height. The system is originating from sailing boats (Ali and Moon, 2007). Cables are used here to stabilize the mast, which is subjected to wind forces on the canvas. For buildings subjected to horizontal load, it works in a similar way. Load on a building leads to a horizontal deflection. This deflection is confined by the outrigger system. In this way the outrigger is activated (figure 3.6). The outriggers also lead to a reduction of bending moments. Outriggers can be executed with steel trusses or concrete walls. To effectively transfer bending moments to the facade columns, a belt truss can be applied. This is a stiff frame at the perimeter of the building. The disadvantage of an outrigger is that one or two floors of the building have to be offered to create space for the frame. Nevertheless, this space can be used for installations.

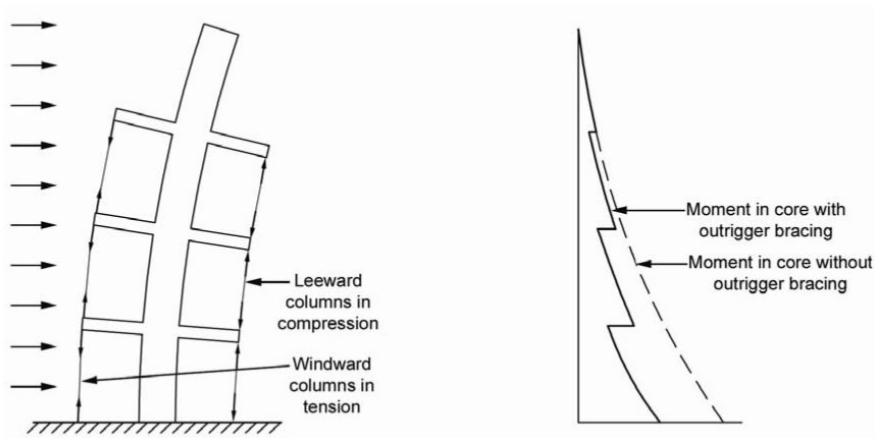


**Figure 3.6** Activation of the outrigger (Ali and Moon, 2007)

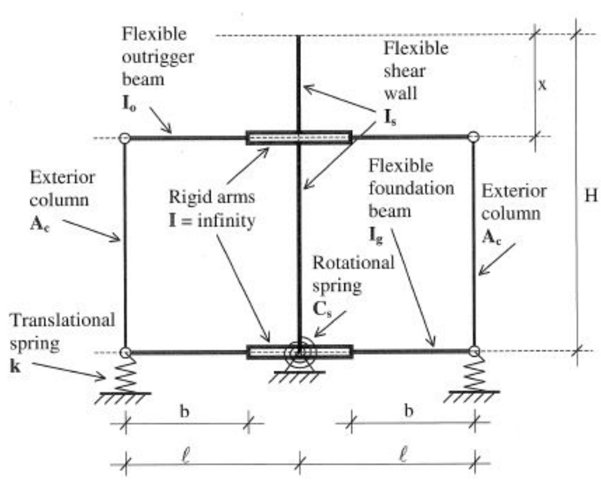


**Figure 3.7** Schematisation of the outrigger (Hoenderkamp, Snijder, and Bakker, 2003)

To rapidly analyse the behaviour of an outrigger, a simplified model has to be applied (Hoenderkamp, Snijder, and Bakker, 2003), as shown in figure 3.7. The outrigger part is modelled with rigid elements at the position of the central shear wall or core. The facade columns are schematised with pin-connected links. The outrigger structure can deform due to lateral load and which is restrained by the bending moment in the foundation and at the outrigger position. The outrigger can be modelled as an Euler-Bernoulli beam, but with reduced bending moments. The total restraining moment at the base of the structure is described by:

$$M_f = \frac{wH^2}{2C_s} * \frac{K}{l/6EI_f} + M_r(K-1) \;\; with \;\; K = \frac{l/6EI_f}{l/6EI_f + 1/C_s + 1/C_k} \tag{3.4}$$

The horizontal deflection at the top of the building is described by:

$$y_{top} = \frac{wH^4}{8EI_s} + \frac{wH^3}{2C_s} - \frac{M_r(H^2-x^2)}{EI_s} - \frac{M_rH}{C_s} - \frac{M_fH}{C_s} \tag{3.5}$$

For the derivation of these equations, the paper of Hoenderkamp, Snijder, and Bakker (2003) can be consulted. The optimum position of the outrigger can be determined manually (Hoenderkamp, Snijder, and Bakker, 2003). The equation of the deflection at the top of the structure is used for this. This equation originates from equation 3.5, but now is rewritten with a number of simplifications.

$$y_{red} = \frac{w * H^5}{12(EI_s)^2}(1 - \bar{x}^2 - \bar{x}^3 + \bar{x}^5 + \frac{5 - 3\bar{x}^2 - 2\bar{x}^3}{\gamma H})(\frac{1}{1 - \bar{x} + \omega}) \tag{3.6}$$

The optimal outrigger position $x$ can be found by differentiating this equation for the horizontal deflection with respect to $x$, setting it equal to 0 and solve for $x$. The outcome of this equation is a function that only depends on $x/H$, $\gamma H$ and $\omega$. $x/H$ is equal to the location parameter $\bar{x}$, $\gamma H$ is a non dimensional parameter which is equal to $\frac{C_s * H}{K * EI_s}$ and $\omega$ is the ratio between two structural parameters.

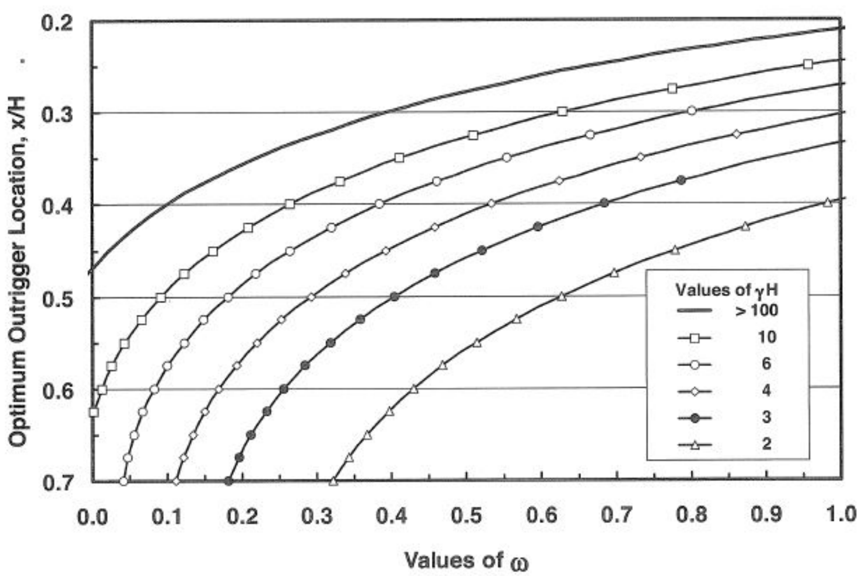


**Figure 3.8** The optimal position of the outrigger (Hoenderkamp, Snijder, and Bakker, 2003)

Reference

| | |
|---|---|
| Name | New York Times Tower |
| Location | New York (United States) |
| Year | 2007 |
| Height | 228 m |
| Source | Outrigger design for high-rise buildings (Choi et al., 2012) |

### 3.1.5 Tube

A tube is a three-dimensional structural system around the building parameter to resist lateral loads (Ali and Moon, 2007). A tube is normally used in combination with a core. The term *tube-in-tube* is commonly used for this system. Stiffness can be gained by concrete walls in the facade or clamped connections between closely spaced beams and columns. A disadvantage of a tube is that these stiff elements lead to restrictions in the design of the facade (Smith and Coull, 1991). A phenomenon in a tube system is shear lag (Ham and Terwel, 2017). In a beam subjected to bending, a linear stress distribution is expected. However, due to shear lag between columns, much higher forces in the corner columns are obtained. This makes the inner columns less effective in resisting lateral loads.

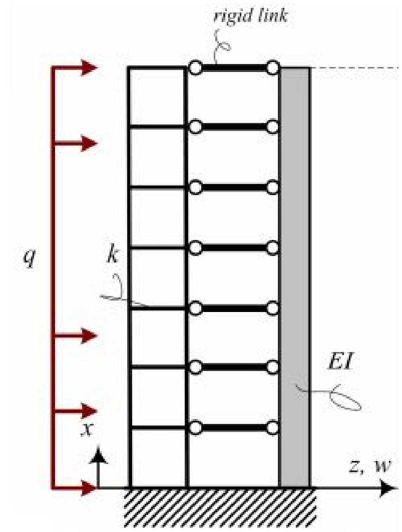


**Figure 3.9** Structural model of a tube (Simone, 2011)

A tube in combination with a core can be seen as coupled system of an Euler-Bernoulli beam with a shear beam. These two elements are connected by rigid links as can be seen in figure 3.9. The bending beam and shear beam work here as a parallel system. In the shear equation is $\gamma$ the rotated angle due to shear. $V$ is the shear force ($kN$) and $GA$ is the shear stiffness ($kN$) of the frame, in figure 3.9 indicated with $k$. The ordinary differential equation of the system can be found as the summation of a beam subjected to bending and shear.

$$\gamma = \frac{\mathrm{d}w}{\mathrm{d}x} \qquad V = GA * \gamma \qquad \frac{\mathrm{d}V}{\mathrm{d}x} = -q \qquad GA * \frac{\mathrm{d}^2 w}{\mathrm{d}x^2} = -q \tag{3.7}$$

$$EI * \frac{\mathrm{d}^4 w}{\mathrm{d}x^4} = q \qquad + \qquad GA * \frac{\mathrm{d}^2 w}{\mathrm{d}x^2} = -q \qquad = \qquad EI * \frac{\mathrm{d}^4 w}{\mathrm{d}x^4} - GA * \frac{\mathrm{d}^2 w}{\mathrm{d}x^2} = q \tag{3.8}$$

An expression for $w$ can be found by evaluating equation 3.8, making use of the boundary conditions:
$for \ \ x = 0 : w = 0 \ \ and \ \ \phi = 0 \ \ for \ \ x = l : V_{bending} + V_{shear} = 0 \ \ and \ \ M = 0$
The stiffness $GA$ in $kN$ is obtained from the equation:

$$GA = \frac{12 * E}{h_{grid}(\frac{1}{\frac{n*I_b}{b_{grid}}} + \frac{1}{\frac{n*I_c}{h_{grid}}})} \tag{3.9}$$

$b_{grid}$ and $h_{grid}$ represent here the vertical and horizontal grid size, $n$ is the number of grids and $I_b$ and $I_c$ are the moment of inertia of the beam and column of the frame.

Reference

| | |
|---|---|
| Name | John Hancock Center |
| Location | Chicago (United States) |
| Year | 1969 |
| Height | 344 m |
| Source | Structural Developments in Tall Buildings |
| | (Ali and Moon, 2007) |

## 3.2 Important factors in high-rise

In the structural design of a high-rise building, there are many factors that determine the behaviour of the building. The factors that are taken into account are material choice, reinforcement design, floor type, horizontal and vertical loads, foundation stiffness, second order effects, comfort, connections and positioning of perforations. A theoretical explanation of these factors is given below. In chapter 4 is explained how they are taken into account during modelling.

### 3.2.1 Material choice

Common used materials for high-rise buildings are concrete, steel or a combination of the two. In this research only concrete cast-in-situ will be used to make a clear and objective comparison between the systems. The strength class of the concrete as input can be determined manually, but for the results presented in this research, a strength of C50/60 will be used. A reduction factor in the young's modulus of the concrete can be applied to account for cracks and creep. This is usually around one third of the uncracked value. The choice to apply the standard young's modulus or the reduced one, depends on the kind of element and the way of loading. Normally the core, shear walls without cutouts and columns are assumed as uncracked. This assumption can be verified by checking the occurrence of tensile forces in the element. At the position of lintels between two parts of a wall, the concrete presumably cracks. Here a cracked situation has to be assumed. The floor elements are assumed to crack under lateral loads. Possible tension forces are directly visible in Karamba, this can be used to verify these initial assumptions.

### 3.2.2 Reinforcement design

**Reinforcement of columns**

The possibility of tension forces in the columns necessitates the application of reinforcement (Ham and Terwel, 2017). Reinforcement in the columns of a high-rise building have to be tested on the combination of normal force and bending. The relative normal force and bending moment in a column can be expressed with:

$$n = \frac{N_{ed}}{A_c * f_{cd}} \ and \ m = \frac{M_{ed}}{f_{cd} * A_c * h} \tag{3.10}$$

The amount of reinforcement can be checked with a design graph from GTB-2013, with $n$ from equation 3.10. The value of $\rho * \frac{f_{yd}}{f_{cd}}$ can be found here, from which the required percentage reinforcement $\rho$ can be retrieved. This amount of reinforcement is the minimum amount of reinforcement in the cross section of the column. A first order calculation will suffice if the slenderness ($\lambda$) is equal to or smaller than the limit slenderness ($\lambda_{lim}$). For the slenderness, the following equation given on page 359 of Constructieleer Gewapend Beton (Braam and Lagendijk, 2011) can be assumed:

$$\lambda_{lim} = \frac{20 * A * B * C}{\sqrt{n}} \ with \tag{3.11}$$

$$A = \frac{1}{1 + 0.2 * \phi_{eff}} \ and \ \phi_{eff} = 1.2, \tag{3.12}$$

$$B = \sqrt{1 + 2 * \omega} \ and \ \omega = \frac{A_s * f_{yd}}{A_c * fcd}, \tag{3.13}$$

$$C = 1.7 - r_m \ and \ r_m = \frac{M_1}{M_2}, \tag{3.14}$$

$$and \ \lambda = \frac{3.46 * l_k}{i} \tag{3.15}$$

**Reinforcement of (core) walls**

The wall of the core can be divided into two categories. The front and back wall are in compression and tension when subjected to horizontal loading, while the two side walls are subjected to shear. An indication of the amount of reinforcement in the horizontal and vertical direction is obtained from Lankhorst (2018). A reinforcement net is assumed of ⌀8-150/250 with 150 mm the vertical spacing and 250 mm the horizontal spacing. The minimum amount of shear reinforcement can be determined with:

$$A_{s;w}/s_{req} = \frac{V_{Ed}}{z * cot(\theta) * f_{ywd}} \tag{3.16}$$

$V_{Ed}$ represents the shear force in the core and $z$ is the center to center distance of the front and back wall. $\theta$ is the crack inclination angle of the concrete and is assumed to be 45°.

**Reinforcement of floors**

The reinforcement design of the floors is based on a one-way spanning slab. The minimum amount of reinforcement in the main direction can be determined from:

$$A_{min,x} = \frac{M_{Ed,x}}{z * f_{yd}} \tag{3.17}$$

Following the analogy of the one-way spanning slab, the minimum amount of reinforcement in y direction can be found with $M_{Ed,y} = 0.2 * M_{Ed,x}$.

### 3.2.3 Floors

The function of a floor in a high-rise building is to bear all vertical loads and to transfer the horizontal loads to the stabilising elements (Lagendijk, 2016). It also ensures horizontal stability through the rigid floor diaphragms. Other functions of floors are (sound) insulation, fire resistance, installations and aesthetics. In general, two concrete floor types can be distinguished, the precast floor and the cast-in-situ floor. The most used precast floors are the hollow core slab, bi-axial hollow core slab, poly slab and the solid slab floor. The most suitable floor type can be determined based on multiple criteria which can be found in Concrete Building Structures (Lagendijk, 2016). The most important criteria are design freedom, maximum span, construction, core activation and necessity for additional beams. Thickness of the floors only depends on the vertical load and floor span. A consequence of this is that this value can be constant over the height of the building, as long as the floor spans and load are also constant. The cooperation with the core and the fact that no beams are required makes the cast in-situ floor an appropriate floor type for the model.

A failure mechanism of concrete cast-in-situ is punching shear. It occurs in structural members as slabs under concentrated loads. The acting shear stress follows from:

$$v_{Ed} = \beta * \frac{V_{Ed}}{u_1 * d} \tag{3.18}$$

$\beta$ is here the ratio between the full perimeter of the column $u_1$ and the effective perimeter of the column $u_1^{\star}$. The shear resistance and the minimum shear resistance are:

$$v_{Rd} = 0.12 * k(100 * \rho * f_{ck})^{1/3} \quad and \quad v_{min} = 0.035 * k^{3/2} * \sqrt{f_{ck}} \tag{3.19}$$

When the criterion $v_{Ed} < v_{Rd}$ is not satisfied, the floor is likely to fail on punching shear. Other measures have to be taken by the engineer in the form of drop panels or additional shear reinforcement.

### 3.2.4 Loads

Loads on a structure can be divided into horizontal and vertical loads. Both are explained in more depth below, with numerical values from Eurocode 1 (2002).

**Vertical loads**

The vertical loads on a building can be divided into dead load and variable load. The amount of variable load depends on the category in Eurocode 1 (2002). Five categories are specified here. Category A describes loads for residential buildings and B for office areas. The static load on a floor depends on the function. This is expressed in categories in the Eurocode. For category A, residential use, the variable load is 1.75 $kN/m^2$. For category B, offices, this is 2.5 $kN/m^2$. The dead weight is a summation of the contribution of structural and non-structural elements. Structural elements here are floors, columns and (core)walls. The dead load of the concrete floors is the thickness multiplied with the density of concrete and will be constant over the building height. The weight of the the other structural elements follows from optimisation. Loads of non-structural elements are 1.2 $kN/m^2$ for floor finishing, 0.15 $kN/m^2$ for the ceiling and 0.1 $kN/m^2$ for mechanical installations (Sarkisian, 2016). The load of facade elements depends on the type of facade. For metal with glass, stone with glass and concrete with glass, this is subsequently 0.75, 1.2 and 2.5 $kN/m^2$.

### Horizontal loads

The wind force on a structure can be determined by the following formula:

$$F_w = c_s c_w * c_f * q_p(z_e) * A_{ref} \tag{3.20}$$

In this formula, $c_s c_w$ is the structural factor, $c_f$ is the force coefficient for the structure, $q_p(z_e)$ is the wind pressure at height $z_e$ and $A_r ef$ is the reference area of the structure. The structural factor $c_s c_w$ takes the effect on wind actions from the non-simultaneous occurrence of wind peak pressures on the surface into account, together with the vibrations due to turbulence. Because $c_s c_w$ cannot be assumed as 1 in this context, it has to be calculated with the formula:

$$c_s c_w = \frac{1 + 2 * k_p * I_v(z_s) * \sqrt{B^2 + R^2}}{1 + 7 * I_v(z_s)} \tag{3.21}$$

Here, $k_p$ is the peak factor of the fluctuating part of the load, $I_v$ is the turbulence intensity, $B^2$ is the background factor, $R^2$ is the resonance response factor and $z_s$ is the reference height. The force coefficient $c_f$ for rectangular cross sections is described by the formula:

$$c_f = c_{f,0} * \psi_r * \psi_\lambda \tag{3.22}$$

With $c_{f,0}$ the force coefficient of rectangular sections, $\psi_r$ the reduction factor for square sections with rounded corners and $\psi_\lambda$ the end-effect factor for elements with free-end flow. $q_p(z_e)$, the wind pressure can be found with the formula:

$$q_p(z_e) = (1 + 7 * I_v(z)) * 1/2 * \rho * v_m^2(z) \tag{3.23}$$

With $\rho$ as the wind density and $v_m$ the wind speed. To determine this normative wind speed $v_m$, The Netherlands is divided into three wind zones. Within these zones, distinction is made between a coastal, rural and urban environment. The wind velocity pressure for buildings with a height to width ratio higher than two is distributed over the building height as shown in figure 3.10. For the exact values of the parameters in these formulas, appendix B of the report of Dijkstra (2008) can be used. The exact values of the wind pressure for building heights within the range of the project can be found in figure 3.1. In this table, distinction is made between three different wind areas in The Netherlands. The three cities with the most inhabitants, Amsterdam, Rotterdam and Den Haag are located in wind area II.

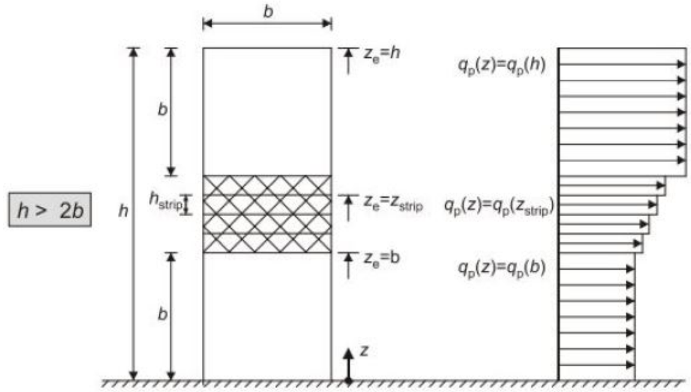


**Figure 3.10** Wind pressure over the building height according to Eurocode 1 (2002)

| Hoogte boven maaiveld | Gebied I | | | Gebied II | | | Gebied III | |
|---|---|---|---|---|---|---|---|---|
| | Kust | Onbebouwd | Bebouwd | Kust | Onbebouwd | bebouwd | Onbebouwd | bebouwd |
| 100 | 2,38 | 1,96 | 1,77 | 1,99 | 1,64 | 1,48 | 1,35 | 1,22 |
| 110 | 2,42 | 2,00 | 1,81 | 2,03 | 1,68 | 1,52 | 1,38 | 1,25 |
| 120 | 2,45 | 2,04 | 1,85 | 2,05 | 1,71 | 1,55 | 1,41 | 1,28 |
| 130 | 2,48 | 2,08 | 1,89 | 2,08 | 1,74 | 1,59 | 1,44 | 1,31 |
| 140 | 2,51 | 2,12 | 1,93 | 2,10 | 1,77 | 1,62 | 1,46 | 1,33 |
| 150 | 2,54 | 2,15 | 1,96 | 2,13 | 1,80 | 1,65 | 1,48 | 1,35 |
| 160 | 2,56 | 2,18 | 2,00 | 2,15 | 1,83 | 1,67 | 1,50 | 1,38 |
| 170 | 2,59 | 2,21 | 2,03 | 2,17 | 1,85 | 1,70 | 1,52 | 1,40 |
| 180 | 2,61 | 2,24 | 2,06 | 2,19 | 1,88 | 1,72 | 1,54 | 1,42 |
| 190 | 2,63 | 2,27 | 2,08 | 2,20 | 1,90 | 1,75 | 1,56 | 1,44 |
| 200 | 2,65 | 2,29 | 2,11 | 2,22 | 1,92 | 1,92 | 1,58 | 1,46 |
| 225 | 2,70 | 2,35 | 2,35 | 2,26 | 1,97 | 1,97 | 1,62 | 1,62 |
| 250 | 2,74 | 2,40 | 2,40 | 2,30 | 2,01 | 2,01 | 1,66 | 1,66 |
| 275 | 2,78 | 2,45 | 2,45 | 2,33 | 2,05 | 2,05 | 1,69 | 1,69 |
| 300 | 2,82 | 2,5 | 2,5 | 2,36 | 2,09 | 2,09 | 1,72 | 1,72 |

**Table 3.1** Wind pressure per building height from Eurocode 1 (2002)

#### Load combinations

Load combinations for vertical loads in the ultimate limit state and serviceability limit state design are shown below. $G$ stands for gravity load, $Q$ for the variable load, $\gamma$ for the partial load factor and $\psi$ is the combination factor when multiple variable loads are applied. The exact values of $\gamma$ and $\psi$ follow from the design tables in Eurocode 1 (2002).

$$ULS : \gamma_G * G_k + \gamma_{Q;1} * Q_{1;k} + \sum \gamma_{Q;i} * \psi_{0;i} * Q_{i;k} \tag{3.24}$$

$$SLS : G_k + \gamma * Q_{1;k} + \sum \psi_{0;i} * Q_{i;k} \tag{3.25}$$

### 3.2.5 Foundation

The total deflection of a high-rise building is the summation due to both the building itself and the foundation. For high-rise buildings, the ultimate deflection at the top of the building is $1/500 * h$, with $h$ the height of the building. This is a requirement from Eurocode 1 (2002). This includes both the influence of the foundation and the building itself. The expression for the total deflection of a bending element is:

$$u = \frac{M * l}{C} + \frac{ql^4}{8EI} \tag{3.26}$$

The rotational stiffness of the foundation here is the factor $C$ in $kNm/rad$. To take both the influence of the foundation and building into account, the structure can be simplified to a vertical cantilever with a bending stiffness $EI$ and a rotation stiffness $C$ as can be seen in figure 3.11. The exact value of $C$ depends on the type of foundation and the accessory stiffness. The type of foundation that will be considered is a pile foundation. The calculation of the deflection due to the foundation exists of two steps: First the number of foundation piles has to be calculated, followed by the calculation of the deflection itself.

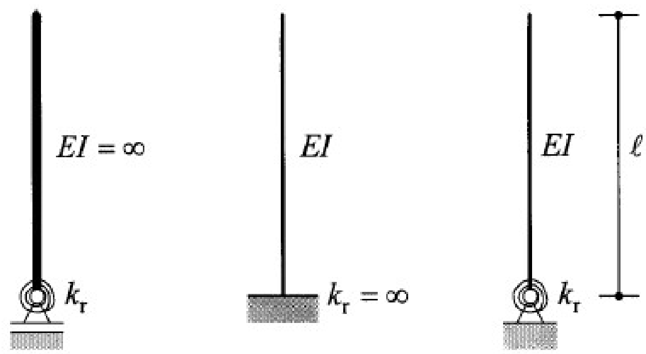


**Figure 3.11** Combination of bending stiffness and foundation stiffness (Simone, 2011).

As stated in the previous paragraph, the resistance per pile has to be determined first. For this a static calculation method is used, in combination with a a cone penetration test. This calculation procedure is derived from Eurocode 7 (2013). The resistance of one pile ($Q_t$) is the summation of the influence of the shaft resistance ($Q_s$) and the base resistance ($Q_b$). The working load of the pile ($Q_{all}$) is the total resistance divided by three, where three is a factor of safety. Subsequently, the number of piles required, is the mass of the building ($m$), divided by the working load of the pile.

$$Q_s = c_u * \alpha * A_s \quad Q_b = c_u * N_c * A_b \quad Q_t = Q_s + Q_b \quad Q_{all} = \frac{Qt}{3} \quad n = \frac{m}{Q_{all}} \tag{3.27}$$

$c_u$ represents the undrained shear strength of the soil, which is assumed to be 360 $kPa$ for clay ground. $\alpha$ is a reduction factor which depends on soil type and strength, in this case 0.33 is assumed for this. $N_c$ can be obtained from Skempton's Chart and is usually taken as 9. The required number of piles can now be used to calculate the rotational stiffness and deflection due to the foundation (Ham and Terwel, 2017). This stiffness can be applied to equation 3.26. As a first step, the moment of inertia ($I_p$) of the pile configuration can be found, based on the positioning and the number of piles. This is used to find $P_n$, the moment force in $kN$ in one pile. Subsequently, $\Delta l$ is calculated. This is the elongation of the most heavily loaded pile. Finally $u$, the horizontal deflection due to the foundation and $C$, the rotation stiffness can be found.

$$I_p = \sum_{i=1}^{n} a_i^2 \quad P_n = \frac{M * a_i}{I_p} \quad \Delta l = \frac{P_n * l_p}{E * A_p^2} \quad u = \frac{\Delta l * l_p}{a_i} \quad C = \frac{M}{\Phi} \tag{3.28}$$

The influence of foundation can be compared now with the influence of the building. This influence can have a maximum value of 33% of the total deflection, which is $h/1500$. If this value is higher, either the number of piles, pile length or pile diameter has to be adapted and the calculation procedure has to be done again.

### 3.2.6 Second order effects

Wind on a high building will lead to a deflection at the top of the building. As a result of this, the center of mass of the building displaces. In a linear calculation, this is not taken into account. When a second order calculation is considered, the displacement causes eccentricity in the building, with an additional deflection as result.

The first order deflection is the summation of the foundation stiffness and the bending stiffness of the building. As a result of this deflection, the center of mass of the building moves horizontally over a distance of $0.5 * u_1$. This movement leads to an additional bending moment at the bottom. The ratio of the original bending moment and the new bending moment, can be expressed in a ratio $n = M_1/M_2$. This factor $n$ can be used to find the second order deflection at the top of the building as well, by using the second order factor $N = n/(n-1)$. This leads to a second order deflection of $u_2 = u_1 * N$.

### 3.2.7 Comfort

Accelerations in a high-rise building are not allowed to exceed a certain limit. This to meet the comfort requirements. Too high accelerations can lead to an unsafe experience for the users. The Eurocode gives a graph to verify this (figure 3.12). Here the maximum allowable acceleration in $m/s^2$ is plotted versus the frequency in $Hz$. The calculated acceleration at the top of the building should not exceed this line. Line 1 is meant for offices and line 2 for residential buildings.

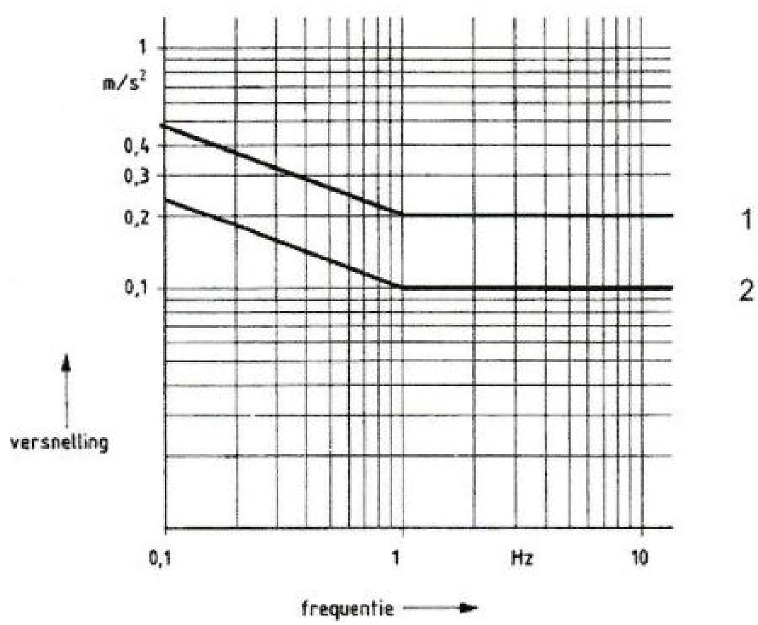


**Figure 3.12** Limits for accelerations in a building from Eurocode 1 (2002)

Factors that have influence on the dynamic behaviour of a building are wind speed, wind direction, building height, width and depth, stiffness, mass density and damping ratio (Paauwe, 2020). The wind speed and wind direction are related to the acceleration of the building and the other factors are related to the frequency. The first frequency of a building can be estimated by the formula $n_1 = \frac{46}{L}$, with $L$ the height of the structure in meter and $n_1$ the frequency in Hertz. An expression for the acceleration in $m/s^2$ at the top of the building is found in the rapport of TNO (Staalduinen, 1992).

$$a = \frac{1.6 * \phi_2 * p_w * C_t * b}{m} \tag{3.29}$$

$\phi_2$ is a dynamic factor which takes the fluctuation of the wind load into account:

$$\phi_2 = \sqrt{\frac{0.0344 * n_1^{-2/3}}{D(1 + 0.12 * n_1 * h)(1 + 0.2 * n_1 * b)}} \tag{3.30}$$

with $D$ the damping coefficient of the building. For buildings with a natural frequency below 1 Hz, the damping coefficient can be set on 0.01. $p_w$ is the fluctuating part of the wind pressure:

$$p_w = 100 * \ln \frac{0.2}{h} \tag{3.31}$$

$C_t$ is the shape factor of the building, $b$ the width perpendicular to the wind and $m$ the mass of the building.

### 3.2.8 Influence of perforations

Perforations in wall elements are unavoidable due to the presence of doors, windows and openings for ducts (Lagendijk, 2016).The rigidity of walls decrease around openings and the wall element becomes more vulnerable for cracking, which leads to a further decrease in rigidity. In walls this is most likely to happen at the position of a lintel above a door. Without opening, the bending stiffness of the element is calculated with full cooperation between the two parts of the wall. In this situation the lintel forms the connection between the left and right side of the wall. The lintel has to transfer the change in bending stress, which deviates over the height. This resulting force is transferred through the lintel as shear force. The maximum bending moment in this lintel is the shear force multiplied by half of the width, plus a value $a_i$.

$$M_{max} = \Delta F_{vert}(\frac{b}{2} + a_i) \tag{3.32}$$

$$a_i = \frac{\Delta F_{vert}}{d * f_{cd}} + c \tag{3.33}$$

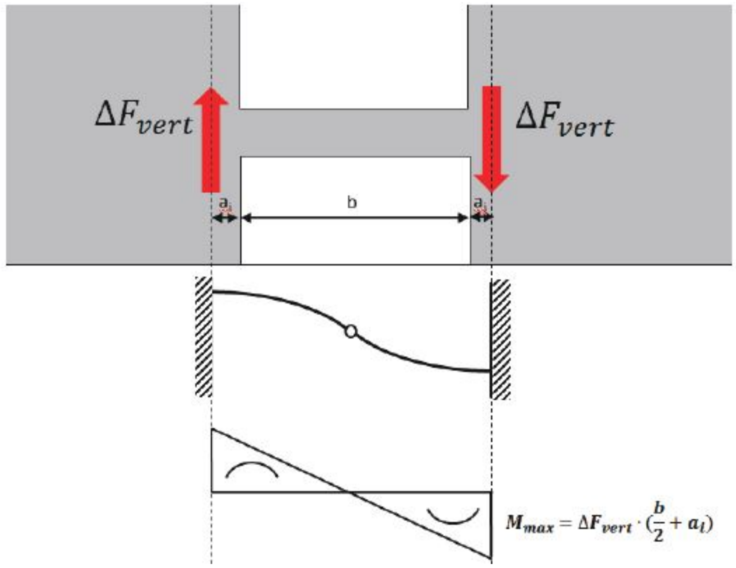


**Figure 3.13** Force in a lintel connection between two walls (Lagendijk, 2016)

## 3.3 Parametric design

The third part of the literature study covers parametric design. First a definition to parametric design is given, followed by an overview of the software and tools that will be used.

### 3.3.1 Definition and steps

Parametric engineering can be seen as an over-coupling term for parametric design, computational design, algorithmic design, associative design and generative design. In the reader Parametric Engineering it is described as:

*'Parametric engineering implies the use of logic – in the form of algorithms driven by input parameters – as a digital design medium to assess engineering problems'* (Van Der Linden, 2018).

Digital applications, the parametric tools, are used to perform a task in a parametric way. With these tools it is possible to increase the level of complexity, dependent on the requirements. When working with parametric tools, five steps are distinguished (Van Der Linden, 2018). These steps are explained below and in figure 3.14

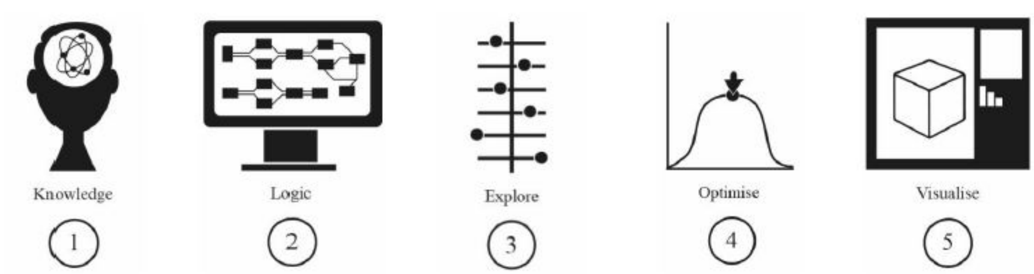


**Figure 3.14** Parametric framework (Van Der Linden, 2018)

1. **Knowledge:** Gather all possible information. Here the design problem is formulated. This problem is translated to an abstract model, in order to solve a generic problem. Fixed numbers are replaced by parameters.

2. **Logic:** In this step the relation between the parameters has to be found. The design problem is translated into logic.

3. **Explore:** When the relation between parameters is set, the computer will create a certain output based on your parameters. This is called optioneering. When the domains of the parameters are set, the design space can be explored.

4. **Optimise:** After defining the design space, the computer can search for the best solution within these boundaries. This is called optimising.

5. **Visualise:** It is important to clearly show the outcomes of your model to others. Good visual models help to obtain a clear overview of the project and to take decisions.

### 3.3.2 Software and tools

There is a wide range of parametric environments that is used nowadays. This is not only in the field of structural engineering and architecture, but also in automotive, industrial design and mechanical design. Grasshopper (Rutten, 2020) in combination with Rhinoceros (McNeel, 2020) is the most used parametric environment by structural engineers. Other often used environments are Solidworks, Dynamo, CATIA and FreeCAD.

#### Geometry

Rhinoceros is an environment developed byMcNeel (2020). It is a computer-aided design tool that can be used to create three-dimensional elements. The geometry is based on a model of NURBS, with free form surfaces and a mathematically precise representation of curves. With the use of Grasshopper, these elements can be made parametric. Grasshopper is a visual programming language in Rhinoceros developed by Rutten (2020). Programs can be created by dragging and connecting components to the canvas. Within Grasshopper several plugins can be applied, with a wide range of purposes. Useful plugins for the scope of the thesis are mentioned below.

**Figure 3.15** Rhinoceros (McNeel, 2020) and Grasshopper (Rutten, 2020)

#### Structural engineering

Before computers were used, structural engineering was done by hand sketches and calculations. Later a transition was made to digital tools with FEM packages. Nowadays parametric tools are providing extra possibilities to the engineer. Karamba (Preisinger, 2018) is used to perform structural analyses. Geometry created in Grasshopper can be converted into structural elements. By creating supports, loads and cross sections, the geometry can be analysed and visualised.

**Visualisation**

The aim of visualisation is to communicate a message or a design with sketches, diagrams, impressions or animations. A user friendly interface for Grasshopper can be made with Human UI (NBBJ, 2019). The fact that this interface is separated from the Grasshopper canvas makes it easily accessible. It can be used for outputting results, defining geometry or presenting a legend. A tool to explore all design alternatives within the boundaries is Design Explorer. The tool works in combination with TT Toolbox, Colibri or Excel.

## 3.4 Optimisation

With optimisation you search for the options that suffice within the design space, so satisfying all constrains (Van Der Linden, 2018). The solution which best satisfies the defined criteria is called fitness. In the optimisation process single and multi-objective optimisation can be differentiated. For this research, single-objective optimisation will be used, executed within Karamba. The Karamba element can be linked to a range of values. Together these form the design space. The most optimal design option depends on the goal of the optimisation, this can be for example the lightest, cheapest or most sustainable construction.

### 3.4.1 Types of optimisation

Baldock (2007) describes three different ways of optimisation: size, topology and shape. In size optimisation the size of structural members is varied. With topology optimisation the amount of available material is optimal distributed over the design domain. In shape optimisation the most optimal shape of the structure is found. The three ways of optimisation described above can be linked to the input of the model. Shape optimisation could be used to find the height or slenderness where a change of structural system could be considered. Topology optimisation can be seen as the system choice. It can be used to find the most suitable system for a building when dimensions are set. Size optimisation can be linked to the element size, so the thickness of columns and walls.

In the design process, it is logical to start with shape or topology optimisation, followed by size optimisation. This is because enlarging the cross sections of structural elements is limited and elements can become unpractical and uneconomic. In chapter 5 is explained how these ways of optimisation are applied on the model.

### 3.4.2 Optimisation tools

There are different tools within Grasshopper that are suitable for optimisation. The most used ones are Karamba, Galapagos, Octopus and Opossum. In Karamba it is possible to optimise for the size of the cross section, based on requirements from the Eurocode. The Galapagos tool can be linked to multiple sliders from the input. One optimisation objective can be determined by the user. Afterwards, the input sliders are varied to find the optimised solution within the design space. With Octopus, solutions for multi-fitness criteria can be found. This is used to explore a wider range of possible design options, between the extremes of each goal. Opossum can be seen as a combination of Galapagos and Octopus. It can be used both for single and multi-objective optimisation.

### 3.4.3 Optimisation goals

**Flexibility**

The term flexibility is a broad term which can be interpreted in many different ways. In this scope, it is defined as the ability to be easily modified. When this is linked to a construction or more specific to a high-rise building, it gives an indication about the design freedom, both in the facade and the floor plan. This freedom can be related to the structural system, adaptation in volume and layout and permanent versus temporary use. Flexibility can be divided into three time ranges (Hubar, 2009). Service flexibility: this is the possibility for fast changes in use and function. Adaptability: this is adaptation to the wishes of a new user. Change in function: a total new use of the building, which cannot be predicted beforehand. In this research, the relation between the structural system and flexibility will be judged. To express this in exact values, the calculation procedure of Hubar (2009) is used. The background of the used expression can also be found in his report. The expression is presented below.

$$\%_{flex} = 1 - \sum (\%_{constr} * \zeta) - \%_{vert} * \zeta \tag{3.34}$$

$\%_{flex}$ is the flexibility index, this is the criterion that quantifies flexibility. $\%_{constr}$ is the percentage of the floor area that is occupied by the stability system, including all load bearing elements. It is defined as the area taken by the stability system, divided by the gross floor area. $\%_{vert}$ is the part of the floor area that is occupied by vertical transport. $\zeta$ is a factor that gives an indication about the divisibility of the floor plan. For each structural element, a ratio has been determined to express this.

**Total weight and embodied carbon**

The total weight of a construction is the summation of the weight of all elements. In this scope, only structural elements will be considered. These are columns, floors, and (core) walls. Other elements as facade elements, floor finishing, installations, staircases and elevators are left out. Carbon emission is a term that is used in multiple phases of the building process. One of these is the calculation of shadow prices of materials. This is a prize that is related to the environmental impact of 1 kg of that material. For concrete grade C35/45 for example, this is 0,007500 €ev/kg and for reinforcement steel FeB500, this is 0,24711 €ev/kg (Gibbons and Orr, 2020). This means that the multiplication of this value with the total weight of the material leads to the environmental cost of that material. The estimated embodied carbon during the building process can be seen in figure 3.16. The product stage is only one of the four stages in the life cycle of the building. However, this stage is responsible for 50% of the embodied carbon during the total life span (Gibbons and Orr, 2020). This means that a decrease in raw material supply can significantly contribute to the carbon footprint of the building. This also shows the relevance of reducing the total weight. Due to the fact that only the amount of concrete is considered in the research, it can be said that total weight and carbon emission are directly related. As a consequence of this, optimisation to minimise both carbon emission and total weight can be done simultaneously.

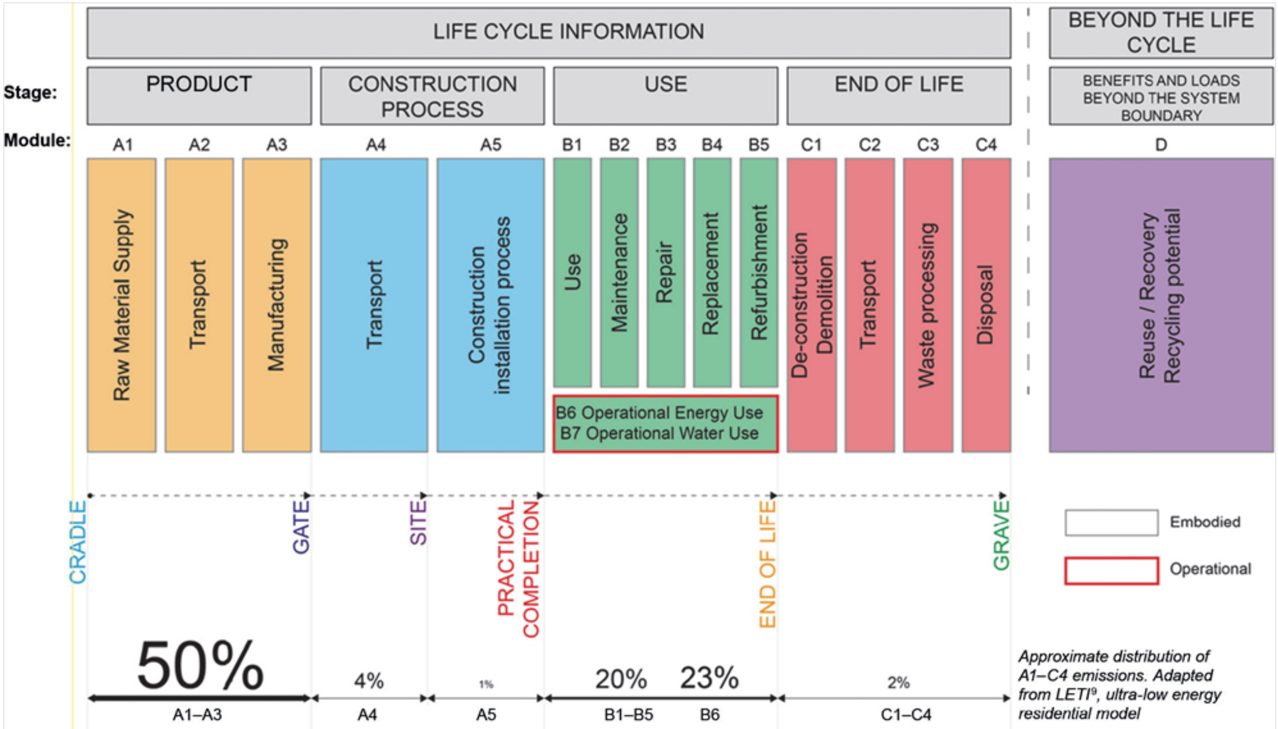


**Figure 3.16** Quantitative overview of embodied carbon per phase (Gibbons and Orr, 2020)

### Slenderness

The slenderness is defined as the ratio between the height and width of a building. In general, structural engineers consider a building as slender if the slenderness ratio is bigger than 1:10. Optimisation of slenderness can be executed either by finding the maximum height of a building with fixed width or the minimum width for a building with fixed height. This value can be found based on the optimised element sizes of beams and wall elements, when a maximum element size is considered. Besides slenderness of the building itself, slenderness can also be related to the thickness of the elements. This also related to the slenderness of the building. A more slender building, will required extra stiffness, which will probably lead to bigger elements.

# Chapter 4

# Parametric model

## 4.1 Overview of modelling

In this chapter, the development of the parametric model will be described. When following the steps described in figure 2.1, it can be concluded that phase 1 has been completed. From literature study, the gaps in knowledge and relevance are mapped. This has been used to define the goal of the research and forms the starting point of the parametric model. Next step is setting up this model. First the input is defined, which is described in section 4.2. Afterwards the Grasshopper model itself can be set up. The model is composed of eight parts which all refer to a part of the report. An overview of the parametric script is given in figure 4.1. The total script can be found in appendix C. First, the variable and fixed input are determined, which are specified in section 4.2 (red). This leads to the geometry of the parametric model (4.3, orange) and the Karamba model (4.3, yellow). The performance criteria which must be met (4.4, light green) are ran through in the user interface in Human UI (4.5, dark green). The optimisation results of all of the three optimisation goals are gathered and saved in an Excel file (5.3, light blue). A visualisation of both the input and results of each step in Human UI is modelled in the dark blue part of the script (4.5). The optimisation procedure itself (5.1, brown) can be seen below the rest of the script as this part runs parallel with the other steps.

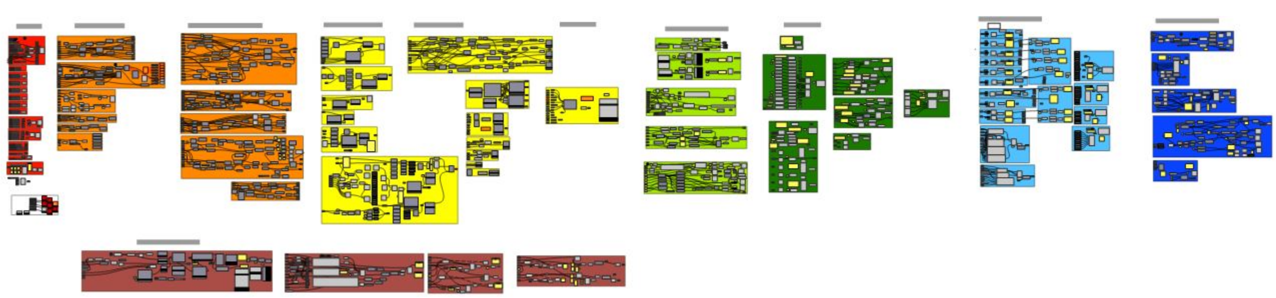

**Figure 4.1** The parts of the script, from left to right: input, geometry, Karamba, performance criteria, Human UI, optimisation results, visualisation and below optimisation procedure

The steps involved in the model are summarised in the scheme in figure 4.2. This scheme includes the workflow of phases 2 and 3 of figure 2.1 in paragraph 2.4. It can also be seen here which part of the scheme belongs to which part of the modelling. This is indicated which the coloured squares. The Number with the Human UI logo show the corresponding step in the Human UI panel, which is explained further in paragraph 4.5.

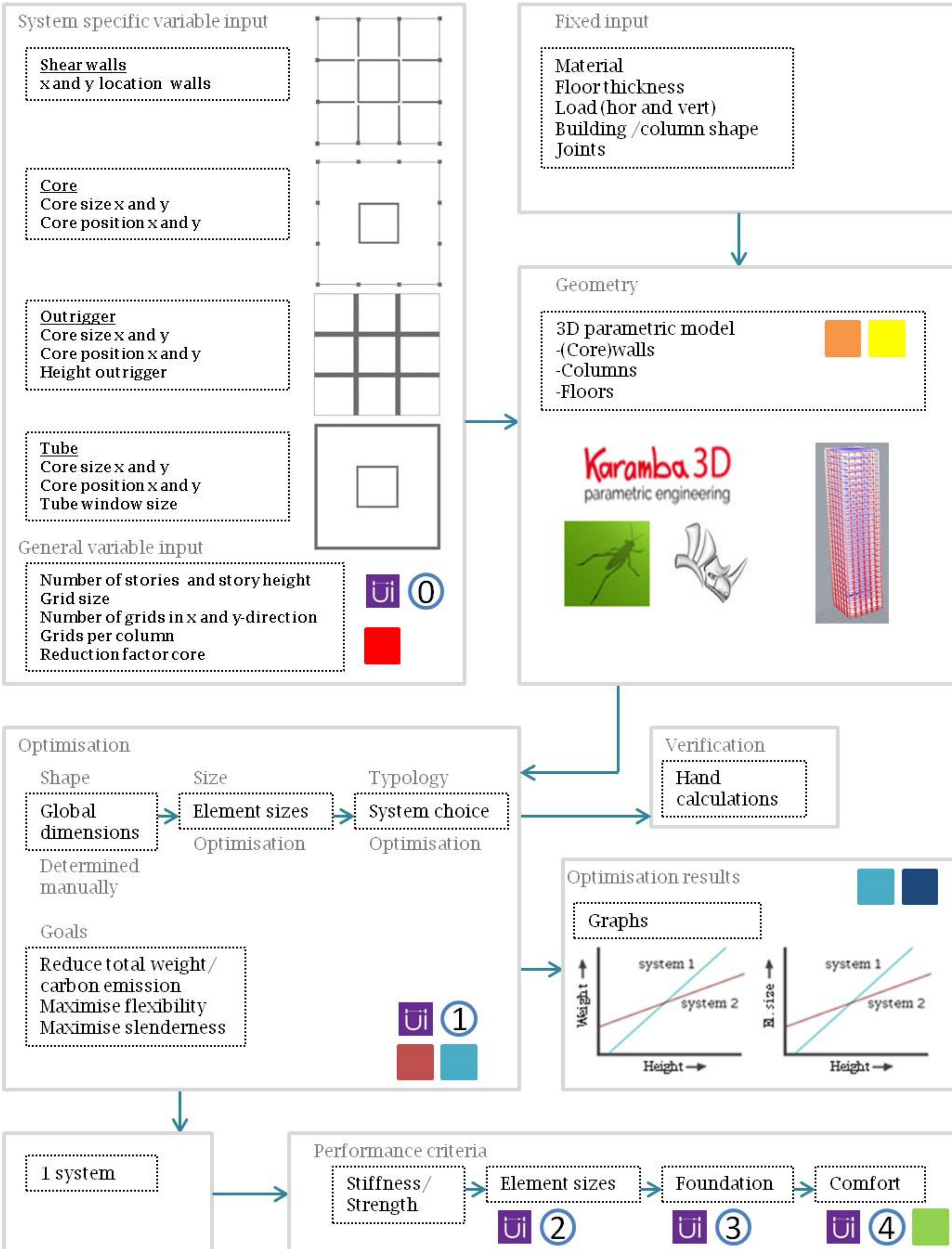


**Figure 4.2** Overview of modelling

## 4.2 Input of the model

### 4.2.1 System specific variable input

The systems shear walls, core, outrigger and tube are considered as explained in chapter 3. The variable input per system is listed below. As can be seen in the figure, shear walls are modelled as unconnected walls spanning from facade to facade, which is equivalent to a core with additional flanges.

| | | | |
|---|---|---|---|
| 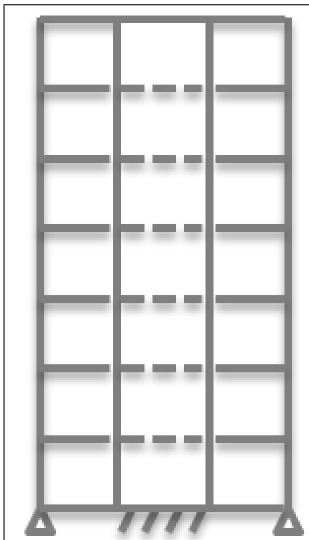 | 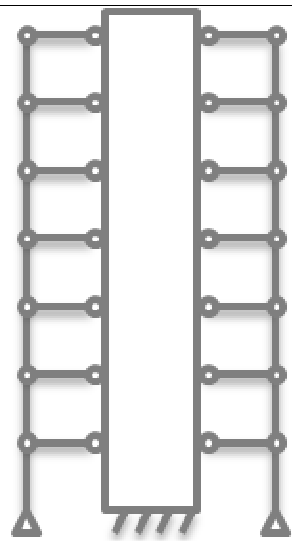 | 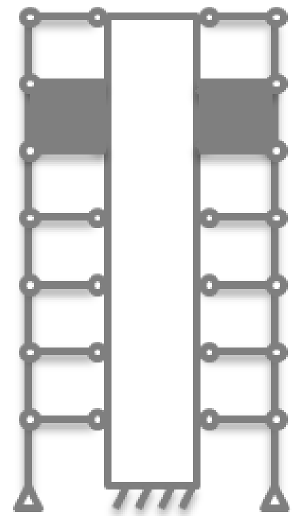 | 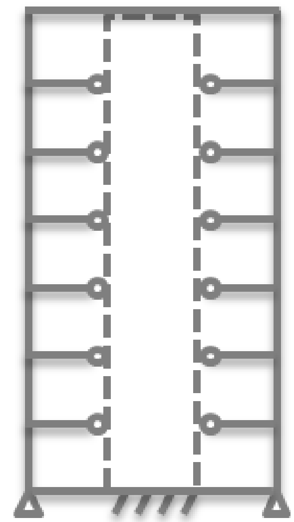 |
| 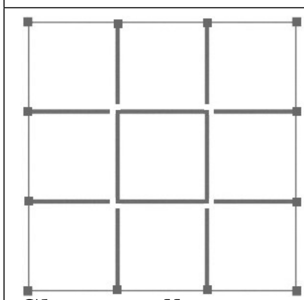<br>**Shear walls** | 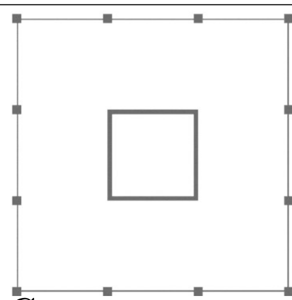<br>**Core** | 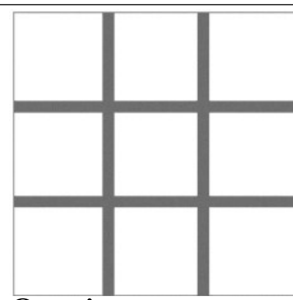<br>**Outrigger** | 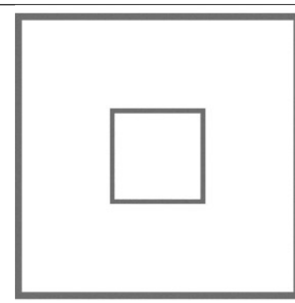<br>**Tube** |
| **Variable input**<br>x and y location of walls | **Variable input**<br>Core size x and y<br>Core position x and y | **Variable input**<br>Core size x and y<br>Core position x and y<br>Height outrigger | **Variable input**<br>Core size x and y<br>Core position x and y<br>Perforation size facade |

**Table 4.1** Variable input per system

### 4.2.2 General variable input

The following parameters can be determined manually, independently of the structural system. This means that these values can be customised depending on the demand of the client.

- Number of stories and story height: The focus will be on rectangular buildings within a height of 100 till 250 $m$. This is a realistic range for high-rise buildings in the Netherlands for now and in the near future. The building height is the multiplication of the story height with the number of stories. A logical story height is 3.6 $m$. This is a summation of the minimum story height of 2.6 $m$ as stated in the Dutch Building Degree, the floor slab (mean value of 0.35 $m$), floor finishing and ducting (0.1 $m$) and space for mechanical systems (0.55 $m$).

- Grid size and number of grids in x and y direction: The building length and width are variable, with only rectangular buildings considered. For the model a grid is defined and both the grid length and number of grids in both directions can be customised manually. Multiplication of these two numbers lead to the floor dimensions. This means that theoretically every length and width is possible. The structural elements are placed on this grid. As a result of this, the distance between the structural elements is always a multiplication of the grid size. The choice was made to constrain the building length and width from 18 till 40 $m$.

- Grids per column: In can be decided to model a column at every grid point in the facade or to do it alternately.

- Reduction factor for core perforations: A reduction factor can be applied, representing a reduced material strength due to perforations in the core.

### 4.2.3 Fixed input

The parameters listed below are determined in advance. This means that reasonable values are chosen to set clear boundaries of the problem.

#### Material

Cast-in-situ concrete will be used. The concrete grade can be chosen manually. As explained in chapter 3, depending on the type of element, cracked or uncracked concrete will be applied. For floors and walls at the position of lintels, cracked concrete will be assumed. As example, for C50/60, the reduced E-modulus is 11000 $N/mm^2$. For walls and columns uncracked concrete is assumed. The most important material properties of C50/60 are given in the table below.

| Grade | $f_{ck}(N/mm^2)$ | $f_{cd}(N/mm^2)$ | E ($N/mm^2$) | $E_{red}(N/mm^2)$ | $f_{ctm}(N/mm^2)$ | $\rho$ ($kg/m^3$) |
|---|---|---|---|---|---|---|
| C50/60 | 50 | 33.3 | 34000 | 11000 | 3.2 | 2400 |

**Table 4.2** Material properties C50/60

#### Load

Horizontal and vertical loads will be considered on the building. Here, normative loads from Eurocode 1 (2002) are used. As earthquakes are not usual in The Netherlands, these kind of loads are neglected. For determination of the horizontal load, the values from table 3.1 are used. For a building located in area II, urban environment, the maximum wind load lies between 1.48 and 2.01 $kN/m^2$ for the predefined height range of 100 till 250 $m$. The load from the bottom till the point where the height is equal to the width of the building has $z = b$ as reference height. The load from the top till $h - b$ uses $z = h$ as height. Between this, the wind load is linearly interpolated as shown in figure 3.10. The vertical load that will be applied is a summation of 1.75 $kN/m^2$ for variable load, 1.45 $kN/m^2$ for non-structural elements and self weight. The loads described above are used as model input with help of load combinations, which are formulated in equations 3.24 and 3.25. Five load combinations are made, with $G$ the own weight, $Q_v$ vertical load and $Q_w$ wind load. The combinations are originating from Consequence Class 3, which is valid for buildings of 100 m and higher. Three equations can be set up for the ultimate limit state:

$$1 : 1.32 * G + 0.5 * 1.65 * Q_v + 1.65 * Q_w \tag{4.1}$$

$$2 : 1.49 * G + 0.5 * 1.65 * Q_v \tag{4.2}$$

$$3 : 0.9 * G + 1.65 * Q_w \tag{4.3}$$

Two equations are assumed to be in the serviceability limit state:

$$4 : G + 0.5 * Q_v + Q_w \tag{4.4}$$

$$5 : G + Q_w \tag{4.5}$$

### Building and column shape

A rectangular shape will be used for the building and for the columns a square shape.

### Floor thickness and system

The cast-in-situ flat slab floor will be considered, with reinforcement both in the top and bottom of the floor. The positioning and the amount of reinforcement will not be specified in the model, but the formulas from section 3.2.2 give a good first indication. The floor thickness is assumed to be constant over the height of the building. A rule of thumb for floors longer than 7 $m$ is $\frac{l}{d} = \frac{245}{l}$. This is a recommended floor thickness, but the thickness can also be inserted by the engineer itself. For example a maximum floor span of 8.8 $m$ leads to an estimated thickness of 0.31 $m$, which can be round to a value of 0.30 m (Lagendijk, 2016).

### Connections

This research is about structural behaviour in early design phases, which means that connections are not worked out in detail. However, the stiffness of the building is influenced by the stiffness of the connections, so this has to be taken into account. Six connections are specified, which are shown in table 4.3 with their position in figure 4.3. Assumptions for the connections are based on the rapport of Hummelen (2015) and the reader Concrete Building Structures (Lagendijk, 2016). Here is stated that for structures with prefabricated concrete, hinged connections are preferred. This because they are simple and can easily be made. Although concrete cast in-situ is applied and it is relatively easy to realise clamped connections here compared with prefabricated concrete, it has been decided to use hinged connections where possible.

| | Connection | Assumption | Model |
|---|---|---|---|
| 1 | Column - Floor | Hinged | Shear wall Core Outrigger |
| 2 | (Core) wall - Floor | Hinged | Shear wall Core Outrigger Tube |
| 3 | (Core) wall - wall | Clamped | Shear wall Core Outrigger Tube |
| 4 | Outrigger - Column | Hinged | Outrigger |
| 5 | Outrigger - Core | Clamped | Outrigger |
| 6 | Tube wall - Floor | Hinged | Tube |

**Table 4.3** Overview of connections in the model

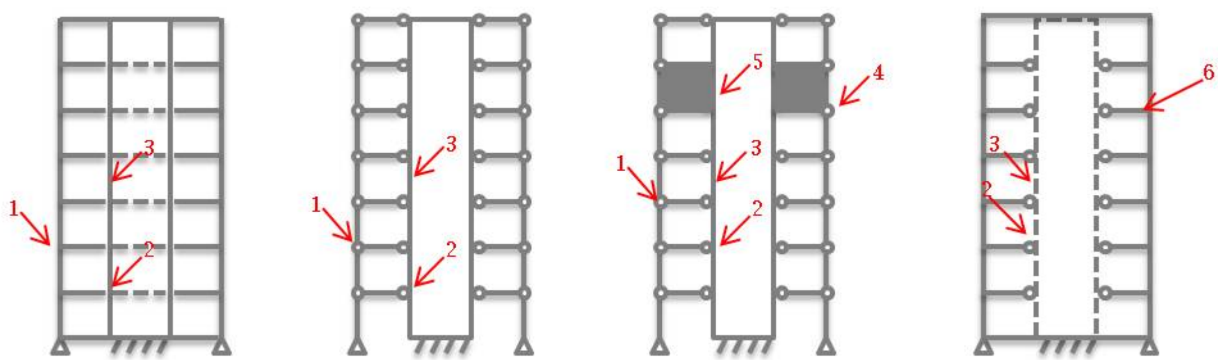


**Figure 4.3** The location of the connections for the systems shear walls, core, outrigger and tube, as described in table 4.3

## 4.3 Setting up geometry

After defining the input, the geometry is defined. The geometry is converted into Karamba elements. These two steps are both described in this section.

### 4.3.1 Basis geometry

The four systems are implemented in one model. Switching between the systems can be easily done with a slider. The value 1 of the slider corresponds to the shear wall model, 2 to the core, 3 to the outrigger and 4 to the tube. 0 corresponds to a free figuration of shear walls, which is not included in the research. This way of modelling is more efficient than modelling the four systems separately, because it can be realised with less components which results in a faster script. To get an efficient material use over the height of the building, it is common use to let the dimensions of the structural elements variate over the building height (Smith and Coull, 1991). To do this, height zones are set up as shown in figure 4.4. For a building between 100 and 150 $m$, three height zones are made. For the range 150 to 200 $m$, there are four zones and five zones for 200 to 250 $m$. The building is automatically divided into zones with about an equal number of floors. An alternative of this could be to take the dimension of elements as constant, but to variate the concrete grade over the building height. An example of these zones is given with a building of 40 floors. Assuming a floor height of 3.6 $m$, this building has an height of 144 $m$, which means three height zones. Two height zones of thirteen floors and one zone of fourteen floors. All these zones can have a different optimised element thickness.

The positioning of structural elements is directly visible in Rhinoceros. This can be seen in figure 4.4 (right). The floor plan of the ground floor is copied, to directly show how the floor is built up. The black lines here represent the grid lines of the building. The structural behaviour of the building is strongly influenced by perforations, as a results of possible door or window openings. That is why the model gives the possibility to reduce the core strength. The influence of the size and position of the perforations on the strength reduction is not specified in this report. This is appointed in the recommendations as potential further research.

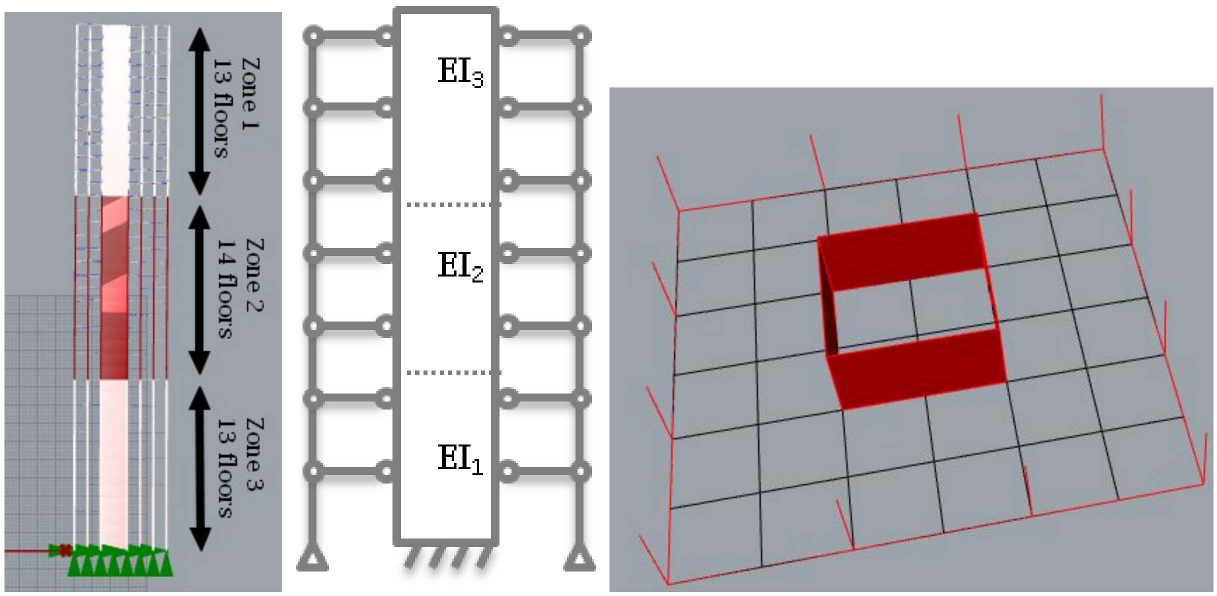


**Figure 4.4** Three height zones (left), the schematising (middle) and visualisation of a core model in Rhinoceros (right)

### 4.3.2 The four systems

Below is explained how the four models are built up. The elements and some information about the geometry of the systems are mentioned. The wall, core and floor elements of the building are converted into shell elements in Karamba and columns are converted into beam elements. Also a scheme and image of the systems is given. A switch between the systems can be made with the 'stream filter component' of Grasshopper in combination with a slider as shown in 4.5. The input of each system is linked to a different filter, which makes switching between the systems quite easy. For the shear wall system, different wall configurations are possible. For the comparison between the systems, one shear wall configuration is chosen, which is named 'fixed shear walls' in the model.

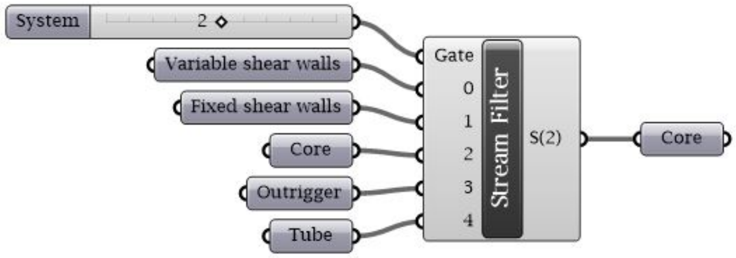


**Figure 4.5** The stream filter component in Grasshopper

### Variable shear walls

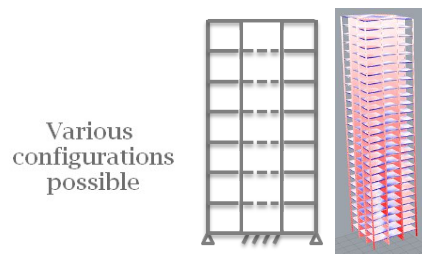


- Elements: Shear walls, columns, floors
- Information: The model can be used to design one, two or three shear walls in both x and y direction, depending on the structure. These walls can be placed at every location on the grid, while the length is variable as well. The walls are supplemented by columns in the facade. This system is not elaborated during the rest of the research.

### Fixed shear walls

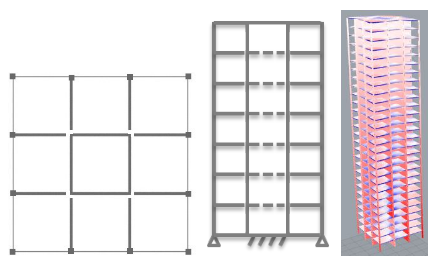

- Elements: Shear walls, columns, floors
- Information: One shear wall configuration is chosen for the comparison with the other systems, which will be executed in chapter 5. For this configuration, two shear walls are modelled, both in x and y direction. They are modelled as a core with additional flanges, with reach to the facade.

### Core

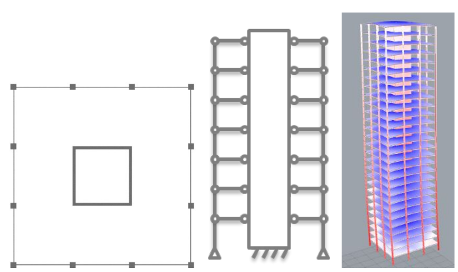

- Elements: Core walls, columns, floors
- Information: The basis of the model is the core, supplemented by facade columns. The position of the core can be varied throughout the grid and the core size is always a multiplication of the grid size.

**Outrigger**

- Elements: Core walls, columns, floors, outrigger walls (outrigger and belt truss)
- Information: The core model is used as starting point for the outrigger model. The outrigger is placed in combination with a belt truss in the facade. In coherence with the rest of the building, the outrigger exists of concrete wall elements. The height can be adapted manually, but figure 3.8 can be used as guideline for this. An advice for this height based on this figure is between 0.65 and 0.7 times the building height. It is only possible to model one outrigger. As well as for the shear wall and core model, additional columns are placed in the facade.

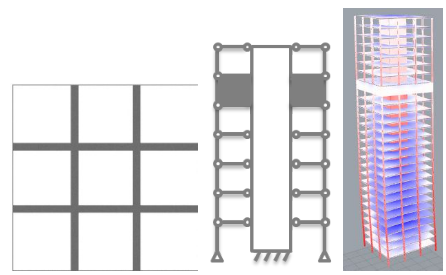

**Tube**

- Elements: Core walls, floors, tube beams, tube columns
- Information: The tube model is based on the core. The tube itself is modelled as concrete beams in horizontal and vertical direction at the perimeter of the building. The choice was made to model them as line elements because the accessory mesh can be modelled faster than when modelled with shell elements.

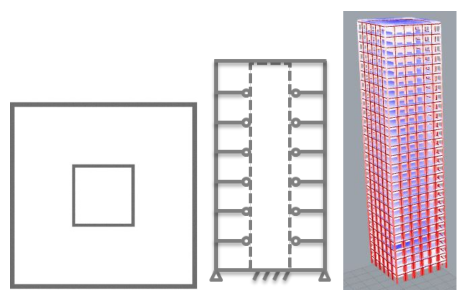

### 4.3.3 Karamba

The Karamba model exists of the following input, with the paragraph where the input was specified between brackets:

- Joints (4.2.3)
- Material (3.2.1, 4.2.3)
- Supports (3.2.5)
- Structural elements( 4.2.2)
  - Columns
  - (Outrigger) walls
  - Floors
  - Tube elements (beams and columns)
- Loads (3.2.4, 4.2.3)
  - Gravity load
  - Vertical load
  - Wind load (three wind zones)

These inputs are assembled in one component to analyse the structure and to view the model. The model is directly used to find the maximum horizontal deflection and the utilisation of the beam and shell elements for the chosen load case.

### Mesh size

Karamba is finite element software. This means that the elements in the model are converted into mesh. In finite element analysis, the accuracy of the results and the computation time depend on the mesh density (Liu, 2013). Models with a fine mesh need more computation time, but also lead to more accurate results. An adequate mesh size has to be chosen based on the required accuracy of the model. The main issue when executing a finite element analysis, is to find the optimum between computation time and model accuracy.

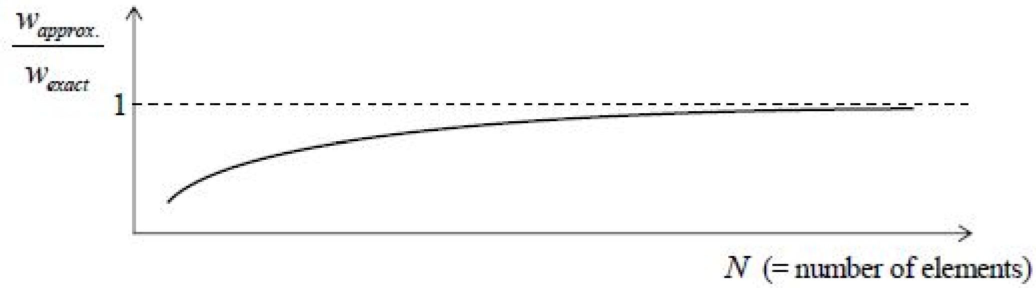


**Figure 4.6** The accuracy increases when the mesh refines (Blauwendraad, 2006)

The theory explained above applies to shell elements in Karamba, which are used to model walls and floors. To check the influence of the mesh size on the computation time and accuracy, a number of mesh configurations will be tested. From the reader of Blauwendraad (2006), it follows that an element size of $2 * t$ is a good first approximation. $t$ is the plate thickness, so in this situation the thickness of the floors and walls. In this small research is chosen to test a mesh size of 2, 1, 1/2, 1/4 and 1/8 times the grid size. This is tested on the model which is also used for the initial verification (Appendix B). This means that a grid size of 3.6 $m$, floor thickness of 0.35 m and a wall and column thickness of 0.3 $m$ are applied. During the test, it needs to be taken into account that high peak stresses can occur around singularities. This can happen at the position of supports. This can be prevented by increasing the number of supports, which leads to a more equal stress distribution. The table below gives the results of the research. The computation time in the last column shows the time needed for one complete calculation of the model. The values in the columns indicated with $\Delta$ show the difference between the current and previous calculation results and give an indication for the degree of convergence.

| Mesh size | ut. slab[%] | $\Delta_{us}$[%] | ut. beam [%] | $\Delta_{ub}$[%] | defl. [$mm$] | $\Delta_d$[%] | time [$s$] |
|---|---|---|---|---|---|---|---|
| 2x grid size | 46.5 | / | 69.9 | / | 437 | / | 2.0 |
| grid size | 60 | 29 | 90.4 | 23 | 553 | 21 | 2.5 |
| **1/2x grid size** | 68.8 | 14 | 98.2 | 8 | 588 | 6 | 3.2 |
| 1/4x grid size | 76.3 | 11 | 100.3 | 2.1 | 600 | 2 | 11 |
| 1/8x grid size | 84.6 | 11 | 100.7 | 0.4 | 603 | 0.5 | 43 |

**Table 4.4** Influence of the mesh size on the model accuracy and calculation speed

From table 4.4, the mesh size is chosen with the most optimal ratio between speed and accuracy. The two finest meshes (1/8 and 1/4 times the grid size) lead to a relative high computation time. This is not desirable for a quick calculation tool. The mesh size of 1/2 times the grid size is relatively fast and the difference in accuracy between this one and the two finest meshes is not significant. This means that this mesh density is suitable to use in the model. However, during optimisation of the model, it has to be kept in mind that stresses in slabs can be up to 15% higher than the model indicates. For deflection and stresses in columns, the difference in results are only 2.5%, which means that they are accurate enough to use directly. With a grid size of 3.6 $m$ and a floor thickness of 0.35 $m$, a mesh size of 1/2 times the grid size leads to a mesh size of 1.8 $m$. This is around five times the floor thickness. This is higher than the advised element size of two times the floor thickness. However, the mesh is fine enough for the scope of this thesis. The mesh size applied to the Karamba model can be seen in figure 4.7.

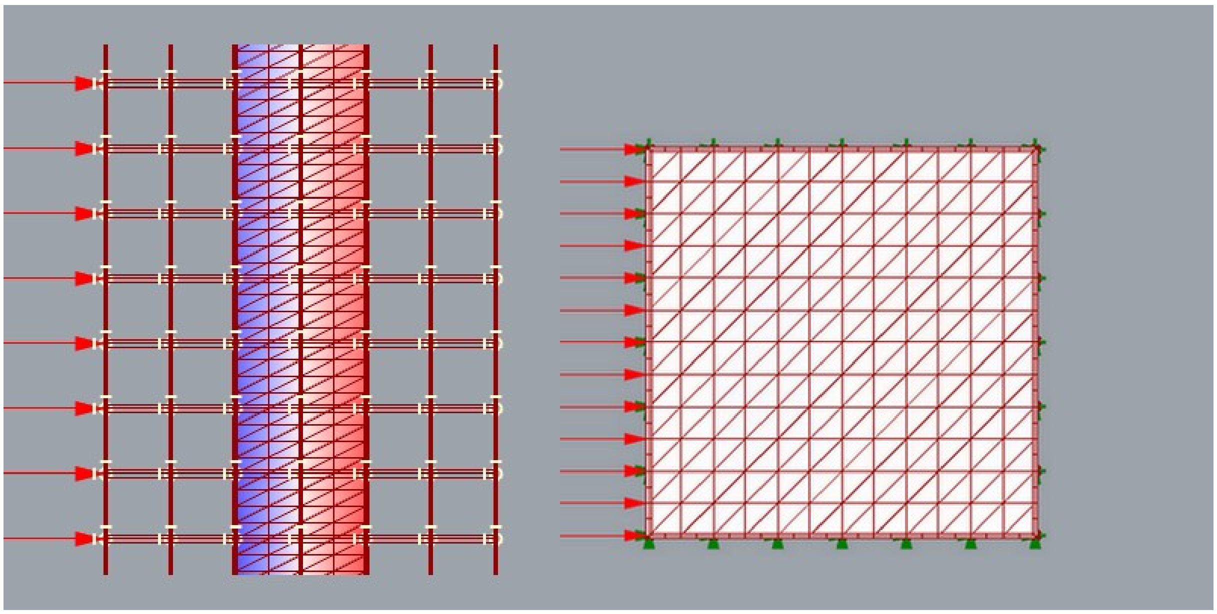

**Figure 4.7** Side and top view of the mesh size in Karamba of a building of 21.6 x 21.6 $m$

## 4.4 Performance criteria

Performance criteria give an indication of how well a building functions, in relation to predefined criteria. The most important criteria for a building are related to the construction, building physics, sustainability, comfort and cost. For this scope, the focus will be on construction related issues. These are stiffness, strength, comfort and foundation.

### Stiffness

The first criterion is the horizontal deflection at the top of the building as described in section 3.2.5 and equation 3.26. This is only the deflection due to the stiffness of the building itself, so only due to the factor $\frac{ql^4}{8EI}$. $q$ is here the load from Eurocode 1 (2002), $l$ the height and $EI$ the bending stiffness of the structural elements. This value can be obtained from the Karamba analysis. The deflection has to be smaller than 1/750 multiplied by the height of the building (Ham and Terwel, 2017). The model is used to obtain rough dimensions in early design stages, that is why a deflection of 0.8 times the maximum deflection will be assumed as optimal. The influence of the second order effect (3.2.6) is automatically taken into account in the model within the analyse component in Karamba.

### Strength

A criterion that is checked simultaneously with stiffness is strength. The maximum utilisation of both the beam and shell elements can be obtained from Karamba. For concrete in compression, an utilisation value of less than 100% is required, but also for the strength a value of 80% will be the target. (Core) walls and columns are expected to be always in compression. This assumption can directly be checked in the model. Dimensions of a construction can be based both on stiffness and strength. In general can be stated that when the height of a structure increases, stiffness will become normative for design of the dimensions (Rolvink, 2010). The criterion which is assumed to be critical at a certain slenderness, is given in figure 5.7 of chapter 5.

### Foundation

The rotational stiffness of the foundation will be considered with a factor $C$ in $kNm/rad$. To assume a reasonable pile configuration and number of piles, which lead to an adequate stiffness, two steps have been followed. First a required pile diameter is determined and afterwards the calculation of the deflection due to the foundation is calculated. A first assumption of the required pile diameter is based on three input parameters. These are building mass, pile configuration and pile length. For the pile configuration, three different options are distinguished as can be seen in figure 4.8: Tube-in-tube, uniform and concentrated around the core. In the model, the piles are located at the grid points, with one or four piles per point. The building mass and pile configuration lead to a required pile resistance, which is divided into a shaft and base resistance. The calculation procedure which was presented in equation 3.27 of section 3.2.5 is followed here. The pile length can be chosen based on local soil conditions. This finally leads to a minimum pile diameter, when squared piles are applied. This procedure is schematised in the upper part of figure 4.9.

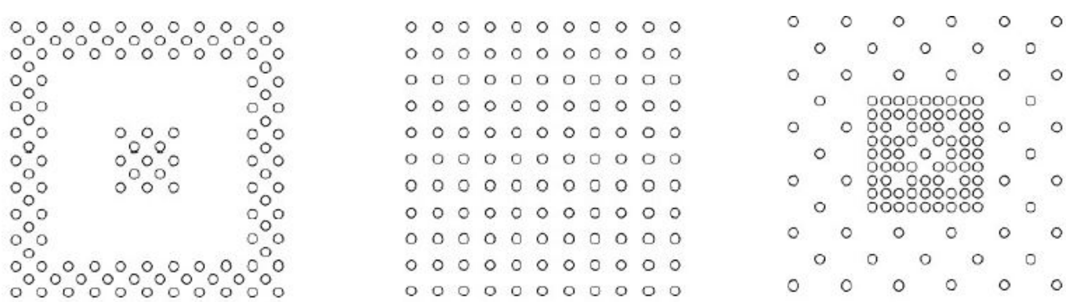

**Figure 4.8** Three pile configurations, tube-in-tube, uniform and concentrated at the core (Bronkhorst, 2018)

The second part of the calculation, the lower part of figure 4.9, is used to calculate the deflection due to the foundation. When this is known, the ratio between the deflection caused by the foundation and the total foundation can be calculated as well. The formulas applied here can be found in equation 3.28. When the influence of the foundation is more than 33% of the total building, either the number of piles, pile length or pile diameter has to be adapted. This can be repeated until the influence of the foundation is below 33%, which makes the total deflection of building and foundation $1/500{*}h$. A limitation to the input is that the soil conditions cannot changed manually. Soil conditions of a clay ground are assumed in the model. Which can be applied for example on Rotterdam. This will be mentioned in the conclusion as potential extension.

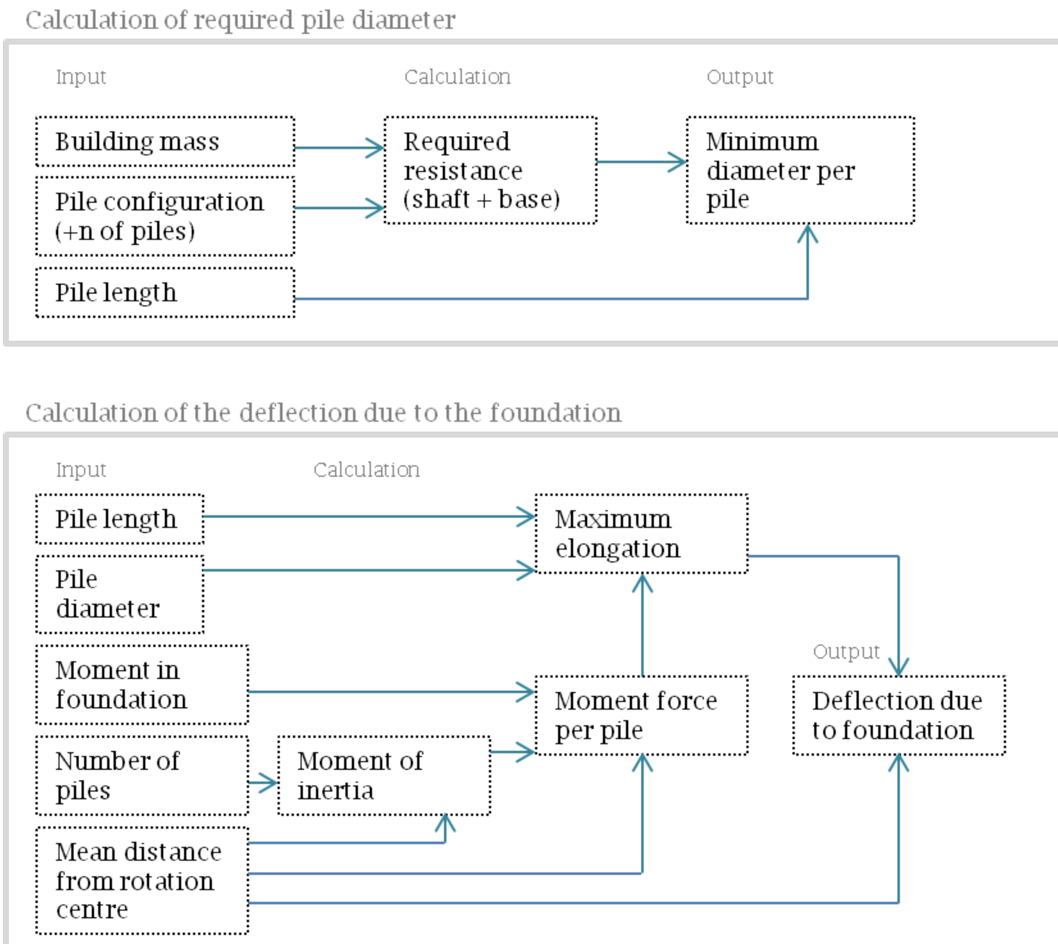


**Figure 4.9** The calculation procedures of the pile resistance and deflection of the foundation

### Comfort

In the area of comfort, there are some limitations regarding the maximum allowed accelerations in a building. These are described in section 3.2.7. The calculation procedure corresponding to the formulas presented here is shown in figure 4.11. To check the comfort requirement, figure 3.12 is rebuilt in Grasshopper, as can be seen in figure 4.10. Both acceleration and frequency are obtained from the input of the Grasshopper model. These values are compared with the maximum values, both for offices and residential buildings. The criterion has to be checked in two directions, this means that the most unfavourable direction can be seen in the graph. When the combination of acceleration and frequency of the building is not within the limits, this is communicated to the user. Subsequently, building sizes or element sizes can be adapted. The upper red line in figure 4.10 represents the critical acceleration for offices and the lower red line for residential housing.

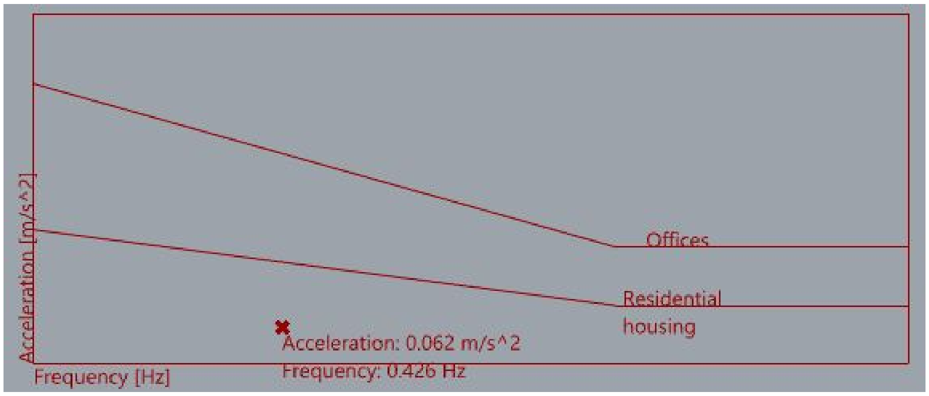


**Figure 4.10** Comfort visualised in Grasshopper

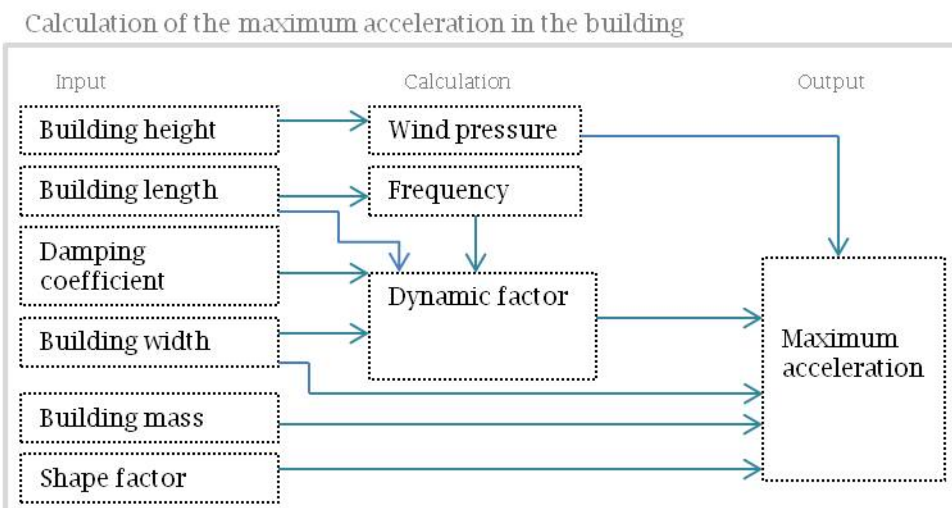


**Figure 4.11** Calculation procedure to calculated maximum accelerations

## 4.5 Human UI

The model in Grasshopper is used to make a tool in Human UI (3.3.2). With Human UI, a panel can be made to manually change the input of the model. The advantage of Human UI is that it can be used separately from the Grasshopper script. The advantage of this is that no extensive prior knowledge of Grasshopper is needed when the tool is used. This makes the tool easily accessible. The tool is divided into five steps. In step 0, the global dimensions of the building can be inserted. In step 1, the structure is optimised for one of the three optimisation goals. The requirements for stiffness and strength of the optimised structure are checked in step 2. Finally, in step 3 and 4, the foundation and comfort are verified. The steps form an iterative process. This means that if a requirement is not met during a step, the input parameters in step 0 can be changed. The tool and all steps are explained further in chapter 6.

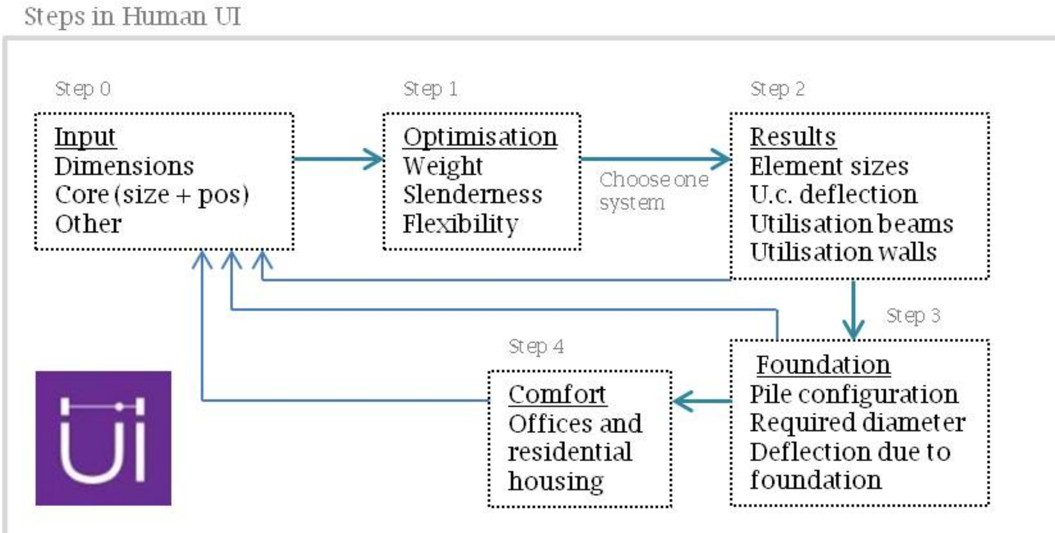


**Figure 4.12** Steps in Human UI

# Chapter 5

# Parametric studies

This chapter gives an overview of the output of the model. First the optimisation procedure is explained. In the first place the optimisation approach and later the optimisation of the element size and system choice. A verification of the results is executed by comparing the model results by an expectation. Optimisation of system choice results in a comparison for flexibility, total weight or embodied carbon and slenderness. Finally, the appropriateness of the four systems over the height is visualised in a number of graphs. For the results presented in this chapter, the following input is taken, unless otherwise specified:

- Grid size: 3.6 $m$
- Concrete: C50/60
- Load: Load case 1 as defined in section 4.2.3
- Floor thickness: 30 $cm$
- Floor height: 3.6 $m$
- Grids per column: one column on each grid point in the facade
- Reduction factor for core perforations: 0.8
- Building size: 36 x 36 $m$ (10x10 grids)
- Core size: 14.4 x 14.4 $m$ (4x4 grids, centrally positioned)
- Outrigger: Located at 65 % of the building height
- Tube: A perforation of 2 x 2 $m$ at every grid along the facade

## 5.1 Optimisation

### 5.1.1 Optimisation approach

Three ways of optimisation can be distinguished, as described in chapter 3.4. These are shape, size and topology optimisation. The optimal structure can be obtained following the approach of figure 5.1. First the outer dimensions of the building are determined manually. These are height, length and width. Also size and positioning of the core can be determined. The next step is to find the optimal size of the structural elements. Finally the most logical system is found for these dimensions, based on one of the optimisation criteria.

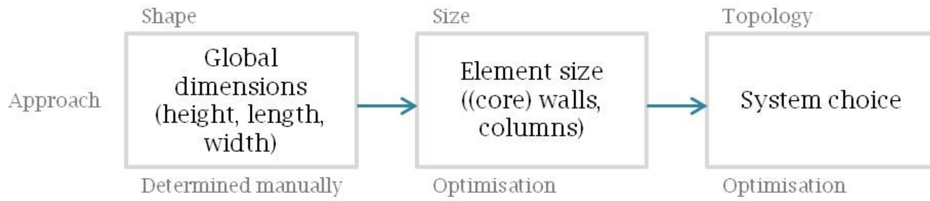


**Figure 5.1** Approach of the optimisation process

### 5.1.2 Optimisation element size

The element size optimisation as described in figure 5.1 is executed with the optimize cross section component in Karamba. With this component, the structure can be optimised both for strength and stiffness. A strategy for the optimisation is to optimise every single element in the construction. This means that all wall and column elements can have their own optimised cross section. Based on these cross sections, for each height zone one cross section can be determined as described in section 4.3. This method however, is not the most logical way of cross section optimisation. Optimisation of all single elements is quite a time consuming process, while there is no need to optimise them all separately. Besides this, it turned out that the optimisation results became inaccurate when the number of elements in the model increased and that the optimisation could only be executed based on the total deflection instead of the horizontal deflection.

To deal with the problems as stated above, a different optimisation strategy is used, in which a one dimensional model is used. The structure is simplified to a vertical cantilevering beam consisting of one element (step 1, figure 5.2 ). The beam is loaded with the same wind load and a square cross section is applied with the same concrete strength as the normal model. Subsequently, the cross section optimiser of Karamba is used to find for this element the optimal cross section (step 2). This cross section is used to calculate the required moment of inertia in the building (step 3).

Besides this, for each of the four systems, the moment of inertia is calculated manually (step 4 and 5). This equation is presented as a function of the column thickness and wall thickness. To ensure enough stiffness in the normal model, the equation of the moment of inertia of the small and the normal model can be equated to each other. The column and wall thickness are unknown here. When assuming a ratio between the column thickness and wall thickness, these two unknowns can be found. From engineering practice, a column thickness of 1.5 times the wall thickness has been applied. Now the required column and wall thickness can be obtained (step 6). These element sizes can be used as input in the normal model.

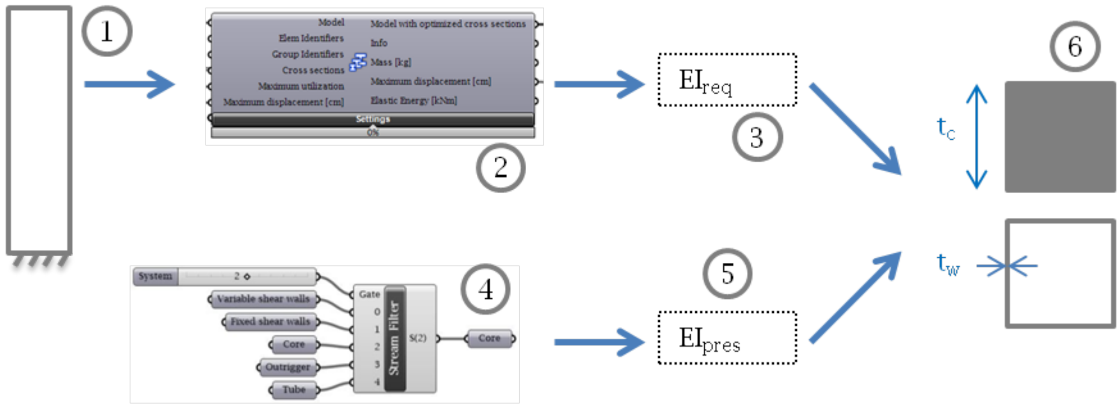


**Figure 5.2** First steps of the cross section optimisation

The element sizes obtained with this method give a good first approximation of the element sizes in the normal model (step 7, 5.3). The simplification of the model and the lack of vertical load however, lead to a certain inaccuracy for the required element size. This is solved by putting the obtained values in a loop and executing an iteration. Iterating is not possible within the default Grasshopper toolbox, because of the occurrence of a recursive data stream. A recursive data stream means that output data is used as input in the same model. This leads to an infinite data flow and no output data. To solve this, the iterating component Anemone is used (Zwierzycki, 2015). Within Anemone, it is possible to select one or more values as input, apply a calculation procedure and use the output values again as input for the model. The calculation procedure in Anemone exists of three checks:

1. Deflection (step 8): The input of this step is the first approximation of the element sizes from the simplified model. This is compared with the maximum allowed deflection. The ratio between the two is used as multiplication factor for the elements, which leads to new element sizes.

2. Stress (step 8): The optimised elements for deflection are used here as input. These values are compared with the maximum allowed stresses. If the stresses are below the predefined value, nothing is done. If the stresses are too high, a multiplication factor has to be applied as well. This factor is the ratio between the current utilisation and the maximum one. This leads to element sizes which fulfill the criteria of both deflection and strength.

3. Minimum element sizes (step 9): From engineering practice, a minimum wall and column thickness can be appointed for buildings of 100 $m$ and higher. If one of the calculated thicknesses are lower, the minimum value is applied.

Now a cross section for walls as well as for columns is applied that fulfills the requirements for stiffness, strength and minimum element size. However, the building is divided into height zones (section 4.3). This means that every zone gets a different element size, to get a more optimal division of mass over the height (step 10). To realise this, for each zone another multiplication factor is applied for the cross sections. The factors used are gained from engineering practice are can be seen in 5.1. Finally the values are rounded to a plurality of 50 $mm$.

| | 3 zones (100-150 $m$) | 4 zones (150-200 $m$) | 5 zones (200-250 $m$) |
|---|---|---|---|
| Zone 1 | 0.85 | 0.8 | 0.7 |
| Zone 2 | 1 | 0.93 | 0.85 |
| Zone 3 | 1.15 | 1.07 | 1 |
| Zone 4 | / | 1.2 | 1.15 |
| Zone 5 | / | / | 1.3 |

**Table 5.1** Multiplication factors per zone

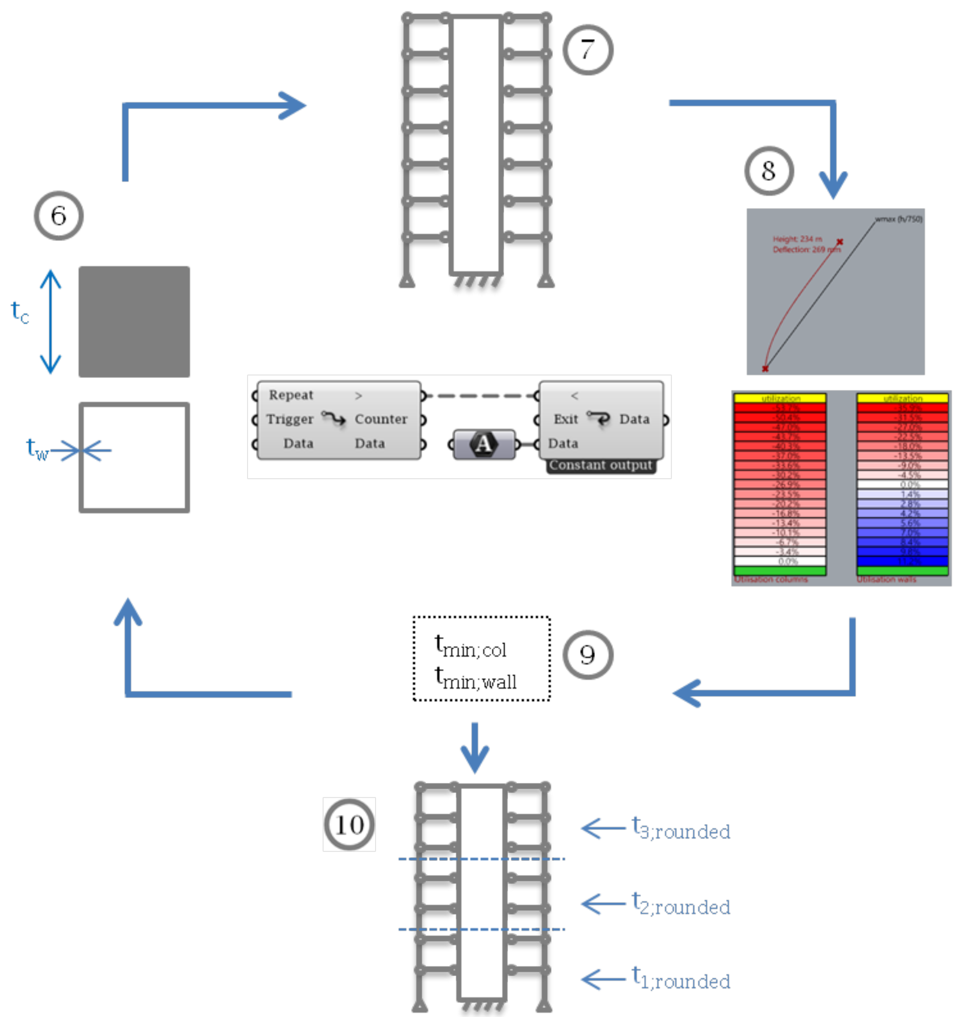


**Figure 5.3** Steps of the optimisation procedure within Anemone (Zwierzycki, 2015)

The iterated values of the optimisation procedure (step 6 to 10) can now be used to compare the four stability systems, the topology optimisation. This is further explained in the next section.

### 5.1.3 Optimisation system choice

Optimisation of system choice is optimisation based on typology. Goal of this optimisation is to find the most suitable system based on input parameters and optimisation goal. Input parameters are defined in section 4.2 and the optimisation goals are explained in section 3.4 and below. The desired output of this part of the optimisation is a quantification of the suitability of each system. This can be used to appoint the most optimal system depending on the input and optimisation goal. By separately optimising the four systems, the suitability of each of them can be found. The four values linked to the optimisation are hereafter stored on a listed, to compare them easily. This is done with the value listener component in Grasshopper. For every optimisation goal, an example of the optimisation results is given as well. This is done for a building with the parameters as defined at the beginning of the chapter and a height of 144 $m$ (40 floors of 3.6 $m$).

#### Total weight and embodied carbon

Goal of the optimisation for total weight is to find the stability system which leads to the lightest structure, given the global dimensions of the building. In this building phase, reinforcement is not taken into account, which means that the weight of the building and the amount of concrete are directly related to each other. Because of this direct relationship, also the embodied carbon of the concrete can be determined, as explained earlier in section 3.4.

Slenderness    Weight/ carbon emission    Flexibility

Total weight, embodied carbon and difference with most optimal one

| | | | |
|---|---|---|---|
| 1: Shear walls - | 529000 kN | 396750 €ev | 3 % |
| 2: Core - | 528100 kN | 396075 €ev | 3 % |
| 3: Outrigger - | 511900 kN | 383925 €ev | 0 % |
| 4: Tube - | 590300 kN | 442725 €ev | 15 % |

**Figure 5.4** Example of optimisation results for total weight and embodied carbon

#### Slenderness

Slenderness is the ratio between the width of a building and the height, where the width is smaller than the length. The appropriateness of a system based on slenderness is defined as the maximum height that can be built within the limits of maximum deflection. A structure with a fixed x dimension, y dimension and height is used here as input. After this, for each system the maximum element size is found. These sizes can be compared with a maximum element size. This maximum element size can be for example 100 cm for column elements and 60 cm for wall elements.

Weight/ carbon emission    Slenderness    Flexibility

Maximum required column/tube wall thickness

| | | |
|---|---|---|
| 1: Shear walls - | columns:55 cm | walls: 30 cm |
| 2: Core - | columns:70 cm | walls: 45 cm |
| 3: Outrigger - | columns:60 cm | walls: 35 cm |
| 4: Tube - | facade walls:35 cm | core walls:30 cm |

**Figure 5.5** Example of optimisation results for element slenderness

### Flexibility

An expression for the flexibility in a building was earlier defined with equation 3.34. This formula is related to construction, structural system, vertical transportation and adaptability. This thesis only focuses on construction and structural system. That is why two simplified formulas are used to calculate the flexibility based on the model. The first one gives the useful floor area and the second one the ratio facade openings. In other words, the formulas give the relation between the available space in the floor and facade versus the total space. For both formulas, the total calculation is given for a core system.

$$\%_{useful;area;floor} = \frac{A_{free;floor}}{A_{total;floor}} = \frac{l_x * l_y - 2 * t_w(l_{cx} + l_{cy}) - t_c^2 * n}{l_x * l_y} \tag{5.1}$$

$$\%_{ratio;facade;openings} = \frac{A_{free;facade}}{A_{total;facade}} = \frac{h(l_x - n * t_c)}{h * l_x} \tag{5.2}$$

In the first formula, $l_x * l_y$ is the total area of one floor. $2 * t_w(l_{cx} + l_{cy})$ is the area of the core walls. $t_c^2 * n$ is the total area of all columns. In the second formula, $h$ is the building height and $l_x - n * t_c$ is the free width in the facade. $h * l_x$ is the total area of the facade.

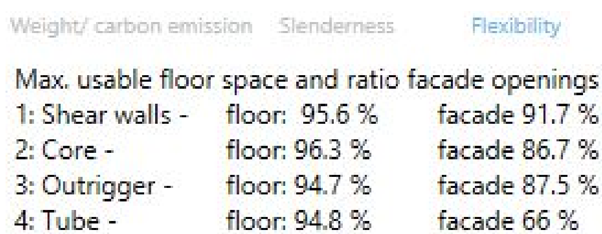


**Figure 5.6** Example of optimisation results for flexibility

## 5.2 Verification

To check the reliability of the model, the results have to be verified. To do this, first some expectations are made based on theory. After this, the global deflection is checked with a hand calculation. Also some other comparisons are made between expectation and reality.

### Expectations

To make an expectation of the behaviour of a high-rise structure, two questions are tried to answer in beforehand: Which failure mechanism is normative at which height and until which height can a system effectively be used? To answer the first question, figure 5.7 can be consulted. This figure shows the dominating failure mechanism versus the slenderness. This is the slenderness of the most dominant stabilising element. For buildings with a slenderness lower than 1:8, strength is assumed to be dominating. For buildings with a slenderness between 1:8 and 1:20, deformation is expected to be normative. Vibrations are dominating for 1:20 and more slender. The second question, regarding the effective height per system, can be answered based on the theory of paragraph 3.1 and accessory images 3.1 till 3.4. Here a first prediction was given about the maximum number of stories that can be applied in the system to be efficient. For shear walls this is 60, for a core 40, for an outrigger 140 and for a tube 80 floors. However, the maximum reachable height for an outrigger depends strongly on the number of outriggers. For a building with only one outrigger, the maximum number of storeys will be around 70, in line with figure 3.1. Besides the utilisation of the walls, columns or deflection, is it also possible that minimum element size is normative. For column elements, this is 350 $mm$ and for wall elements 250 $mm$.

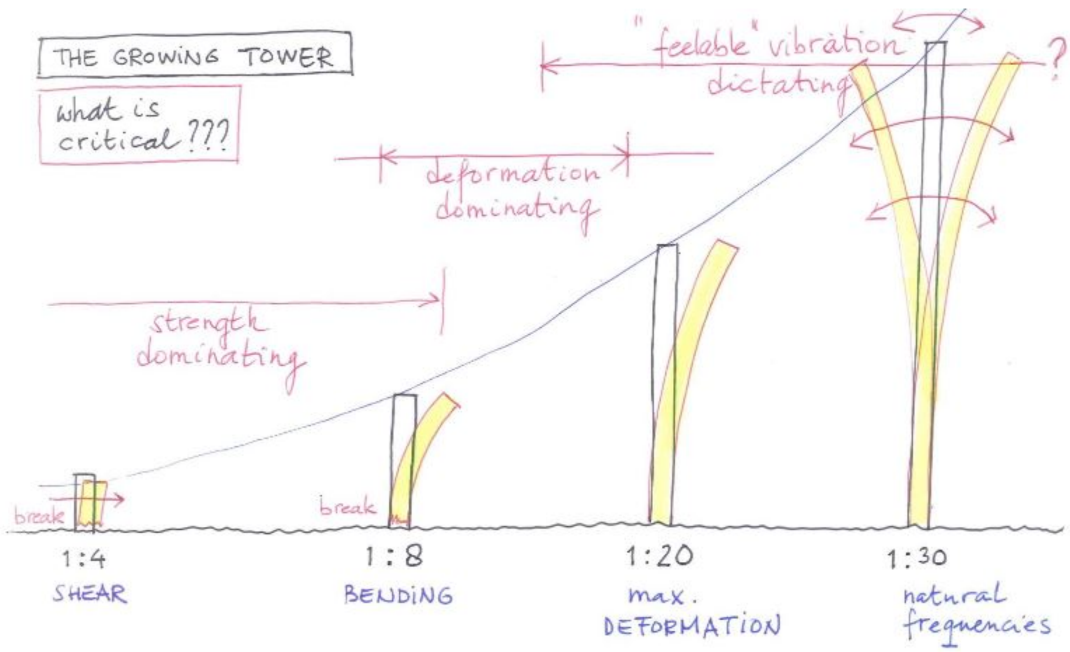


**Figure 5.7** Dominating failure mechanism per slenderness (Nijsse, 2012)

**Reading guide verification pages**

The overviews on the next pages show for each system a building with input as defined at the beginning of chapter 5. Only height is varied. For consecutively the systems shear walls, core, outrigger and tube, a height is taken of 198, 126, 162 and 234 $m$. This corresponds to 55, 35, 45 and 65 floors of 3.6 $m$. For each system, the unity checks are plotted over the building height for the utilisation of walls, columns and deflection. A comparison of deflection according to differential equation and the model is given as well. Also one other calculation is presented. The dot in the graphs indicates the point from where element sizes have to increase to keep the unity check below one. This dot is also visible in the graphs with maximum element sizes (section 5.3.1). In the graphs, three different zones can be differentiated, zone A, B and C. In zone A, the minimum element size is normative. This is the minimum element size for high-rise, to prevent local failure mechanisms as defined in the previous paragraph. In zone B, the material strength is normative. This means that the element sizes are based on the compression strength of the walls and columns. In zone C, the deflection is normative, the element size here is based on the deflection at the top of the building. This to keep this value below the maximum allowable one.

| | |
|---|---|
| • | Height where element sizes have to increase |
| A | Minimum element size normative |
| B | Material strength normative |
| C | Deflection normative |

**Table 5.2** Legend for the unity check graphs

### Shear walls (55 floors, 198 m)

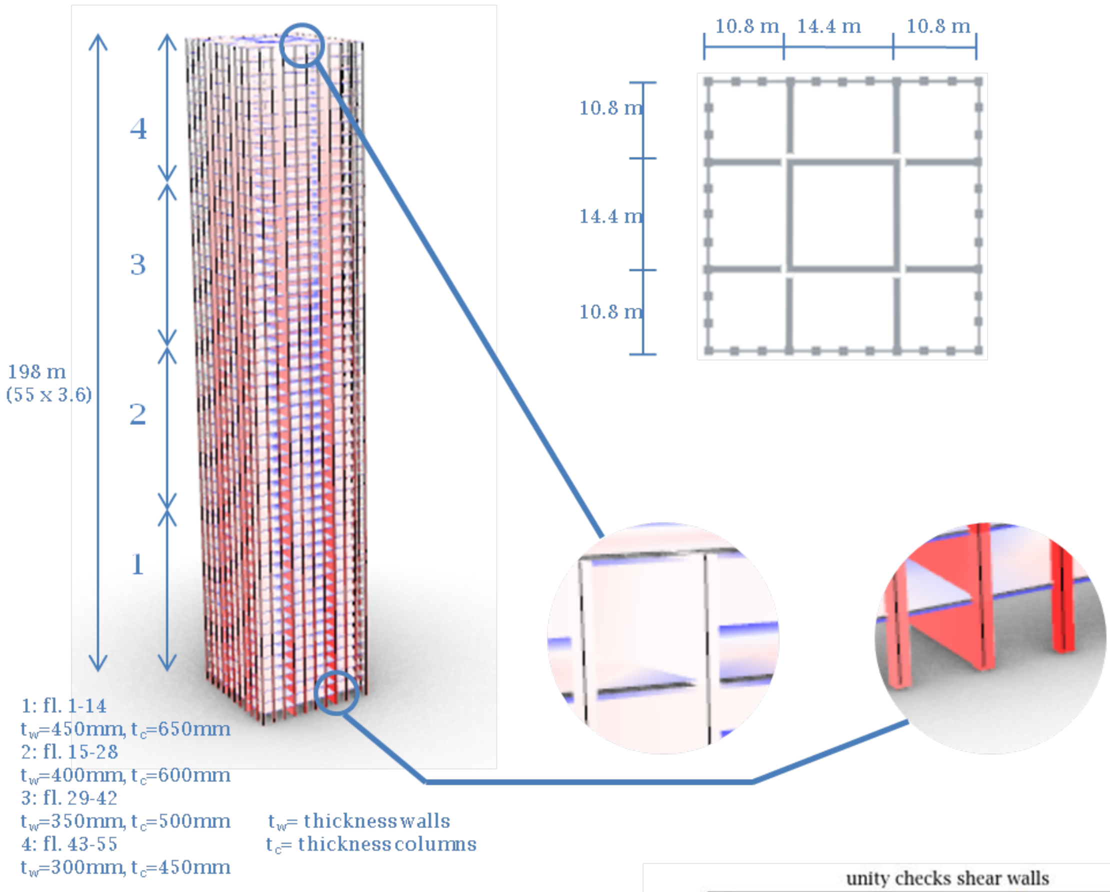


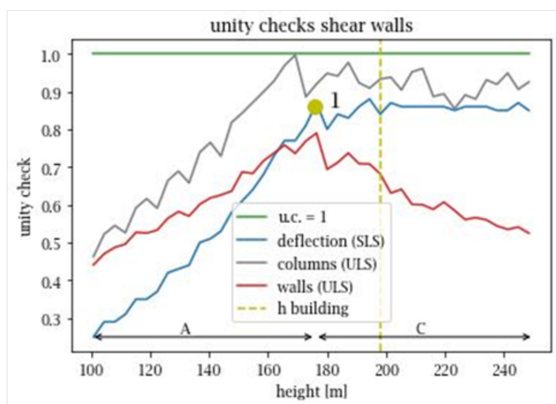


**Unity checks**
<u>Model</u>
Slenderness stabilising part
*25.6/198=1:8*
u.c. deflection = *0.84*
u.c. columns = *0.87*
u.c. walls = *0.68*

**Deflection**
<u>Manual verification</u>
$E = 29.6\ kN/m^2$
$I = 3548\ m^4$
$q = 108\ kN/m^2$
$l = 198\ m$
$w_{dv}$=198 mm
<u>Model</u>
$w_{kar}$=221 mm

$$w = \frac{ql^4}{8EI}$$

**Normal force to foundation**
<u>Expectation</u>
Building mass: *810*10³ kN*
Vertical load: $3.2\ kN/m^2 * 362\ m^2 * 55 = 228*10^3\ kN$
Load combination: $1.32*810*10^3 + 0.5*1.65*228*10^3 = 1.26*10^6\ kN$
<u>Model</u>
Summation of vertical reaction forces in foundation:
$1.26*10^6\ kN$

**Figure 5.8** Verification shear walls

## Core (35 floors, 126 m)

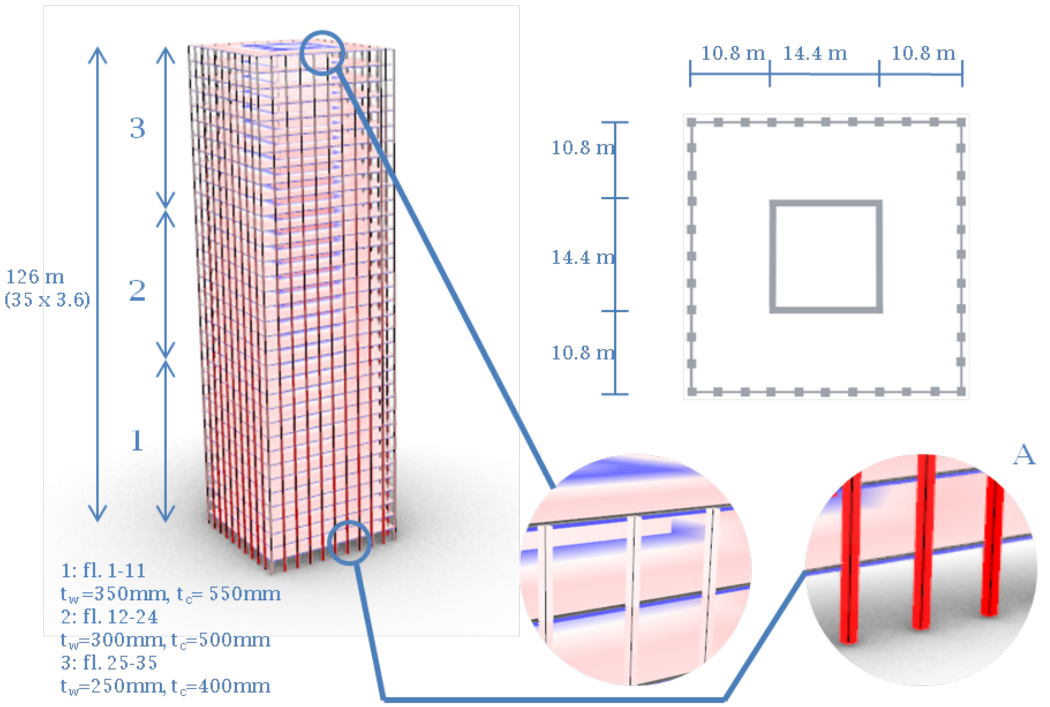


**Unity checks**
<u>Model</u>
Slenderness stabilising part
*14.4/126 = 1:9*
u.c. deflection = *0.805*
u.c. columns = *0.986*
u.c. walls = *0.800*

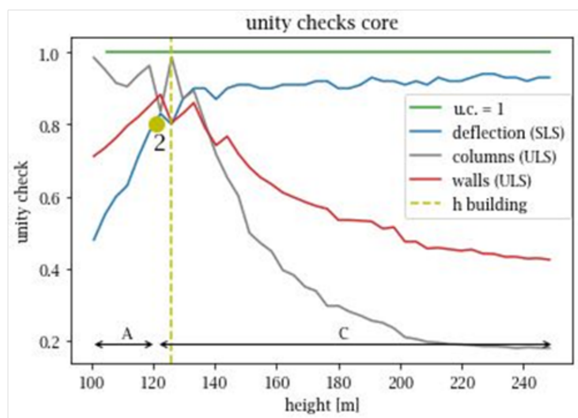


**Deflection**
<u>Manual verification</u>
$E = 29.6$ kN/m²
$I = 692$ m⁴
$q = 109$ kN/m²
$l = 126$m
$w_{dv}$=143 mm
<u>Model</u>
$w_{kar}$=135 mm

$$w = \frac{ql^4}{8EI}$$

**Detail A**
Heaviest loaded column
Column size: *500 mm*
<u>Expectation</u>
Floor area carried by one column: *3.6*5.4 = 19.44 m²*
Load on the column: *1.32*G + 0.5*1.65*Qv + 1.65*Qw*
*35(1.32*24(19.44*0.3+0.3²*3.6) + 0.5*1.65*3.2+0) =*
*8621 kN*
<u>Model</u>
Normal force in Karamba: *8194 kN*

**Figure 5.9** Verification core

## Outrigger (45 floors, 162 m)

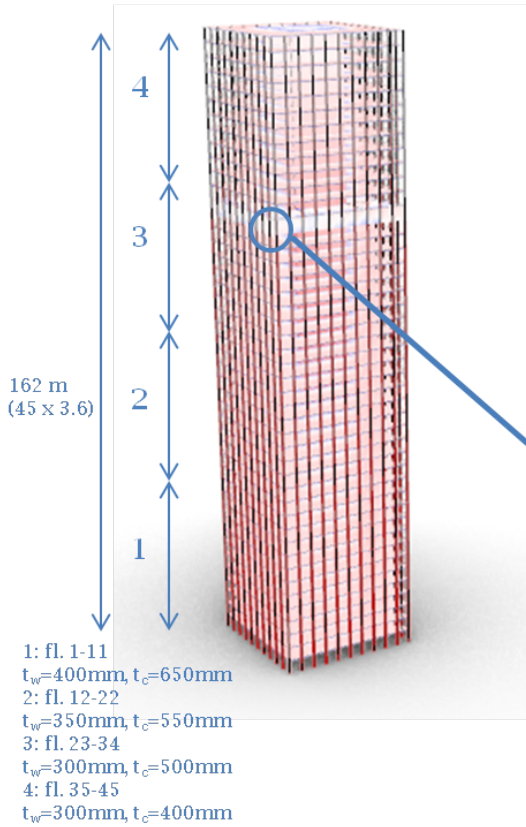


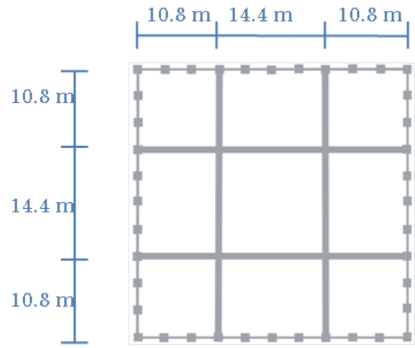


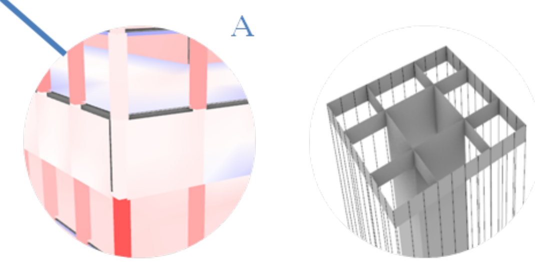


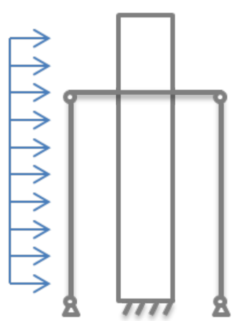

**Unity checks**
<u>Model</u>
Slenderness stabilising part
*14.4/162=1:11*
u.c. deflection = *0.79*
u.c. columns = *0.88*
u.c. walls = *0.91*

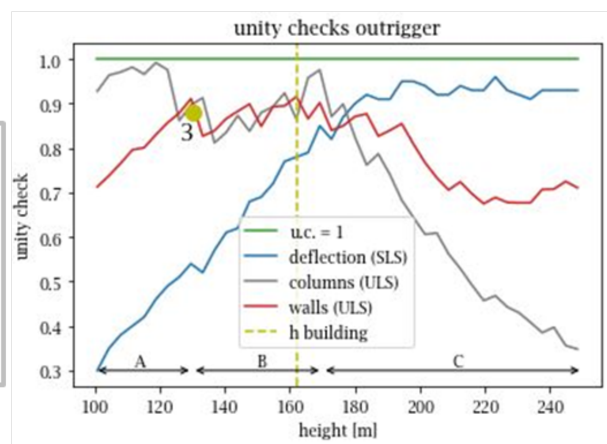


**Deflection**
<u>Manual verification</u>
*E = 29.6 kN/m²*
*I = 962 m⁴*
*q = 117 kN/m*
*l = 162m*

$$w = \frac{ql^4}{8EI}$$

$w_{dv}$=*172mm*
red. due to outrigger 43%
<u>Model</u>
$w_{kar}$=*171 mm*

**Normal force in outrigger columns**
Only due to wind load
<u>Expectation</u>
Result from MatrixFrame: Tension/compression: *9.3*10³ kN*
<u>Model</u>
Normal force in Karamba: Sum of forces in columns below outrigger: *8.8*10³ kN* (position A)

**Figure 5.10** Verification outrigger

### Tube (65 floors, 234 m)

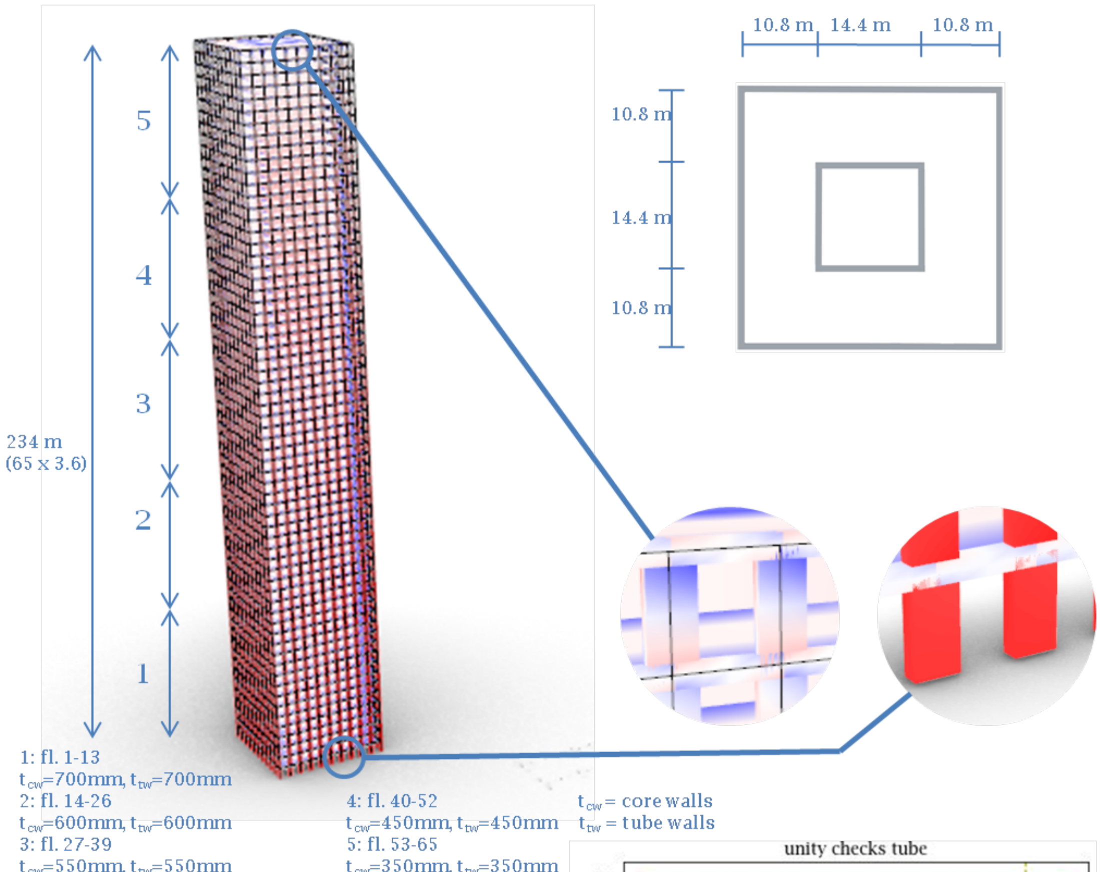


**Unity checks**
<u>Model</u>
*36/234=1:7*
Slenderness stabilising part
u.c. deflection = *0.84*
u.c. tube walls = *0.85*
u.c. core walls = *0.71*

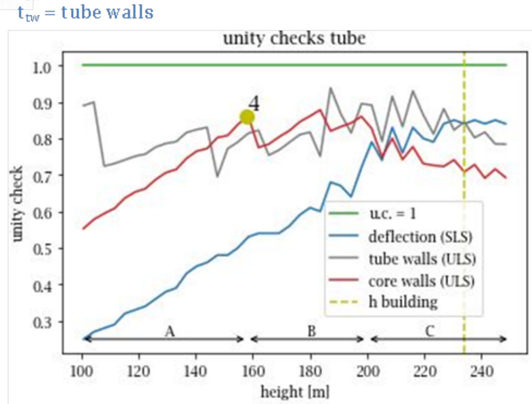


**Deflection**
<u>Manual verification</u>
$h_{grid} = 3.6\ m$ $E = 29.6\ kN/m^2$
$b_{grid} = 3.6\ m$ $I = 1094\ m^4$
$I_b = 0.023$ $q = 133\ kN/m$
$I_c = 0.188$ $l = 234\ m$
$n = 20$ $GA = 1.1*10^7$
*defl. due to EI & GA*
$w_{dv} = 207mm$
<u>Model</u>
$w_{kar} = 262\ mm$

$$GA = \frac{12 * E}{h_{grid}\left(\frac{1}{\frac{n*I_b}{b_{grid}}} + \frac{1}{\frac{n*I_c}{h_{grid}}}\right)}$$

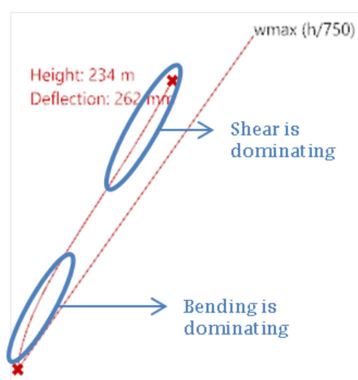


**Figure 5.11** Verification tube

**Conclusions**

The second column of table 5.3 shows the height from the model and graphs where deflection becomes normative. This can be compared with the theory (third column), based on the expectation from figure 5.7 and a height corresponding to a slenderness of 1:8. For the core, outrigger and tube, the expected height is close to the theoretical height. For the shear wall, there is a small difference. This can be due to the way of modelling and the effective width of the stabilising element. The theoretical height of the outrigger is based on a single core with 43 % additional stiffness.

| Model | $h_{modelandgraph}(m)$ | $h_{theory}(m)$ | Difference |
|---|---|---|---|
| Shear walls | 170 | 201.6 | 18% |
| Core | 125 | 115.2 | 8% |
| Outrigger | 170 | 164.7 | 3% |
| Tube | 200 | 201.6 | 1% |

**Table 5.3** Heights where stiffness is normative, according to the model and theory

The results presented above apply to buildings with input as stated at the beginning of the chapter. However, many variations are possible on this building input, leading to other optimisation results. That is why a prediction is made of the influence of three building parameters on the results.

- Increased building slenderness: A higher slenderness means less stiffness in the building, with more deflection as result, when height is constant. As a result of this, slenderness will earlier be normative. The systems shear walls and tube are expected to be more favourable in this situation.
- Higher concrete strength: A higher concrete strength will lead to a lower utilisation of walls and columns. A consequence of this is that smaller elements can be applied in situations where strength is critical. This applies for example to the outrigger system below 180 $m$.
- Thicker floors: Thicker floors lead to more interaction between the stabilising elements on the floor map. This will lead to a higher stiffness for the same stability system, but also higher vertical loads on the structure

## 5.3 Optimisation results

In this section, the optimisation results are presented. This is done with graphs in Python. The optimisation results are obtained from the Grasshopper model with the animate function from the slider. Within this function, optimisation can be executed for every single value in the domain of the slider. For a graphical representation of the optimisation results, one of the optimisation results is plotted as function of the height. At the same time, the other quantities are constrained. The three optimisation goals which are shown are slenderness, total weight and carbon emission and flexibility, as defined in section 3.4.3 and 5.1. All numerical values used for the graphs are as stated at the beginning of this chapter.

### 5.3.1 Optimisation results slenderness

The optimisation results for slenderness show the maximum required column and wall thicknesses over the height. The goal of this is to compare the element sizes of the four systems. It can also be checked what the maximum building height can be without exceeding a maximum element size. For columns, this is around 1000 $mm$ and for walls 600 $mm$. The dots in the graphs represent the points where the wall size has to increase to keep the unity checks below one. The dots correspond to the dots in the unity check graphs of figure 5.8 till 5.11.

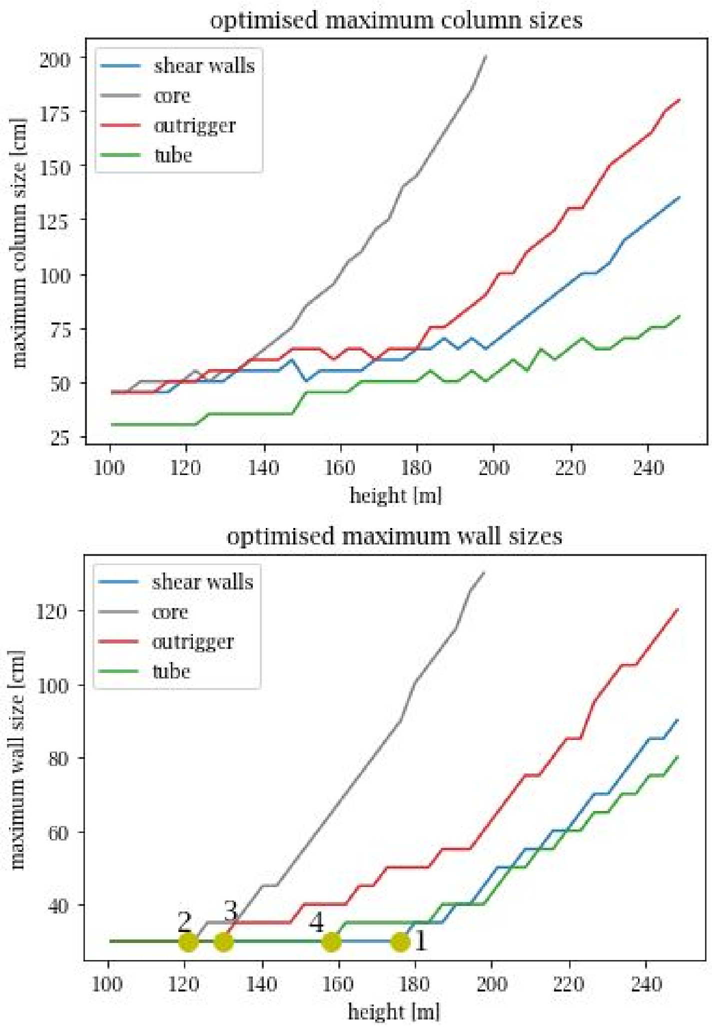


**Figure 5.12** Maximum column and wall size per system

A number of conclusions can be drawn from the optimisation results of the maximum column and wall sizes. The first thing that strikes is that the element sizes of the core increase rapidly in size above 150 $m$. In this situation, all stiffness of the tower comes from the core. This leads to uneconomically big element sizes above 150 $m$, which makes the core unsuitable. Applying one outrigger is a good option until a height of 200 $m$. When building higher, two or more outriggers should be considered. For the shear walls and tube, the building limits, based on maximum column size of 100 $cm$ and 60 $cm$ for walls, are about equal with the end of the height range which is 250 $m$. For completeness, also the total height range for walls and columns per systems is added. This means that all optimised elements for a certain height are between the upper and lower boundary of the graph. Again, the dot with number shows the point where the maximum wall size starts to increase.

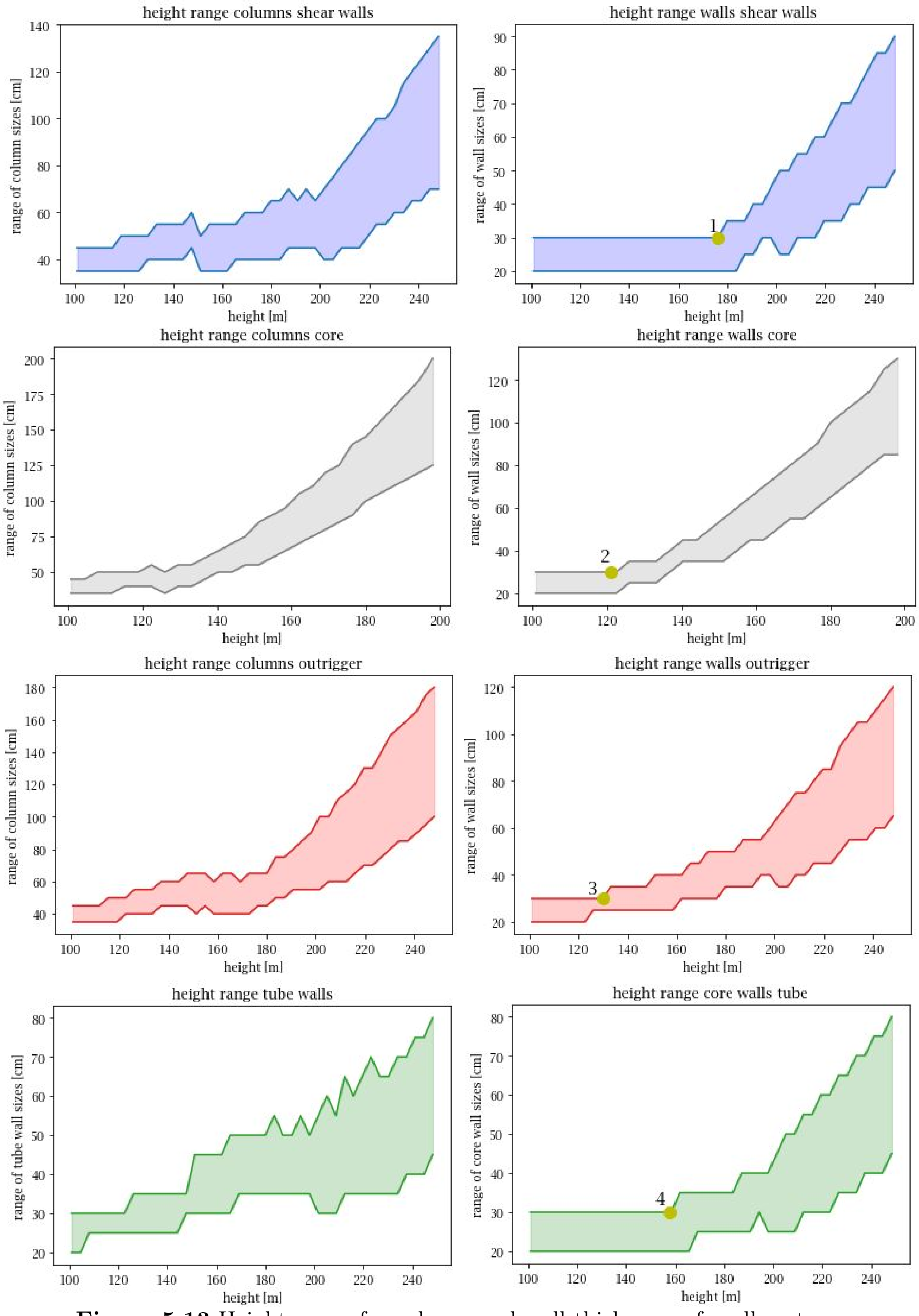


**Figure 5.13** Height range for column and wall thicknesses for all systems

### 5.3.2 Optimisation results total weight and carbon emission

For this optimisation, total weight and carbon emission is shown versus the building height. This is used to select the lightest structure, based on the height and the other input parameters. As carbon emission in this study is directly related to the total weight, the graphs show a similar behaviour. The impact of the foundation is excluded in the results.

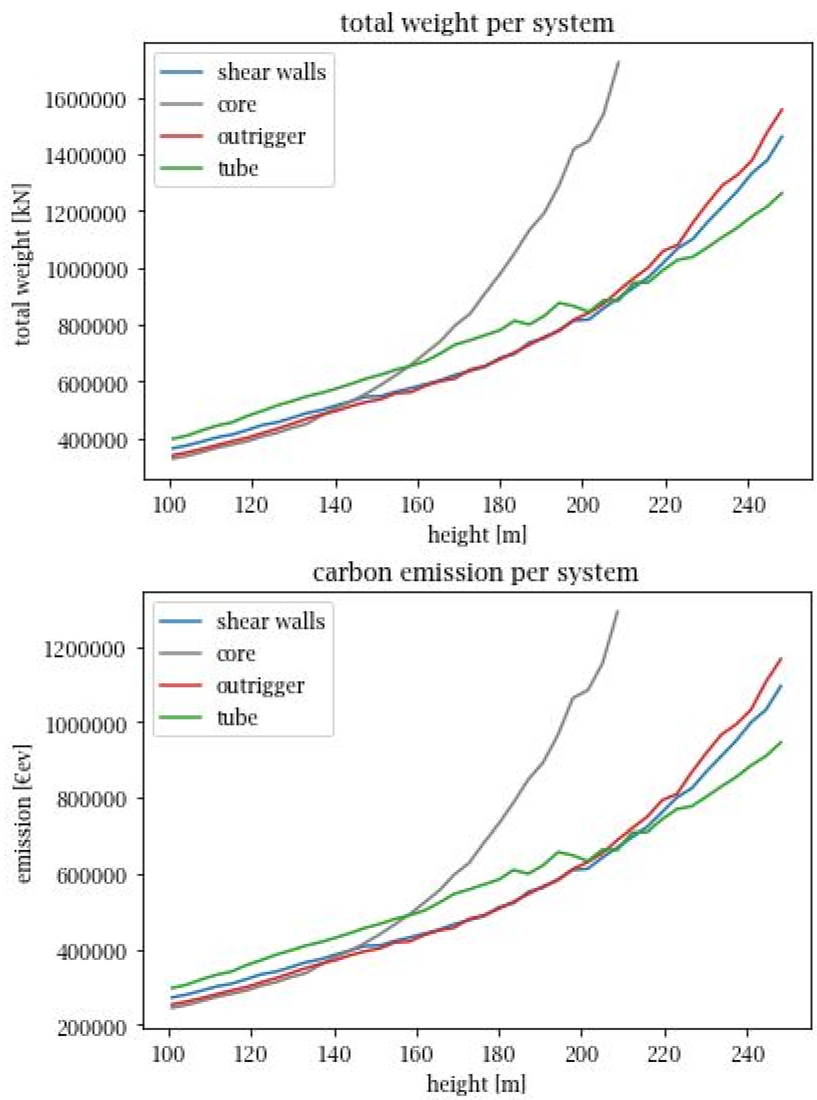


**Figure 5.14** Optimised mass and carbon emission per system

When looking to buildings below 150 $m$, it can be said that the optimised building masses are close, but a core is the best option. From 150 $m$ till 220 $m$, applying an outrigger or shear walls leads to the lightest solution. Above 220 $m$, the tube walls are used optimally, which leads to the smallest element sizes and lightest construction. For carbon emission, the graphs can be explained in a similar way. What is not directly visible in the graphs, is the high influence of the floors on the total mass. When assuming a building of 108 $m$ and 30 floors of concrete cast-in-situ with a thickness of 0.3 $m$, the total floor mass in the building is 291600 $kN$ or 0.29*$10^8$ $kg$, which is about 75 % of the building mass according to the graph. This shows the high influence of the floor thickness and system on the total weight. As a consequence of this, the graphs have to be interpreted carefully and are mainly meant as comparison of four systems instead of a quantitative analysis.

### 5.3.3 Optimisation results flexibility

The graphs below show the results for flexibility over the height of the building. Flexibility is executed for the four systems for both the facade and floor. Flexibility is defined here as the useful floor area and ration facade openings.

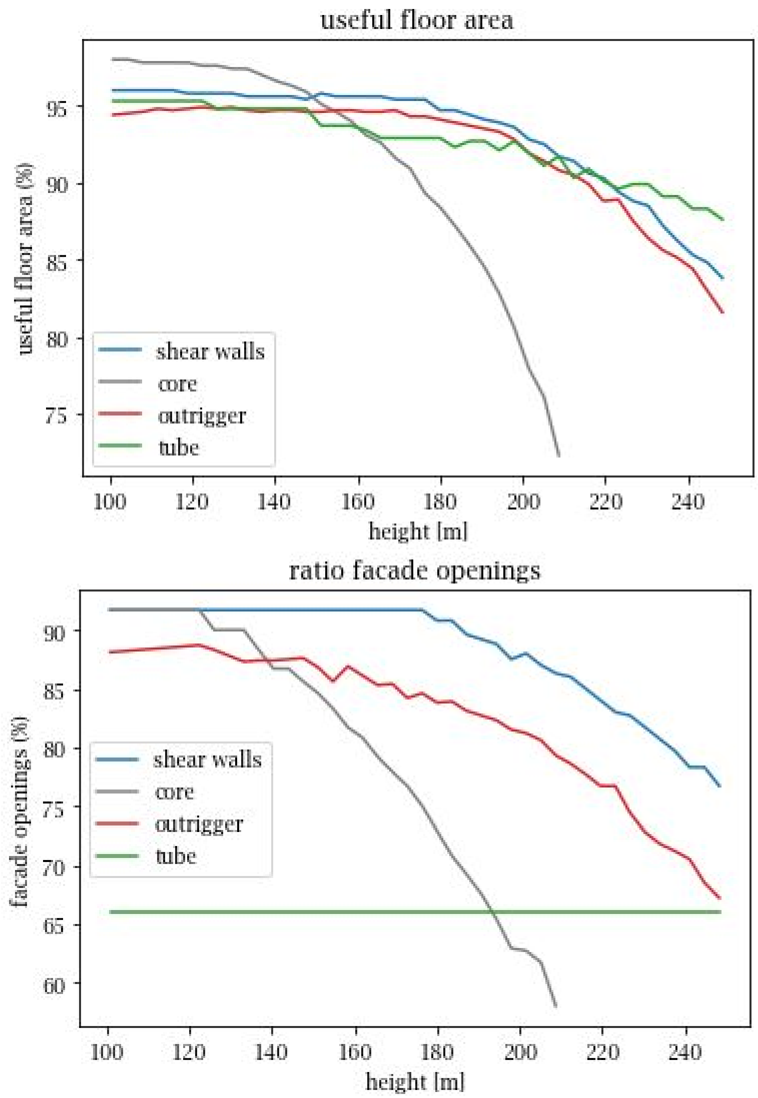


**Figure 5.15** Useful floor area and ratio facade openings

About the optimisation of useful floor area can be said that until a height of 150 $m$, the core system has the highest useful floor area. With increasing height, more space is taken by structural elements, which makes the core less suitable above 150 $m$. When construction height increases, the tube becomes more favourable. This because it is an exterior system, with the main stabilising elements in the facade. It strikes that the outrigger is the worst choice for low heights, due to the sacrificed outrigger floor, but this additional stiffness also leads to better results for buildings between 160 and 200 $m$. For the ratio facade openings, it can be said that shear walls are the best option throughout the total height range. The shear wall system obtains its stability by the walls in the floor plan, which results in a low influence on the facade openings. This in contrary to the tube system, where the window size in the facade element is normative for the ratio of facade openings.

# Chapter 6

# User interaction

In this chapter, the user interaction between the tool and client is described. In section 4.5, the tool in Human UI (NBBJ, 2019) was introduced as part of the parametric model. In this chapter, the tool is explained further. First the general goal and requirements of the tool are mentioned, then the testing procedure is explained, the steps in the tool are followed to show the process and finally, this is applied on De Zalmhaventoren.

## 6.1 Goal and requirements

### Goal

The goal of the project was mentioned earlier in section 1.4. Here was stated that the model and tool should give insight in the early design of high-rise buildings between 100 and 250 $m$. Besides this, the model should help decision making and speed up the design process in this phase. The tool can be used in a situation where a new high-rise building has to be developed. The first sketches are made and the outer dimensions of the building are roughly set. The next step is to make the first decisions for the structural design. This contains the decision for structural system, determining the element sizes and making the first estimations concerning the foundation.

### Requirements

Users of the tool are required to have a basic knowledge in the area of structural engineering and high-rise. The tool is made in Human UI, which means that no deep knowledge of Grasshopper is needed to use it. Only if the script itself has to be changed, some knowledge is required. To use the tool, a number of software packages are required. These are listed below, as well as the used version and a link to the reference list, where a corresponding link can be found.

- Rhino 6 (McNeel, 2020)
- Grasshopper(Included in Rhino 6) (Rutten, 2020)
- Karamba 1.3.3(Preisinger, 2018)
- Human UI 0.8.1.3 (NBBJ, 2019)
- Anemone 0.4 (Zwierzycki, 2015)

The output of the tool originates both from predefined input parameters and calculations in Grasshopper. To use the tool properly, it is important to make a clear distinction between the input defined by the user and the calculations of the tool. This was shown earlier in figure 5.1. Here could be seen that the general shape of the building has to be determined by the user. Subsequently, the element sizes are determined by the tool. The system choice can be chosen by the user, although this is based on optimisation.

## 6.2 Testing procedure

In this section the tool is tested. This is done by structural engineers from IMd Raadgevende Ingenieurs. During the test, a number of criteria are checked and this feedback is used to improve the tool. The criteria lead to five questions about usage of the tool. The approach, questions and answers are presented below.

### Approach

At the 9th of December 2020, the tool was tested by Sander van Eerden and Ikram Talib from IMd Raadgevende Ingenieurs. The testing procedure is made up of two parts. First the steps in the tool are followed based on random input parameters. This is done to check the procedure and logic of the steps. The second step is inserting an existing building in the tool, to check the applicability of the tool and to compare the outcomes. A remark is that a reverse procedure has been applied here: Normally, the model can be used to compare building variants. During the test, an existing building is used to check the model.

### Criteria

- Logic: Is the tool clear and can the steps easily be followed? Is the tool also usable for engineers without practice in Grasshopper?

  *The process in the tool is not fully clear. Explanation of the tool is given in the report, but without the report it is difficult to understand the tool. This is especially true for the optimisation procedure.*

- Link to practice: Is the process that is run through similar to the design process in practice? Are there any important steps left out that influence the design process in the early design stage?

  *The process that is followed is similar to the process in practice. However, the way the optimisation results are obtained is slightly different. It would make more sense to optimise the structure for only one of the optimisation goals. Now, one general optimisation is executed, from which the results of each individual optimisation goal are obtained. The way that flexibility of the floors is defined is not fully logical. For example for the shear walls model, with walls from facade to facade. According to the optimisation, shear walls score high on this criterion, despite the fact that the long walls confine the design freedom*

- Speed: Is the tool fast enough during use? Leads the calculation time to any annoyance for the user?

  *For the tested building, the calculation time is acceptable. When the size of the building increases, the number of element increases as well. In this situation, extra calculation time has to be kept in mind.*

- Applicability: At which range of buildings is the tool applicable? Leads the fixation of some of the design parameters to a bad applicability of the tool?

  *In the tool, four different concrete systems can be compared. Often a building is an intermediate form of two systems, this means that a required configuration of stability elements cannot be modelled. The tool gives a clear comparison between the four systems, but other configurations of stability elements cannot be tested.*

- Results: Are the calculated element sizes and the changes in size per height zone logic? How do the element sizes compare with a real building with similar system and dimensions?

*The element sizes and changes per zones are realistic. The tool has been applied on a high-rise building. The element sizes from the tool are similar with the chosen sizes in practice. Although, due to the limited model options, it was not possible to exactly rebuild the building in the tool.*

### Conclusion

The conclusion from the test is that procedure in the tool is not fully clear, this makes it difficult to judge the reliability of the results. This has led to a number of adaptations in the tool. The optimisation results were originally presented in a rose, which showed the results of one optimised system. This is replaced by bar charts with the results of all four systems. Flexibility has been defined in a different way, which better fits the calculation. Another point which can lead to a lack of clarity for the user, is the difference between expectations and possibilities of the tool. In other words, the tool is meant for comparing four stability systems instead of rebuilding existing buildings.

## 6.3 Steps in the tool

In this section, the steps in the tool are presented. Images are added to show both the steps in the tool and the corresponding visualisation in Rhinoceros. The steps were introduced first in section 4.5 and are explained in a more elaborate way now. An overview of all steps and their positioning in the Rhino environment can be seen in figure 6.1

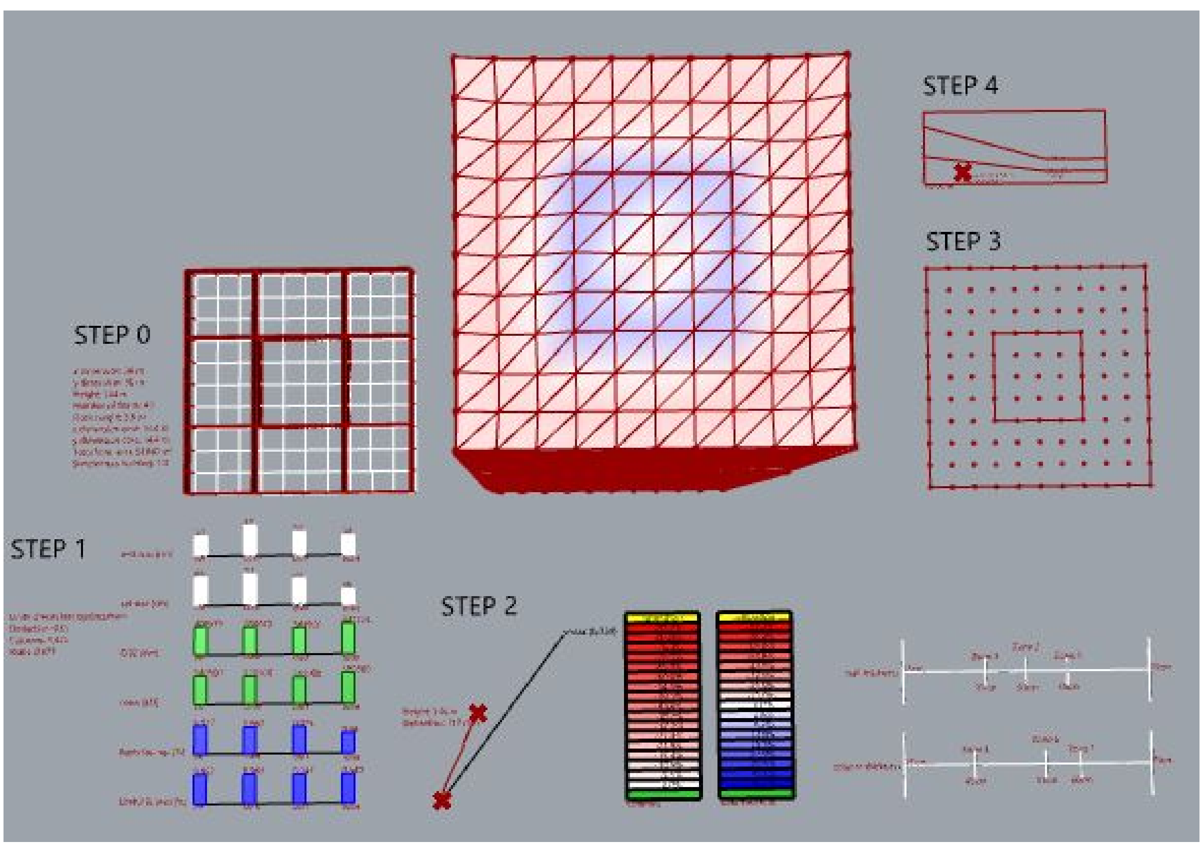


**Figure 6.1** All steps of the tool in Rhinoceros

### Intro

When the tool is activated, first an introduction page can be seen. Here is explained how the tool can be used, in which situation and what the target group is. A link to the report in the repository of TU Delft and explanatory video are added as well.

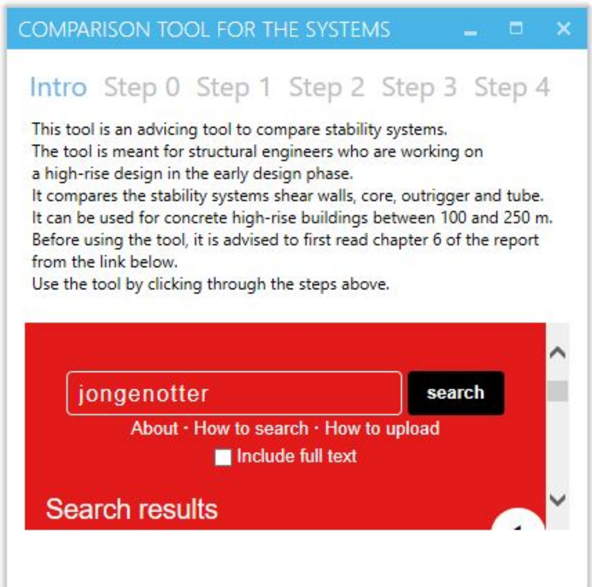


**Figure 6.2** Intro

### Step 0

Step 0 (figure 6.3) is the input step. This is divided into three parts. First the global dimensions of the building can be filled in. These are the grid size, number of grids in x and y direction, number of floors and floor height. After this, the dimensions of the core can be set up. This set of input parameters contains the x and y position of the core and x and y size of the core. It is also possible to apply a reduction factor, representing a reduced core strength due to perforations. Finally, other settings can be inserted. These are the floor thickness, load combination, concrete strength, relative outrigger height, grids per column and tube window size. In grids per column can be decided if a column is placed at every grid point in the facade or if this is done alternately. Simultaneously, the results of the optimisation can be seen in the Rhinoceros environment (6.3, bottom right). First the floor plan can be seen, with the location of structural elements. Besides this, a number of important building inputs can be visualised.

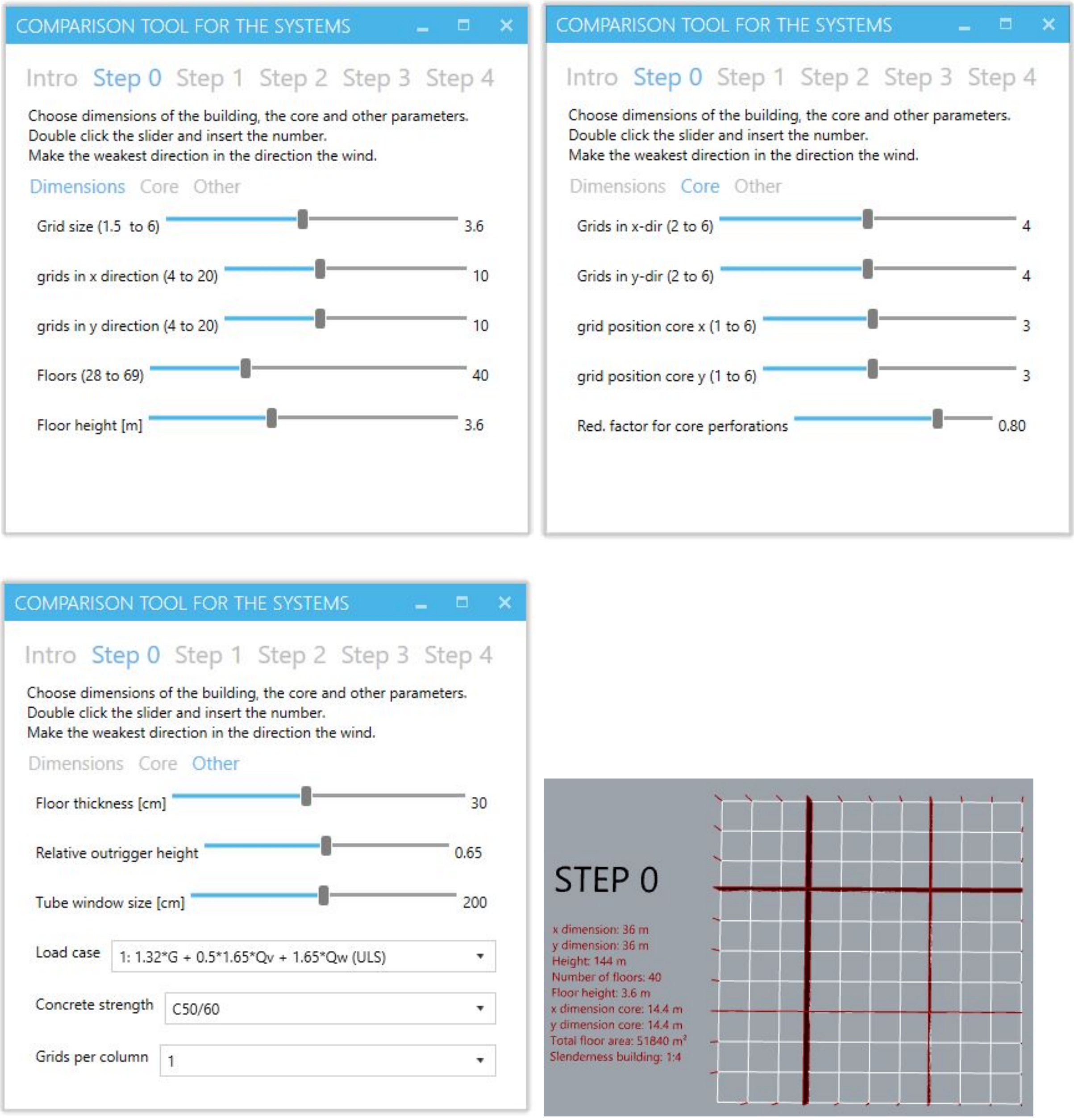


**Figure 6.3** Step 0

### Step 1

In step 1 (figure 6.4), the optimisation process is executed. For all of the four systems a size optimisation is executed. The obtained optimised constructions are compared to find the most optimal system, the typology optimisation. At first, the element size optimisation has to be turned on to activate the optimisation. By default this is turned off, to keep the tool as fast as possible. The next step is to execute the optimisation. This can be done by manually clicking through the systems. First the shear wall system, followed by the core, outrigger and finally the tube. Now the appropriateness per system can be found, based on the preferred optimisation goal (section 3.4.3). This leads to the choice for one of the four systems. Performance criteria of this system are ran through in steps 2,3 and 4. The bar charts on the right image of figure 6.4 show how optimal the chosen solution is, based on each optimisation goal. Also the unity checks of the last optimisation can be checked. In this example, an outrigger is chosen as final system and is worked out further in the next steps.

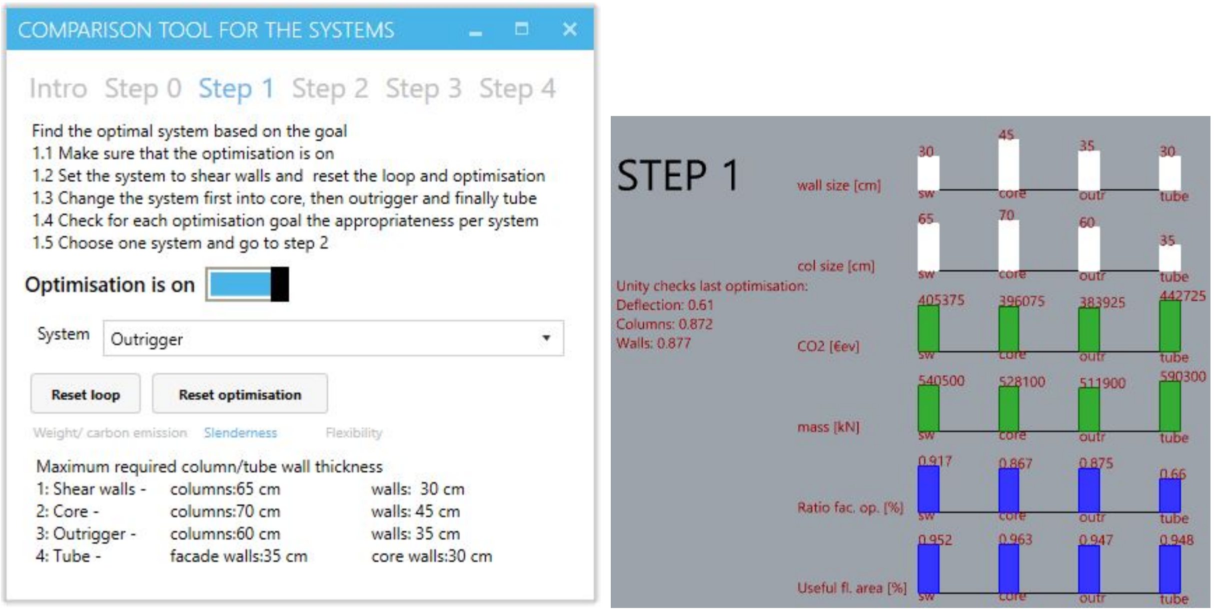


**Figure 6.4** Step 1

## Step 2

An advice for the column and wall sizes per height zone is given in step 2 (figure 6.5). Based on these sizes, the maximum deflection and utilisation of wall and beam elements can be obtained. The colored charts visualise the utilisation of all shell and beam elements. An important remark here is that both (core) walls and floors are shown in the graph for shells. The advised element sizes are plotted on a horizontal line with each zone clearly indicated. The deflection over the height is plotted in a graph, with the maximum deflection in black.

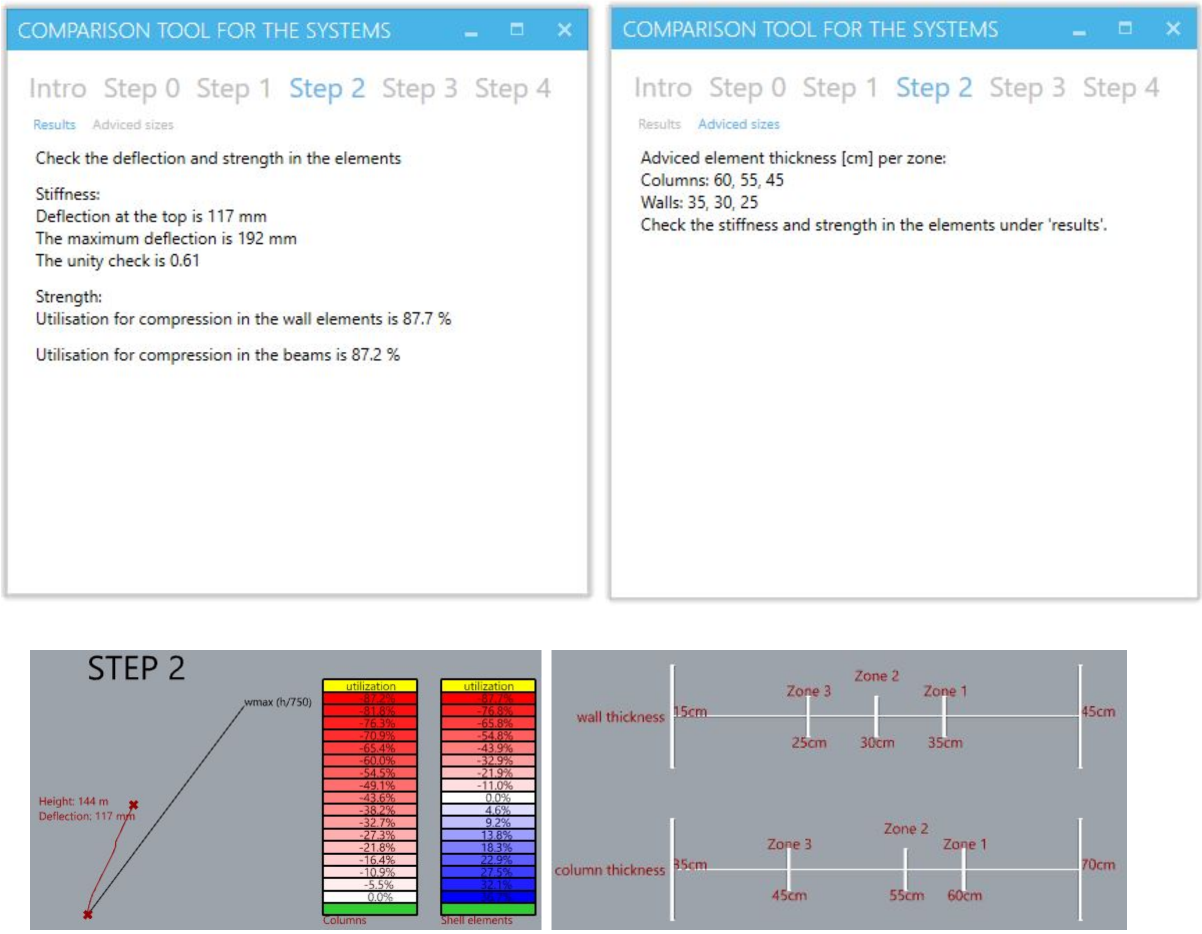


**Figure 6.5** Step 2

### Step 3

In step 3 (figure 6.6), the foundation is tested following the process explained in section 4.4. First a pile length and configuration can be inserted. A pile length can be based on the composition of the soil. For the piles, three different configurations are possible. Subsequently, the tool gives an estimation of the required diameter per pile. This is based on the total weight of the building and the resistance per pile. Hereafter, the applied diameter can be set and deflection due to the pile foundation is given. A limitation for the total deflection is $h/500$, with $h$ the building height. This is used to determine the influence of the foundation on the total deflection.

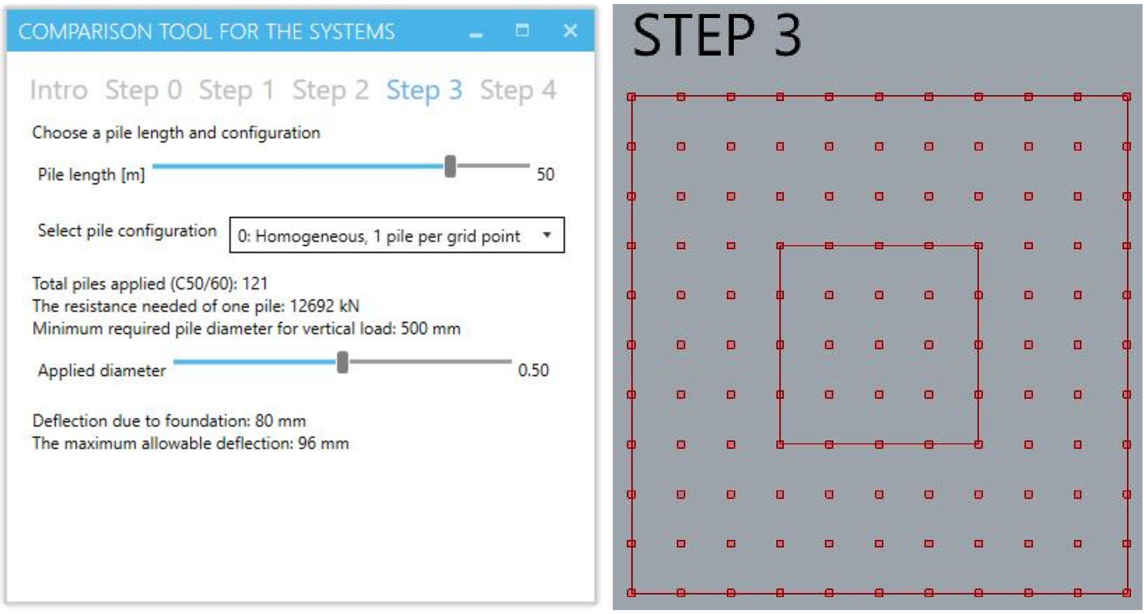


**Figure 6.6** Step 3

### Step 4

In the last step (figure 6.7), the maximum acceleration in the building is compared with the maximum allowable one. This is based on the graph in figure 3.12, which can also directly be seen in Rhinoceros. The tool communicates if the requirements are met, both for residential buildings and offices.

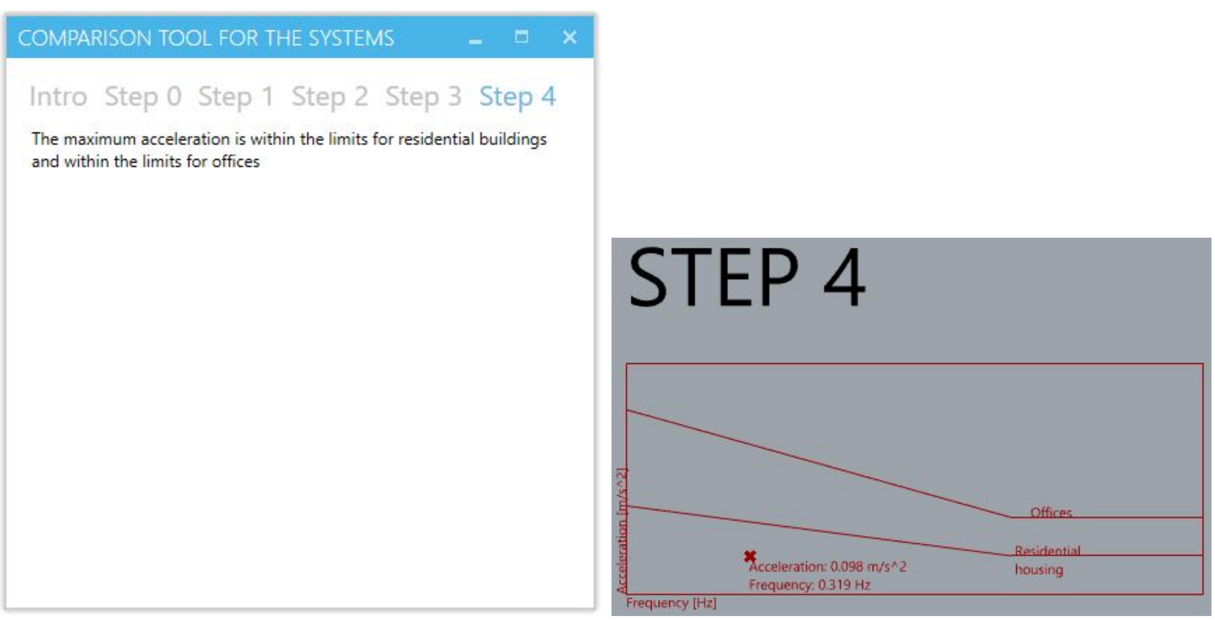


**Figure 6.7** Step 4

Going through the tool is an iterative process. This means that when a criterion in the steps 2, 3 or 4 is not met or results are unsatisfying, it is possible to go back to step 0 to change input values and run through the process again.

## 6.4 A case study: De Zalmhaventoren

So far in this chapter, the procedure concerning the tool was given. To fully prove the validity of the model and results, an existing building is rebuilt in the model. The choice has been made to use De Zalmhaventoren for this. The building was presented earlier in chapter 3.1.2. First the general specifications of the tower are given. This includes the building dimensions, deflection, foundation and comfort.

### 6.4.1 De Zalmhaventoren

De Zalmhaventoren is a high-rise building project, existing of three towers, located in Rotterdam. The highest of these three towers, Zalmhaven I, is designed by Dam  Partners Architecten and will be covered in this study (Van Eerden, 2017). It is expected that the tower will reach its highest point in September 2021 and that the finalised project is delivered in 2022. The height of the construction will be 188 $m$ and the total height of the tower, the crown (the highest three floors) and antenna included, is supposed to reach a height of 216 $m$. This will make it the highest building in The Netherlands.

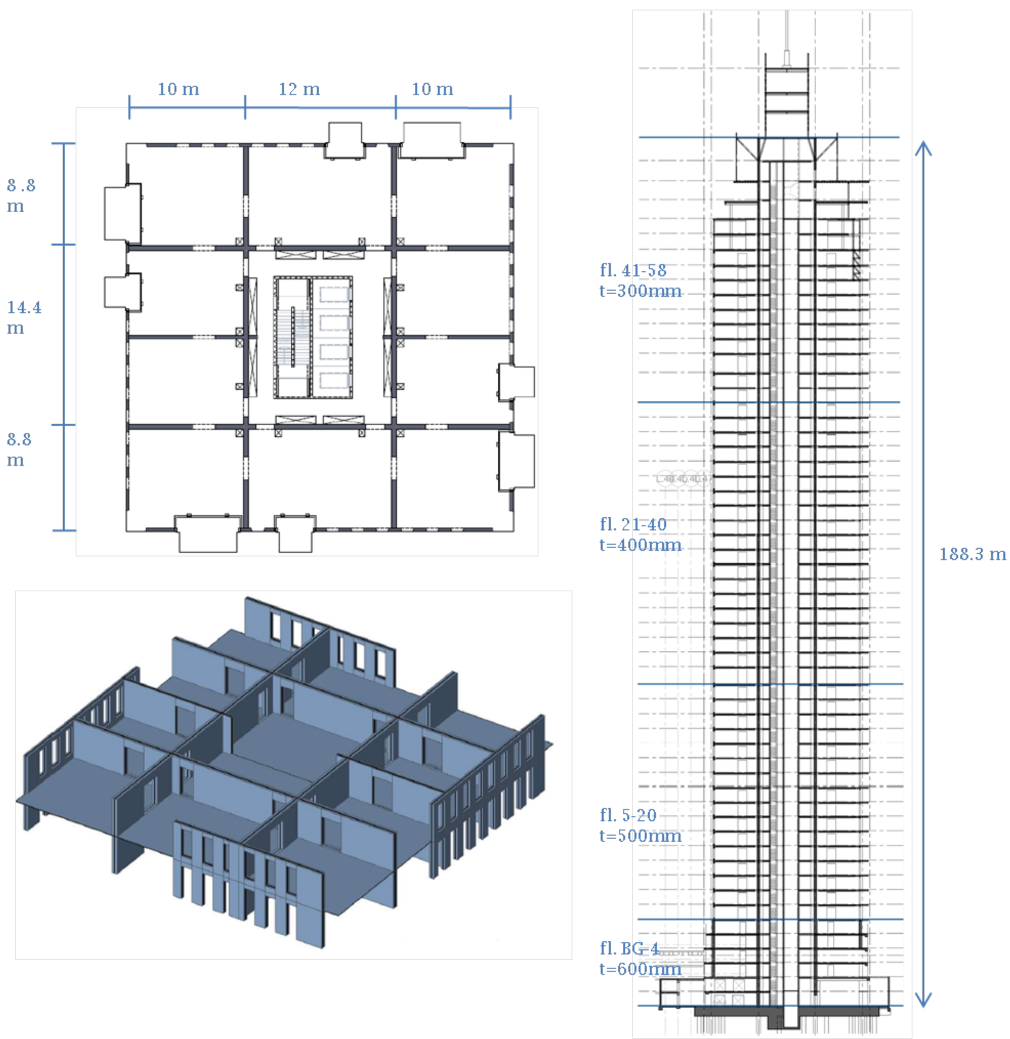


**Figure 6.8** Floor plan and cross section of De Zalmhaventoren (Van Eerden, 2017)

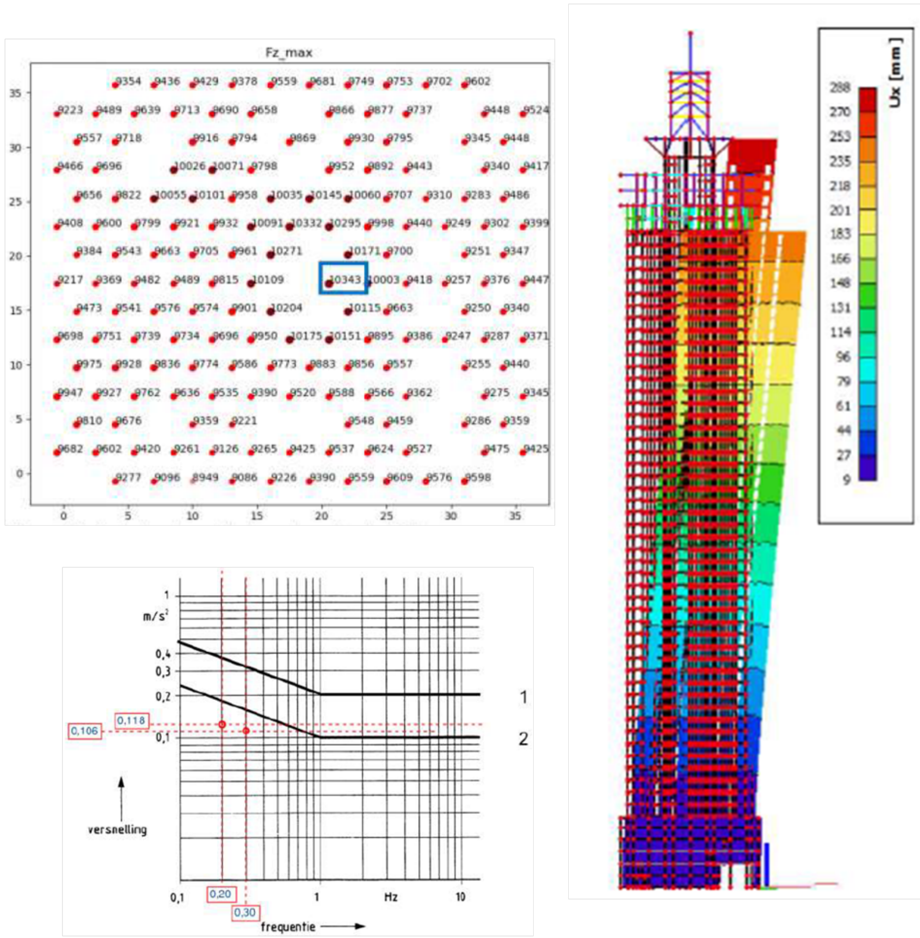


**Figure 6.9** Foundation plan (top left), acceleration (bottom left) and deflection (right) of De Zalmhaventoren (Van Eerden, 2017)

Specifications Zalmhaventoren:

- height: 216 $m$
- x-dimension: 32 $m$
- y-dimension: 32 $m$
- x-dimension core: 12 $m$
- y-dimension core: 14.4 $m$
- Wall dimensions: 300, 400, 500, 600 $mm$
- Floor thickness: 270 $mm$
- Number of floors: 60
- Floor height: 3.06 $m$ (top floors are higher)
- Concrete: C53/63 (old strength class) for floors 0-5, C45/55 for floors 6-22, C35/45 for floors 23 and higher
- Stability system: Two shear walls in both directions spanning from facade, with two additional shear walls in x direction
- Stiffness: Maximum deflection in x direction is 288 $mm$

- Foundation: 163 Tubex GI piles, with a diameter of 762 mm, length is 66 m, homogeneous divided, steel tube drilled in the ground, filled with a grout mixture
- Comfort: Maximum acceleration is 0.118 $m/s^2$. The frequency is 0.20 $Hz$

### 6.4.2 Model

The building as described above is now rebuilt with the model in Grasshopper. The system that is applied from the model is the shear wall system, with walls spanning from facade to facade. It has been tried to approximate the building as accurate as possible, but of course a few simplifications had to be made. The building with crown excluded, has a height of 188.3 $m$ and 59 floors, ground floor included. Until the 50th floor, the floor height is 3.06 $m$. On the floors above, the floor height varies between 3.24 and 4.76 $m$. To accommodate for this, a mean floor height of 3.2 $m$ is applied throughout the whole building. This leads to a building height of 188.8 $m$. The facade elements in the building are modelled with columns, with one column every four meters. The first five stories of De Zalmhaventoren have a divergent construction compared with the rest of the tower. This is left out in the model. The concrete grade shifts over the height of the building from C53/65 to C45/55 to C35/45. A mean concrete strength of C45/55 is applied on the building.

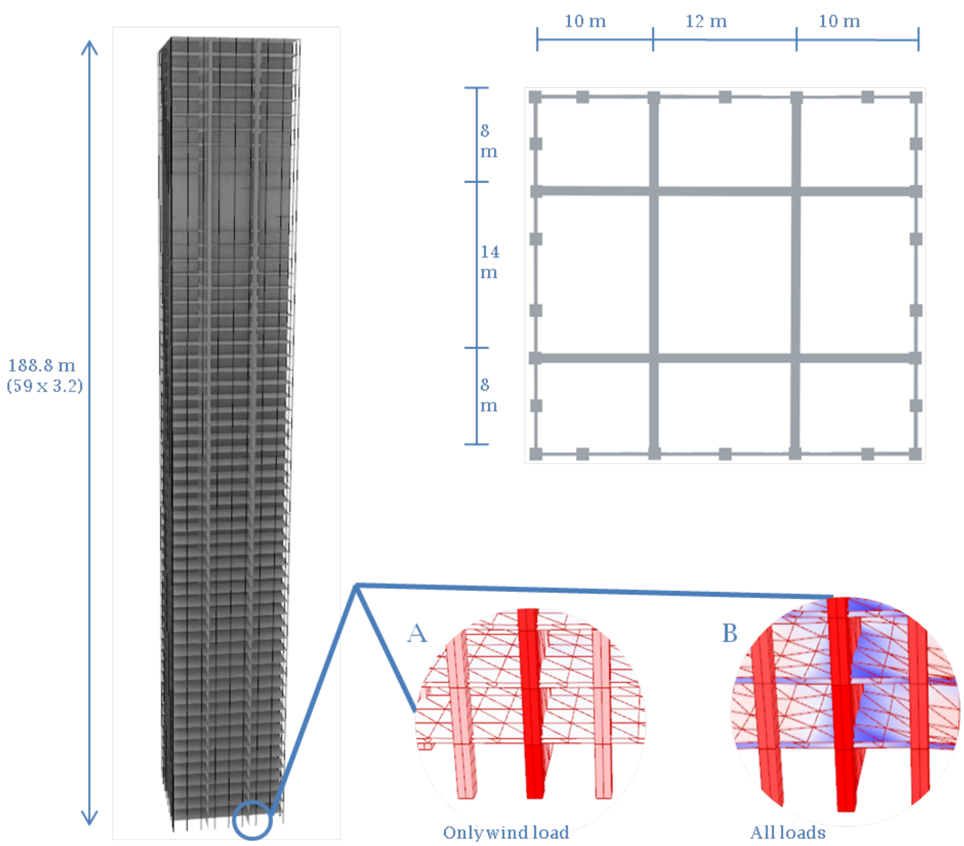


**Figure 6.10** Modelling of De Zalmhaventoren

### Input

The input in Grasshopper which is used to model De Zalmhaventoren can be found below. The input values 'Relative outrigger height' and 'Tube window size' are system specific parameters and not of influence for the shear wall model which is applied in this study.

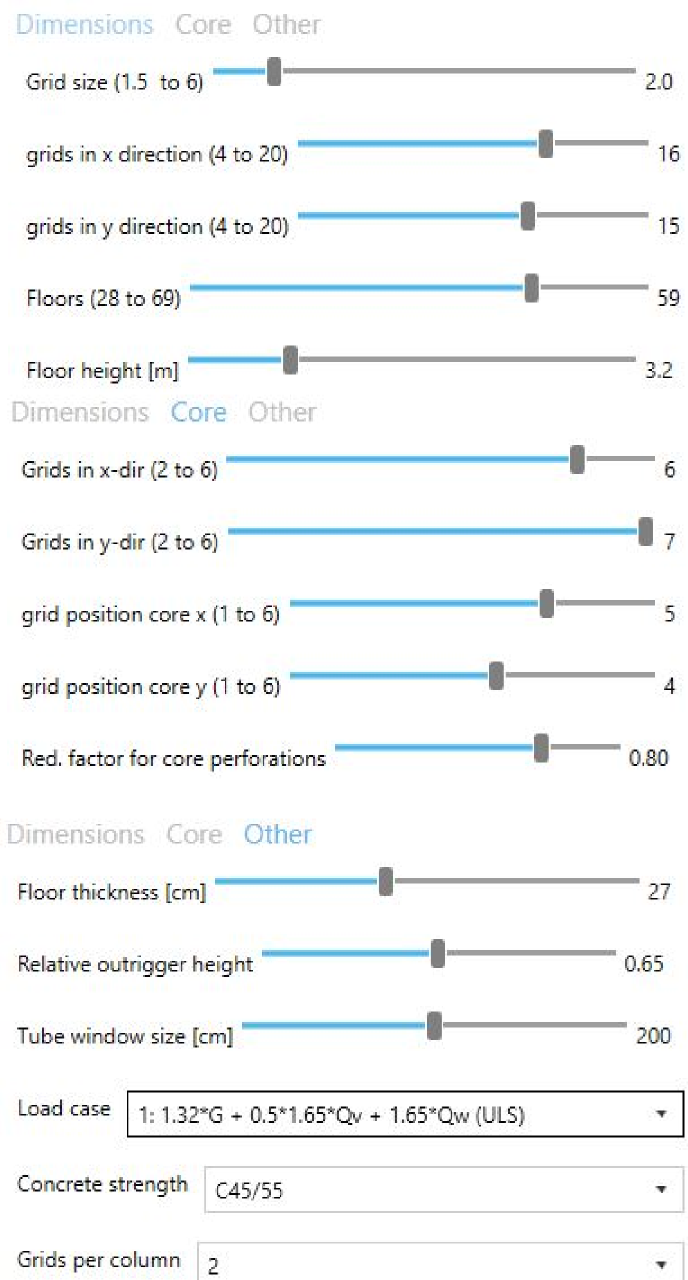


**Figure 6.11** Input in Grasshopper

### Results

The results with regard to stiffness, strength, advised element sizes, foundation and comfort are presented below.

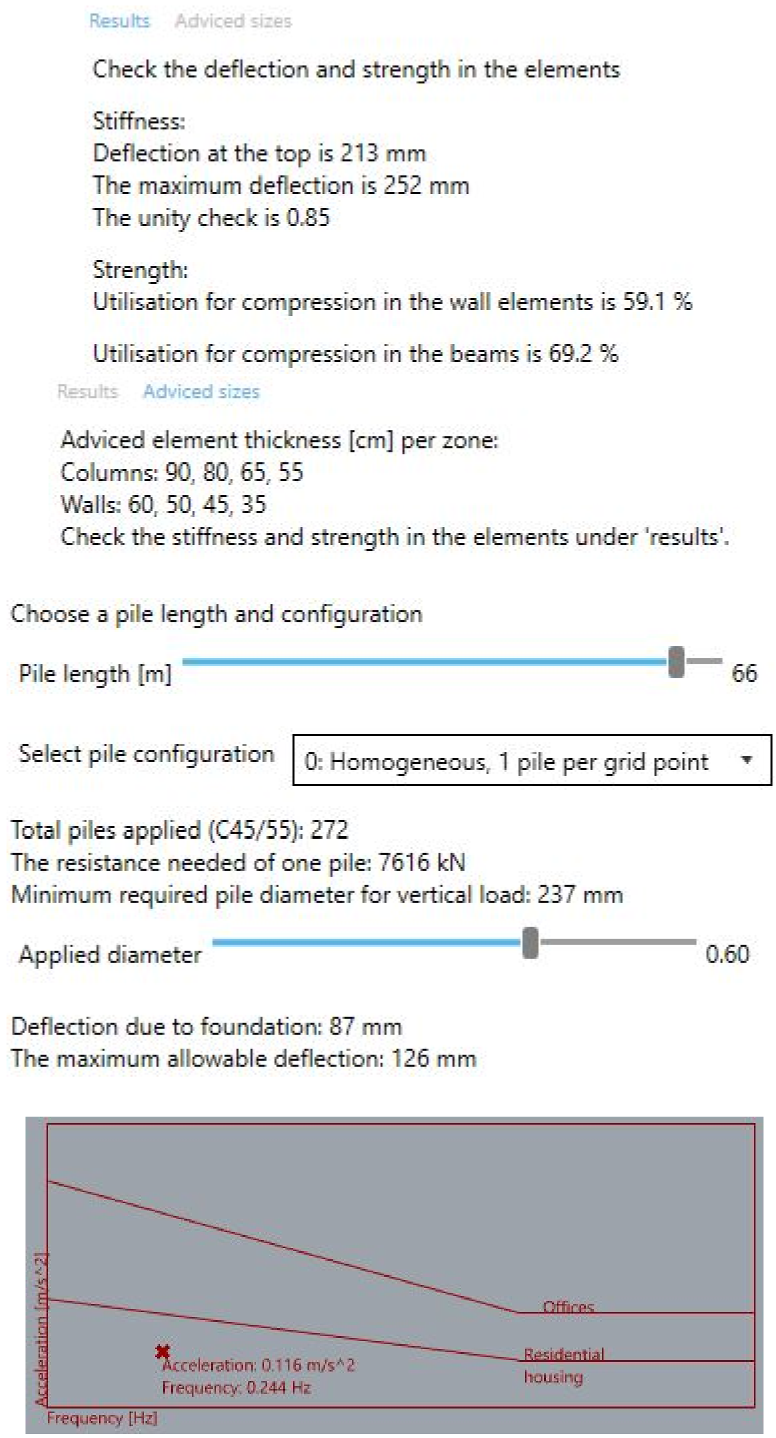


**Figure 6.12** Results from Grasshopper

### 6.4.3 Comparison of results

**Wall sizes**

The results of the calculation procedure of De Zalmhaventoren are now compared with the results of the model. The wall sizes applied in De Zalmhaventoren are 600, 500, 400 and 300 $mm$ (figure 6.8, right), divided over four height zones. The optimisation procedure of the model leads to advised sizes of 600, 500, 450 and 350 $mm$ (figure 6.12, advised sizes). These sizes are roughly the same as applied in reality.

**Deflection**

The deflection of De Zalmhaventoren in the weakest direction was 288 $mm$ (figure 6.9, right) , where the model gives 213 $mm$ as deflection (figure 6.12, results). This difference is due to the height on which the deflection was calculated. This was 188.6 $m$ for the model and 202.7 $m$ for the finite element model used during tower design. When the deflection is rescaled by a factor $(\frac{202.7}{188.6})^4$, the total deflection is 284 $mm$, which is close to the earlier calculated 288 $mm$.

**Foundation**

The foundation of De Zalmhaventoren is located on the clay ground of Rotterdam. That is why a pile length of 66 $m$ had to be used. 163 piles are placed on the second sand layer, with a pile diameter between 762 and 950 $mm$. The model is based on a default number of piles per grid, this means that 272 piles are selected. The pile length is set on 66 $m$. To compensate for the difference in number of piles, a pile diameter is chosen of 600 $mm$. This leads to a deflection due to the foundation of 87 $mm$, which is below the maximum deflection of 126 $mm$.

**Comfort**

The results with respect to comfort of the Zalmhaventoren were presented on the bottom left image of figure 6.9. The maximum acceleration in the weakest direction here is 0.116 $m/s^2$, with a frequency of 0.244 $Hz$ (figure 6.9, bottom left). The maximum acceleration in the model is 0.112 $m/s^2$, with a frequency of 0.228 $Hz$ (figure 6.12, bottom), which is close to the values of the real building.

**Interpretation of results**

From the comparison of the model and the structural calculations can be concluded that the results are quite accurate. For the foundation, the final pile diameter is based on deflection, but for vertical load bearing, also less piles or piles with a smaller diameter could be used. This difference could be a result of the extremely long piles applied to the tower. Although the results in general are quite similar, there are still a few differences that influence the results. The two additional shear walls are not modelled in the model. The facade walls are replaced by columns. This leads to a reduction in stiffness of about 12 %. It can be said that the model can be used in the early design phase to obtain the results presented above. The results can be used as starting point for more in depth calculations in later phases.

### 6.4.4 De Zalmhaventoren as tube

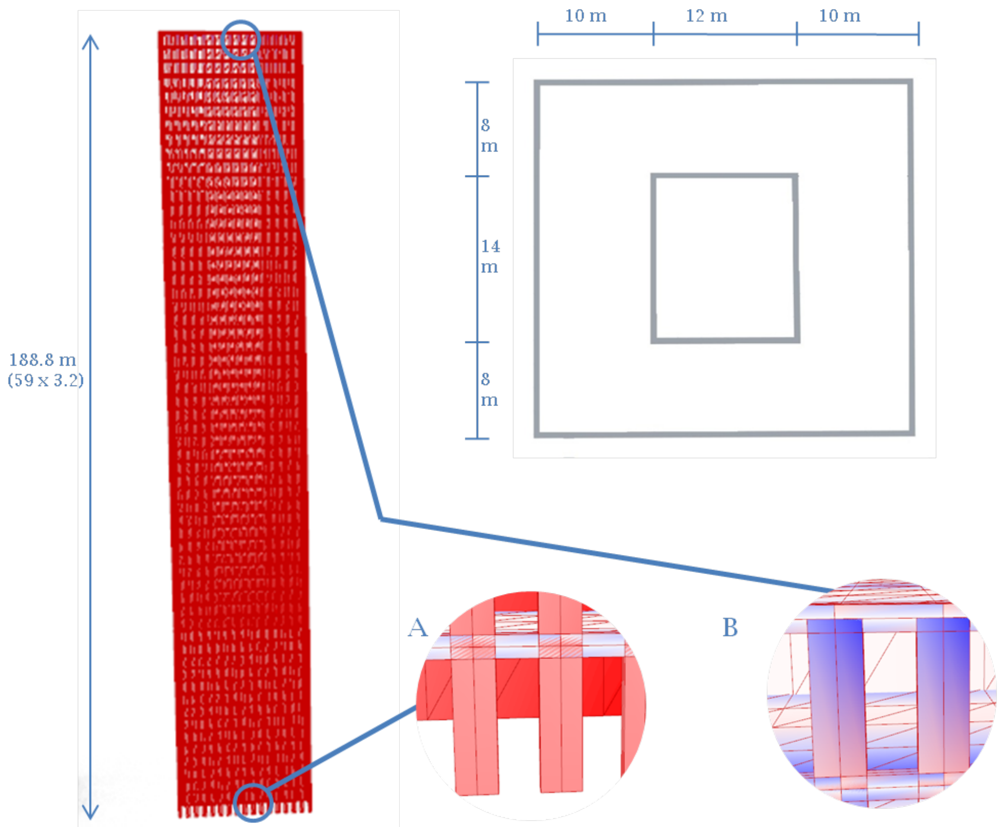


**Figure 6.13** De Zalmhaven as tube

| | Shear walls | Tube |
|---|---|---|
| Core wall sizes | 600/500/450/350 $mm$ | 450/400/300/250 $mm$ |
| Total weight | 6.8*$10^5$kN | 6.4*$10^5$kN |
| Carbon emission | 5.1*$10^5$€$ev$ | 4.3*$10^5$€$ev$ |
| Useful floor area | 88.9 % | 91.8 % |
| Ratio facade openings | 83.7 % | 63.5 % |

**Table 6.1** De Zalmhaven with shear walls and as tube

As could be seen in the case study, De Zalmhaventoren makes use of shear walls as stability system. De Zalmhaventoren is also executed as tube now and both variants are compared. The stiffness of the tube leads to lower optimised core wall sizes compared with the shear wall system. The optimised tube results in a total weight reduction of 5% compared with the shear wall variant. The biggest difference is the ratio facade openings. The tube scores significantly worse on this criterion. It can be concluded that De Zalmhaven executed as tube leads to a more efficient construction concerning element sizes and total weight, but at the expense of design freedom in the facade. The most optimal solution depends on the principles of the design.

# Chapter 7

# Final remarks

In this last chapter of the research, some final remarks will be stated. These final remarks are divided into three parts. First the conclusions are drawn. This includes answering the research questions and checking if the predefined goals of the thesis are met. The second part is the discussion. Here the findings during the research are presented. The reliability and interpretation of the results are discussed. In the last part, further research possibilities are presented. It is mentioned how this research could be extended and improved.

## 7.1 Conclusions

The conclusions form an answer to the research questions as defined in chapter 2.3.

**Theory**

1. *Which stability systems are most likely to consider for concrete high-rise between 100 m and 250 m?*
2. *Which parameters play a role in the design of a high-rise structure?*
3. *Which parametric tools are available for the structural design, optimisation and visualisation of a high-rise structure?*

To determine which stability systems have to be considered during research, different sources have been consulted. Only systems which can be executed in concrete and are suitable for the height range from 100 to 250 $m$ are considered. From this, four systems have been distilled. Shear walls, a core, an outrigger and a tube. These systems all have a core as basis. Based on literature study, a list of eight parameters for high-rise design has been selected:

- Material choice: Concrete cast-in-situ is processed in the model.
- Reinforcement design: Design rules are presented for the reinforcement design of columns, floors and walls. This is not calculated in the model and could be seen as a next step in the design process.
- Floors: Concrete cast-in-situ floors are applied in the model. To deal with the possibility of punching shear, a minimum column diameter is applied in the model.
- Loads: Vertical, horizontal and gravity load have to be taken into account as defined in the Eurocode. Five load combinations can be distinguished, three for the ultimate limit state and two for the serviceability limit state.
- Foundation: Deflection has to be considered as the summation of bending stiffness ($EI$) from the building itself and rotational stiffness ($C$) from the foundation. The total allowed deflection of $1/500*h$ is divided between these two.

- Second order effect: The second order effect must be taken into account by the second order factor $n$.
- Comfort: Comfort can be checked by comparing the maximum acceleration in the building with the maximum acceleration as in figure 3.12.
- Influence of perforations: Perforations can cause peak stresses in wall elements. To compensate for this, a reduction factor can be set up in the model.

Investigation into the modelling options for geometry, structural design, visualisation and optimisation let to the choice for the following software:

- General geometry: Grasshopper (Rutten, 2020)
- Structural design: Karamba (Preisinger, 2018)
- Visualisation (user interface): Human UI (NBBJ, 2019)
- Optimisation: Cross Section Optimizer of Karamba combined with Anemone (Zwierzycki, 2015) for the iteration process

**Parametric model**

1. *Which building parameters are assumed to be variable and which are fixed?*
2. *Which performance criteria have to be taken into account in the model?*

To get a model that is structured logically, a number of parameters are assumed to be fixed and other parameters to be variable. Variable parameters can be set by the user of the model. These are the positioning of structural elements, number of stories, story height, grid size, number of grids and a reduction factor for core perforations. Fixed parameters are material choice, load, building and column shape, floor system and connection type for different details. The four systems introduced in chapter 3, are merged in one model. Changing between these models can be done with a slider. In the model, it is possible to check four performance criteria:

- Stiffness: The deflection of the building itself has to be smaller than $1/750{*}h$.
- Strength: The utilisation of both wall and beam elements in compression have to be smaller than the material strength.
- Foundation: A pile diameter is calculated based on a pile configuration. Afterwards the deflection due to the foundation is determined.
- Comfort: The acceleration in the building is compared with the maximum acceleration, both for offices and residential buildings.

**Parametric results**

1. *What is the most optimal system based on input parameters and slenderness?*
2. *What is the most optimal system based on input parameters and total weight?*
3. *What is the most optimal system based on input parameters and flexibility?*

The graphs plotted in chapter 5 give a good insight in the suitability of the stability systems per optimisation goal. When looking to slenderness and element sizes, it can be concluded that a single core can be used until 150 $m$ and an outrigger system until 200 $m$, based on one outrigger. The other two systems, the shear wall system and tube, are limited at a height of around 250 $m$, which is the maximum height considered in the research. Considering total weight and carbon emission, it can be concluded that a single core system is the best option below 150 $m$, shear walls and an outrigger are best suitable between 150 and 220 $m$ and a tube is the lightest system above 220 $m$. A nuance on the results is the high influence of the floor thickness on the total weight. Beside choosing an adequate stability system, minimising floor spans also contribute to a reduced total weight. The third optimisation goal is divided into flexibility of the floor area and facade. These are plotted as ratio between useful and total space. The optimisation for useful floor area leads to a good applicability of the core below 150 $m$, where for buildings higher than 200 $m$, the tube can be seen as a good option. In between, the shear wall and outrigger are the best choice. For the ratio facade openings, the shear wall system is the best option for all heights. This because stability is provided by shear walls which are placed across the floor space and have minimal influence on the openings in the facade. The ratio is constant for the tube system, as the perforations in the tube are assumed to be constant. What strikes in the graphs of all optimisation goals are the deviant results of the core. Optimisation results show that a single core does not ensure enough stiffness for buildings above 150 $m$. To compensate for this, unrealistically high element sizes are required. This also results in a relatively high total weight and low flexibility. A final remark is that the results of the optimisations have to be considered as rough values, as they depend on the chosen input parameters.

**User interaction**

1. *Which steps must be present in the Human UI tool to run through the early design process?*
2. *How can the tool influence the current design process?*

With the steps of the tool in Human UI, it has been tried to mimic the design process as good as possible. Five steps are introduced for this. First the input has to be defined. This is divided into building size, core size and other input parameters. Subsequently, optimisation of the four systems must be executed, which leads to the choice of one system. For this system, the performance criteria are checked. First strength and stiffness, followed by a first foundation design and comfort. It can be concluded that the tool has led to more insight, flexibility and efficiency in the early design process. The comparison of four systems gives insight in the available options and result in a well substantiated decision for one of the systems. Building dimensions can be easily adapted and the tool can speed up the design process. The tool has been applied on De Zalmhaventoren. Similar results concerning element sizes, deflection, foundation design and comfort show the reliability of the tool. A limitation of the tool is that it is specified on only four systems, all executed in concrete. This makes it only usable in specific situations.

**Main question**

To answer the main question and to get an indication of the reliability of the results, first conclusions of other researches and theory are given. Afterwards, the main conclusion of this research is given. Finally, the results are compared. The main question during this thesis was:

*What is the optimal stability system for a concrete high-rise building based on input parameters and optimisation goal for the early design stage?*

A first prediction concerning the maximum height per system was given in paragraph 3.1, based on the theory of Nijsse (2012), Ali and Moon (2007), Smith and Coull (1991), Ching, Onouye, and Zuberbuhler (2014) and Sarkisian (2016). A core was expected to be be optimal until 40 floors or 144 $m$. For shear walls, this is 216 $m$ (60 floors). The prediction for the tube was a maximum of 80 floors or 288 $m$. For the outrigger, the expected maximum height was 252 $m$ or 70 floors. A second comparison can be made based on sustainability and costs from Koopman (2020). Her comparison tool shows a good applicability of shear walls for structures below 200 $m$, where the outrigger and tube are more favourable above 200 $m$. The results of Lankhorst (2018) do not show a clear winner for structures of 150 $m$. For 200 and 250 $m$, the outrigger seems like most optimal, followed by the tube. These results where based on environmental impact.

In this thesis, four concrete stability systems were considered for buildings between 100 and 250 $m$: Shear walls, a core, outrigger and tube. These systems were modelled in one Grasshopper model. Based on a set of input parameters and a variable building height, for all these systems an element size optimisation was executed, while meeting the performance criteria. This was done for three optimisation goals: Minimise element slenderness, minimise total weight and carbon emission and maximise flexibility of floor and facade. The optimisation graphs provided insight into the suitability per system over height. Based on these results, the following can be said: For buildings between 100 and 150 $m$, a core is the best option. Above 150 $m$, element sizes for the core increase massively, which makes the core totally inappropriate. For buildings between 150 and 200 $m$, both the outrigger and shear walls are the most optimal system, when one outrigger is applied. For buildings between 200 and 250 $m$, the tube is the best option.

A comparison between earlier researches and this research is given in table 7.1. The comparison between this research and theory shows quite similar results. Only the upper limit of the outrigger is expected to be higher. The way of execution of the outrigger can be a reason for this. The results of Koopman (2020) show a good applicability of shear walls for 100 and 150 $m$, where this research shows a core to be most favourable around these heights. According to Lankhorst (2018), an outrigger is most optimal for 200 and 250 $m$, followed by the tube. According to this research, a tube is most optimal, followed by the outrigger. The comparison shows quite similar results compared with theory. The results compared with two earlier executed researches are roughly similar. Differences in results can be explained by different assumptions and optimisation criteria. Considering other optimisation goals would probably lead to a different optimal height per system as well.

| Reference | Criteria | Applicability of the systems |
|---|---|---|
| This research | Slenderness, total weight and carbon emission and flexibility | core: 150 - 200 $m$<br>shear walls: 150 - 200 $m$<br>outrigger: 150 - 200 $m$<br>tube: 200 - 250 $m$ |
| Theory (section 3.1) | General | core: max. 144 $m$<br>shear walls: max. 216 $m$<br>outrigger: max. 252 $m$<br>tube: max. 288 $m$ |
| Koopman (2020) | Sustainability and costs | 100 $m$: 1. Shear walls 2. Outrigger 3. Core 4. Tube<br>150 $m$: 1. Shear walls 2. Outrigger 3. Core 4. Tube<br>200 $m$: 1. Shear walls 2. Other systems (inapplicable)<br>250 $m$: 1. Outrigger 2. Tube 3. Other systems (inapplicable) |
| Lankhorst (2018) | Environmental impact | 150 $m$: 1. Core, outrigger and tube<br>200 $m$: 1. Outrigger 2. Tube 3. Core<br>250 $m$: 1. Outrigger 2. Tube 3. Core (inapplicable) |

**Table 7.1** Applicability per system from four references

## 7.2 Discussion

General findings during the research are presented here, as well as an indication of the reliability of the results.

**Parametric model**

- Modelling of the tube: The tube is modelled with horizontal and vertical beam elements in Karamba. A tube could also be modelled with shell elements with perforations, but this is detrimental to the speed of the model. Modelling with beams might lead to another distribution of stresses compared with modelling with shells. Executing a tube with wall elements in practice could possibly lead to high peak stresses around corners of perforations, which has to be analysed separately.

- Workability in Karamba: A finding during the use of Karamba is the reduction in speed of the model as the model becomes more elaborate. This speed is linked to the number of Karamba elements in the model. It is possible to increase the speed by increasing the mesh size in Karamba, but this leads to less accurate results (section 4.4).

- Clearness of Karamba results: An additional disadvantage about the size of the Karamba model is the visualisation of results. This relates to bending moments, shear forces, normal forces and support reactions. It is possible to obtain these results, but it is not possible to have a clear overview of which result belongs to which element. This makes it difficult obtain and compare model output.

- Inaccuracy of optimisation: It was found that the results of the cross section optimisation are inaccurate when the number of elements in the model increase. This is the reason that an alternative way of optimisation is applied, as explained in section 5.1.

**Parametric results (chapter 5)**

- Influence of the floor on the total weight: The optimisation results of total weight and carbon emission (section 5.3.2) are highly influenced by the floor thickness. This means that system choice only has a small influence on weight and carbon emission. Two examples of probably more efficient weight reducing measurements are reducing the maximum floor span and change of floor type. Reducing the maximum floor span by implementation of internal columns has a negative influence on the useful floor area. During building design, a balance has to be made between optimisation priorities.

- Height where outrigger becomes ineffective: In the conclusion is written that the outrigger is the most favourable system between 150 and 200 $m$. This is based on a building with one outrigger of one floor. The conclusion of this that the outrigger as executed in this research can be efficiently applied until 200 $m$, but applying more outriggers with possibly more outrigger floors will probably lead to a higher maximum.

- Interpretation of flexibility: The results for floor flexibility of the shear wall model might feel counter intuitive. Shear walls are expected to have a low flexibility compared with the other systems, but the graphs show the opposite. This is because of the definition used here: The ratio between the available and total floor space.

**User interaction (chapter 6)**

- System choice: The tool compares four stability systems. However, in reality it often occurs that a system is an intermediate form of two systems or a variation on the systems described. Examples of this are a core with an additional wall, a shear wall with flange or a tube executed along a part of the facade. This means that the tool should be used to make a decision between the four main systems. Further specifications can be added in later stages of a project.

## 7.3 Further research and potential

This research was focused on the early design phase of high-rise structures. When looking to the scope of the thesis and to the obtained results, the following areas might be interesting for further research:

### Multiple shear wall configurations

In the research, one shear wall configuration is taken into account. Two continuous walls, spanning in two directions. In practice, it often happens that another wall configuration is required, in particular when the aspect ratio of the floor plan increases. An useful elaboration of the tool is to create an additional system, where the number of walls in both directions, positioning and length of the walls can be determined by the user.

### Other materials

This research was focused on high-rise systems executed in concrete cast-in-situ. An extension could be to make the material choice parametric. This could be one material or multiple materials for one design. For example steel columns or a composite floor. Change of material will not directly influence the stability system. However, it can influence the optimised element sizes, building mass, carbon emission or connection design. This means that addition of other materials could be an interesting extension to the existing model input.

### Reinforcement design

A logical next step after determining the element sizes is reinforcement design (section 3.2.2). A useful addition to the current tool is to make a first estimation for the amount of required reinforcement. This could be done both for the walls, floors and columns.

### Modelling of perforations

Perforations in wall elements (section 3.2.8) can be seen as weak spots due to possibly high peak stresses. Their positioning can be normative when determining thicknesses. In the research, this was taken into account by a multiplication factor for the concrete strength. Adding perforations would give more insight into the influence on their positioning, size and frequency.

### Internal columns

The results in chapter 5.3 show the relatively high utilisation of columns as well as a high influence of the floor on the total weight. This applies in particular to buildings with a relatively big floor plan. Internal columns can result both in a more equal distribution of normal forces over the floor plan and smaller floor spans. This results in thinner floors and a reduced total weight.

### Parametric grid size in two directions

The tool gives the possibility to input the required grid size. One grid size can be set for two directions. However, it might happen that a different grid size is required in both directions.

### Change of optimisation approach

The optimisation approach during this research was to determine first the global dimensions of the building, followed by the optimisation of element sizes to finally compare the four systems. However, it could be interesting to change this approach. A structural engineer might be interested in the question: If I want to apply walls smaller than 500 $mm$, what would be the minimum core size for this building? Or assuming a certain core size and wall thickness, what is the minimum required concrete grade to fulfil performance criteria? Such questions result in another optimisation approach with different input and output.

### Location dependent soil parameters

The calculation procedure of the foundation stiffness as defined in section 3.2.5 and 4.4, does depend on soil parameters. These parameters are based on a clay ground, for example applicable to Rotterdam. A valuable extension would be to make the soil stiffness parametric, as input parameter for the calculation of the foundation.

# References


*NEN-EN 1991 Actions on structures* (2002). EN. NEN. URL: https://www.phd.eng.br/wp-content/uploads/2015/12/en.1991.1.1.2002.pdf.

*Eurocode 7: Geotechnical Design* (2013). Joint Research Centre. European Commission. URL: https://eurocodes.jrc.ec.europa.eu/doc/2013_06_WS_GEO/report/2013_06_WS_GEO.pdf.

Abspoel, R. (2013). *Building Structures 2 Steel part*. TU Delft.

Ali, M. M. and K.S. Moon (2007). "Structural Developments in Tall Buildings: Current Trends and Future Prospects". In: *Architectural Science Review* 50.3, pp. 205–223.

Baldock, R. (2007). "STRUCTURAL OPTIMISATION IN BUILDING DESIGN PRACTICE. CASE-STUDIES IN TOPOLOGY OPTIMISATION OF BRACING SYSTEMS". PhD thesis.

Blauwendraad, J. (2006). *Plate analysis, theory and application*. TU Delft.

Braam, C.R. and P. Lagendijk (2011). *Constructieleer gewapend beton*. CementBetonCentrum.

Bronkhorst, O. (2018). *Trillingen in hoogbouw. Ontwikkeling van een dempingsmodel*. TNO.

Ching, F.D.K., B.S. Onouye, and D. Zuberbuhler (2014). *Building Structures Illustrated*. Wiley.

Choi, H.S. et al. (2012). *Outrigger Design for High-Rise Buildings*. Council on Tall Buildings and Urban Habitat, p. 50.

Coenders, J. and L. Wagemans (2006). *StructuralComponents*.

Dijkstra, A.J. (2008). "High-Rise. Exploring the Ultimate Limits".

Gibbons, O.P. and J.J. Orr (2020). "How to calculate embodied carbon". In:

Gustafsson, D. and J. Hehir (2005). "Stability of Tall Buildings".

Ham, P.H. and K.C. Terwel (2017). *Structural calculations of High Rise Structures*. TU Delft.

Hoenderkamp, J.C.D. (2002). "SIMPLIFIED ANALYSIS OF ASYMMETRIC HIGH-RISE STRUCTURES WITH CORES". In: *THE STRUCTURAL DESIGN OF TALL BUILDINGS* 11, pp. 93–107.

Hoenderkamp, J.C.D., H.H. Snijder, and M.C.M. Bakker (2003). “Preliminary design of high-rise outrigger braced shear wall structures on flexible foundations”. In: *HERON* 48.2, pp. 281–298.

Hubar, S.C.B.L.M. Van Hellenberg (2009). “Duurzaamheid, flexibiliteit en kosten van hoogbouw”.

Hummelen, J.C. (2015). “Precast Concrete in Framed Tube High-Rise Structures”.

Jayachandran, P. (2009). “Design of Tall Buildings. Preliminary Design and Optimization”. PhD thesis.

Khajehpour, S. (2001). “Optimal Conceptual Design of High-Rise Office Buildings”. PhD thesis.

Khajehpour, S. and D.E. Grierson (2003). “Profitability versus safety of high-rise office buildings”. In: *Struct Multidisc Optim* 25, pp. 279–293.

Koopman, E.M.R. (2020). “Rationalising the Structural Material Choice Process for High Rise Buildings in the Netherlands”.

Lagendijk, P. (2016). *Concrete Building Structures*. TU Delft.

Lankhorst, G.J. (2018). “Sustainable structural design of high-rise. Life-cycle assessment of main load bearing structures of high-rise buildings in the Netherlands”.

Liu, Y. (2013). “Effects of Mesh Density on Finite Element Analysis”. In:

McNeel, R. (2020). *Rhinoceros 6*. URL: https://www.rhino3d.com/.

NBBJ (2019). *Human UI*. URL: https://www.food4rhino.com/app/human-ui.

Nijsse, R. (2012). *Dictaat Draagconstructies 2*. TU Delft.

Paauwe, Y. (2020). “Obtaining Insight into the Influence of the Main Parameters in the Preliminary Structural Design on the Wind Induced Dynamic Response Including Soil Structure Interaction Effects of High Rise Buildings in the Netherlands”.

Paling, R. (2020). *Woningnood: ‘Nederland heeft nog een Rotterdam nodig’*. URL: vastgoedmarkt.nl/projectontwikkeling/nieuws/2020/04/woningnood-nederland-heeft-nog-een-rotterdam-nodig-101152968?_ga=2.257126531.945727773.1590477746-2062216650.1590477746.

Preisinger, Clemens (2018). *Karamba3D*. URL: https://www.karamba3d.com/.

Rhijn, A. Van (2020). “Possibilities of timber high-rise. parametric study on the possibilities of timber high-rise in The Netherlands”.

Rolvink, A. (2010). “StructuralComponents2”.

Rolvink, A., J. Coenders, and J. Breider (2011). “StructuralComponents – a parametric associative design toolbox for conceptual structural design”. In:

Rutten, D. (2020). *Grasshopper*. URL: https://www.grasshopper3d.com/.

Sarkisian, M. (2016). *Designing tall buildings*. Routledge.

Simone, A. (2011). *An Introduction to the Analysis of Slender Structures*. TU Delft.

Slooten, E.C. (2018). “Feasibility study of a wood concrete hybrid super tall building and optimization of its wind-induced behaviour. A case study on a skyscraper in the city-centre of Rotterdam”.

Smith, B. Stafford and A. Coull (1991). *Tall Building Structures, Analysis and Design*. John Wiley Sons.

*Achtergronden van de windbelastingen volgens NEN 6lA2:1991* (1992). TNO bouw. TNO.

To, T.T.P. (2020). “Structural optimization of modular high-rise buildings”.

Van Der Linden, L. P. L. (2018). *Parametric Design*. TU Delft.

Van Eerden, S. (2017). “Hoogtepunt voor binnenstedelijke woningbouw”. In: 16, pp. 22–28.

Viik, L.D. (2019). “StructuralComponents6. An early-stage design tool for flexible topologies of mid-rise concrete buildings”.

Zwierzycki, M. (2015). *Anemone*. URL: https://www.food4rhino.com/app/anemone.

# APPENDICES

# Appendix A

# Primary literature research

The primary sources that are used to map recently executed research are mentioned here. First master theses from TU Delft are mentioned, followed by Structural Components. In the last place other theses, PhDs and articles are presented.

## A.1 Theses TU Delft

In the last years, several master theses are written about high-rise buildings and stability systems, often combined with parametric design. A selection of these is listed below.

Dijkstra (2008) tries to explore the ultimate limits of a skyscraper. From a list of fourteen challenges, six are worked out: Load bearing structure, foundation, economical feasibility, comfort, vertical transportation and evacuation. Input parameters of a building are changed to increase the maximum height based on these criteria. Altering the skyscraper's form by changing the footprint of the building, giving the building a tapering shape and creating a compound structure have the biggest influence on this. It can be concluded that it is not possible to find an absolute limit to high-rise, because the limits that are found are largely dependent on assumptions and boundary conditions.

Hubar (2009) investigates the relation between stability systems for high-rise, building sustainability, flexibility and costs. There has been looked to the traditional way of building. This method turns out to be the cheapest, but does not have enough flexibility. The rapport gives three conclusions: Sustainability is more than only environmental impact, flexibility means sustainability and the traditional way of building is wrong. Based on this, a recommendation is done for the choice of floor type and stability system.

Lankhorst (2018) compares five different kind of stability systems and three floor types on their environmental impact. Buildings with a height of 150, 200 and 250 $m$ in The Netherlands are compared, making use of the materials precast concrete, in-situ concrete and steel and all with a concrete core. The environmental impact was calculated by a life-cycle analysis. It is found that both both types of concrete had a low impact and that the outrigger and diagrid are the most effective systems. Potential further research can cover influence of the foundation, use of internal columns or use of lighter floor systems.

Slooten (2018) executes a feasibility study of a wood-concrete hybrid super tall building. He optimizes for its wind-induced behaviour. A 300 $m$ tall timber concrete building under wind loading is designed. Optimisation is done based on stiffness. A parametric study to find dimensions for the columns, thickness of the core wall and outrigger is executed. A system with a braced tube and the economic feasibility of wood-concrete high-rise could be researched in future.

Paauwe (2020) tries to get insight into the influence of the main parameters in the Preliminary Structural Design on the wind-induced dynamic response for high-rise. The influence of design decisions on the dynamic behaviour of a structure is investigated for buildings from 100 till 300 $m$. This under a wind load. Parameters which are studied are height, width, depth, stiffness, mass density and damping ratio. Parameters for the foundation are mass density, foundation depth and soil profile. A frequently response function is determined with a three degrees of freedom model. The goal of the thesis is to find the influence of the parameters on the acceleration at the top. It can firstly be concluded that when height and slenderness increase, the foundation flexibility becomes more important. Secondly, the across wind response is governing over the along-wind response.

Rhijn (2020) executes a parametric study with Dynamo on the possibilities of timber high-rise in The Netherlands. A case study is used to check the results. The maximum building heights are investigated for stability systems with a parametric model, as well as the timber volume and steel mass. Considered systems are either a shear core, diagrid, tube or a combination of two of them. A diagrid system with infinite stiff connections gives the best results.

To (2020) performs a two way coupled cross section (size) and BESO (typology) optimisation of high-rise buildings. Elements are removed by lowest strain energy density. This results in a logical load path and weight reduction. Modular buildings are considered with standardised column and beam dimensions and multiple load cases. In can be concluded that for rectangular buildings the optimised system is more efficient than a core or outrigger, however not for a diagrid.

Koopman (2020) made a decision making framework for the structural material choice for high-rise buildings (between 50 and 250 $m$) in The Netherlands. The goal of the thesis was to give the structural engineer early in the design process insight in the influence of the structural typology on costs and sustainability. Only the height is used as input. A tool is made in which a top ten of the most optimal combinations is given. These are combinations of stability system, material and floor type.

## A.2 StructuralComponents

Coenders and Wagemans (2006) started with a tool to allow the engineer to quickly compose an early-stage structural concept and analyse its performance. It bridges the gap between rough hand calculations and extensive analysis models. The first step in this process was set by Coenders and Wagemans in 2006 with 'Structural Design Tools'. Goal was to guide the computational developments and strategies so that the engineer can support his or her design decisions. Afterwards the tool NetworkedDesigned was developed by Coenders in 2012. Here the life cycle of a building can be followed to reduce the loss of information and the gaps between design engineering processes. These two inventions formed the basis of StructuralComponents. Up to now there are seven versions of StructuralComponents. All with the goal of helping to make well considered design decisions in early design phases. The first two versions have affinity with high-rise. Because version two is an expansion of version one, only this one will be mentioned.

StructuralComponents 2 (Rolvink, 2010) focuses on high-rise and stability systems. A toolbox is developed with components which can be used for parametric modelling of structures. The toolbox exists of a framework, which comprises the core layers, libraries and a representation layer, with a user interface. The first design method applied here is top-down design. This means that distinction is made between different structural typologies. The second method is the bottom-up design. Here a model is assembled existing of different structural elements. This should give insight in the structural performance of the building. Future extensions of the tool can cover multi-disciplinary design with other disciplines integrated, multi-criteria optimisation, tests on real design projects and integrating of building costs.

In StructuralComponents 6 a tool has been developed, based on previous version StructuralComponents 5, that provides early stage structural validation for concrete mid-rise buildings made of shear walls, cores and floors. First, the requirements of such a tool are investigated. A flexible calculation method was developed to determine the forces and deflections. This was implemented in a tool with user-interface included and examined to a real building design.

Jeroen Coenders founder of White-Lioness and initiator of StructuralComponents says the following about parametric design for high-rise: Our tool StructuralComponents now exists of seven parts and new parts are in development. The first two versions are specifically focusing on high-rise. My colleague can send you the reports. Afterwards no further research has been done on this topic within our company. IASS and IABSE or big American engineering firms as Arup, SOM, Happold and Thornton Tomasetti might have. More information might be available on their websites. The plan is to make a parametric model to compare stability systems for early design phases. I do not have models that can already do this, but maybe they exist on the internet. Interesting aspects of the problem which need extra exploration are difficult to address. For this you have to look to conclusions and recommendations of reports.

## A.3 General theses, PhDs and articles

Khajehpour (2001) develops an optimal cost-revenue conceptual design for a high-rise office building. An algorithm is applied for a Pareto optimisation that minimises capital and operating costs and maximises income revenue. This leads to a set of optimal design concepts. In the article of (Khajehpour and Grierson, 2003) this is summarised and analysed further.

Gustafsson and Hehir (2005) examined methods used for stability calculations. They did this for columns, solid shear walls, pierced shear walls, coupled and uncoupled components, cores, single storey structures and multi storey structures.

Baldock (2007) tried to bridge the significant gap between the state-of-the-art design optimisation in research and its practical application in building industry is bridged. Three types of optimisation are discussed: size, shape and topology. An algorithm is developed for topological design of a freeform tower as well as size optimisation. Practical issues in the application of structural optimisation in the building industry are taken into account. The optimum is found for a two dimensional problem where size and typology are combined.

Jayachandran (2009) executes a manual optimisation of five subsystems for a high-rise building. Design issues are discussed to reduce weight. Optimisation is done for the initial structural systems for drift and stresses, based on gravity and lateral loads with an iterative method.

# Appendix B

# Initial verification of the model

## B.1 Verification procedure

Verification is executed by comparing the deflection of the building in the model with the deflection from the fourth order differential equation. This is the the fourth order differential equation for bending of a cantilever beam, which was presented earlier in equation 3.26 and in equation 3.8 for verification of the combination of bending and shear.

To get the best results out of the verification, it is important that the model in Karamba can be approximated as good as possible. To reach this, a number of simplifications are done in the Karamba model:

- Over the height of the tower, the wind force is constant
- Over the height of the tower, the element thickness is constant
- Over the height of the tower, the concrete strength is constant and assumed to be uncracked
- The reduction factor for cutouts in wall elements is 1
- Only wind force is assumed, own weight and horizontal weights are left out

The influence of the outrigger is compared with the theoretical influence of an outrigger from the paper of (Hoenderkamp, Snijder, and Bakker, 2003). The deflection of the construction with and without outrigger will be measured. The optimal position of the outrigger is obtained from figure 3.8 and is between 65% and 70% of the building height. The theoretical influence of the tube is based on the influence of the shear stiffness ($GA$) as was presented in equation 3.9. The positioning of stabilising elements for each system can be found in figure B.1.

## B.2 Execution of verification

Verification will be done for all four systems and two different heights, 144 $m$ and 216 $m$, corresponding with a building of 40 and 60 floors and a floor height of 3.6 $m$. The verification is based on a load of 50 $kN/m$ and a concrete grade C35/45 ($E$=34 $N/mm^2$). The other input parameters are shown in the table:

| l [m] | b [m] | t walls [m] | t columns [m] | core size [m] | grid size [m] | t floor [m] |
|---|---|---|---|---|---|---|
| 21.6 | 21.6 | 0.3 | 0.3 | 7.2 | 3.6 | 0.35 |

**Table B.1** Input parameters verification

The results of the verification are shown in table B.2 till B.5.

| Model | I [$m^4$] | h[m] | $w_{kar}[mm]$ | $w_{dv}[mm]$ | ratio |
|---|---|---|---|---|---|
| 1.1 | 745 | 144 | 98 | 106 | 0.92 |
| 1.2 | 745 | 216 | 519 | 537 | 0.96 |

**Table B.2** Input parameters verification shear walls

| Model | I[$m^4$] | h[m] | $w_{kar}[mm]$ | $w_{dv}[mm]$ | ratio |
|---|---|---|---|---|---|
| 2.1 | 150 | 144 | 588 | 528 | 1.10 |
| 2.2 | 150 | 216 | 2762 | 2673 | 1.03 |

**Table B.3** Input parameters verification core

| Model | h[m] | theoretical infl. | actual infl. |
|---|---|---|---|
| 3.1 | 144 | 43.6% | 43% |
| 3.2 | 216 | 43.6% | 36% |

**Table B.4** Input parameters verification outrigger

| Model | h[m] | theoretical infl. | actual infl. |
|---|---|---|---|
| 4.1 | 144 | 69% | 84% |
| 4.2 | 216 | 69% | 72% |

**Table B.5** Input parameters verification tube

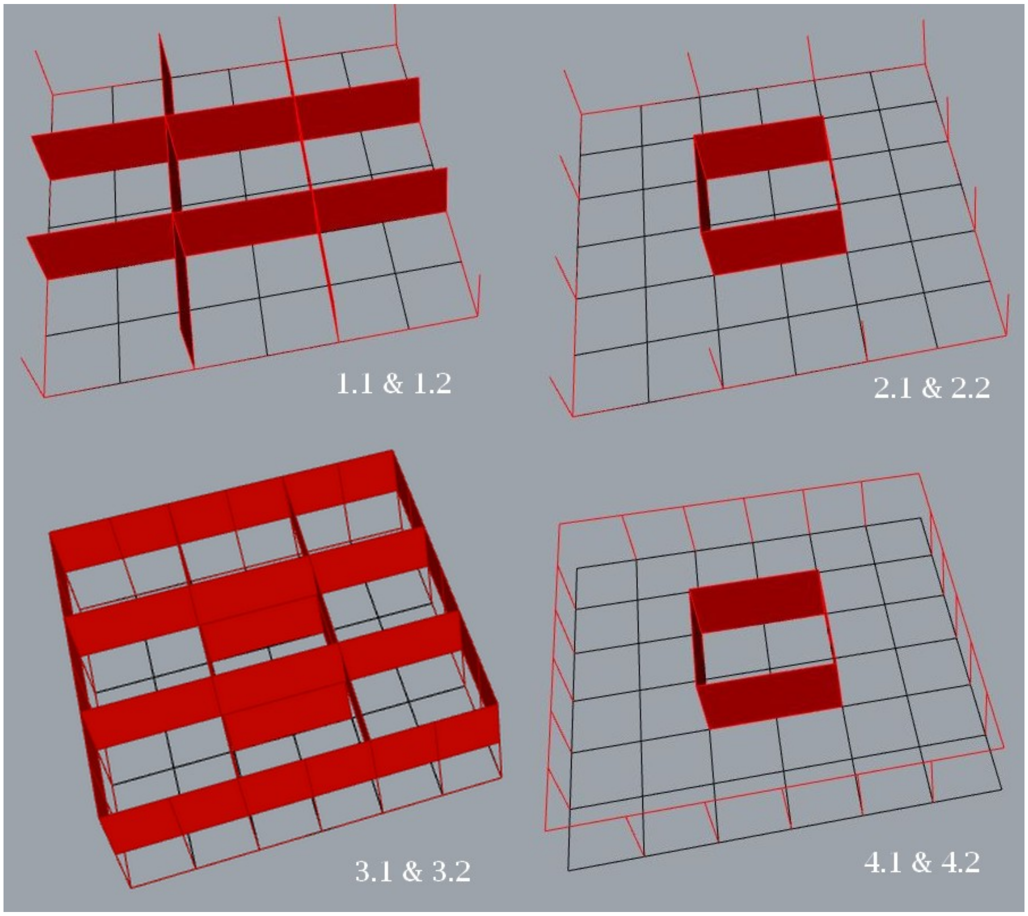


**Figure B.1** Orientation of the structural elements for verification.

## B.3 Conclusion of the verification

It can be concluded that the shear wall model is accurate compared with the differential equation. The maximum difference between them is 8 %, this is an acceptable value. For the core model, the maximum difference is 10 %. This is also acceptable. The outrigger works as expected for the building of 144 $m$. When the height increases, the influence of the outrigger decreases. A reason for this is that one outrigger does not have enough stiffness in this situation. Applying two or more outriggers would be a more logical option in that situation. For the tube model, it can be seen that the influence of the tube is slightly higher than expected. This can be declared with the fact that the calculated shear stiffness with equation 3.9 is a rough estimation, which makes differences in this order of magnitude logical.

# Appendix C

# Parametric modelling

The total Grasshopper script is shown in this appendix. The first image gives an overview of the complete model. The second image shows in which figure the bigger image of that part of the model can be found.

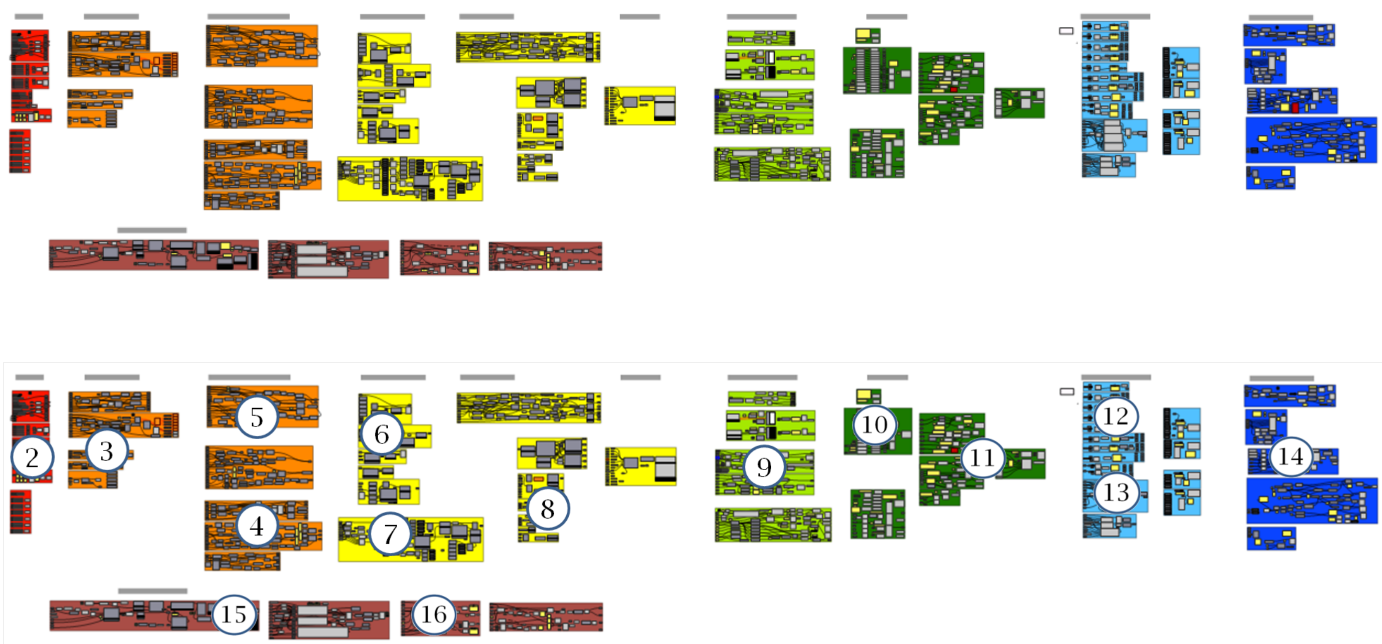


**Figure C.1** Overview of the complete model

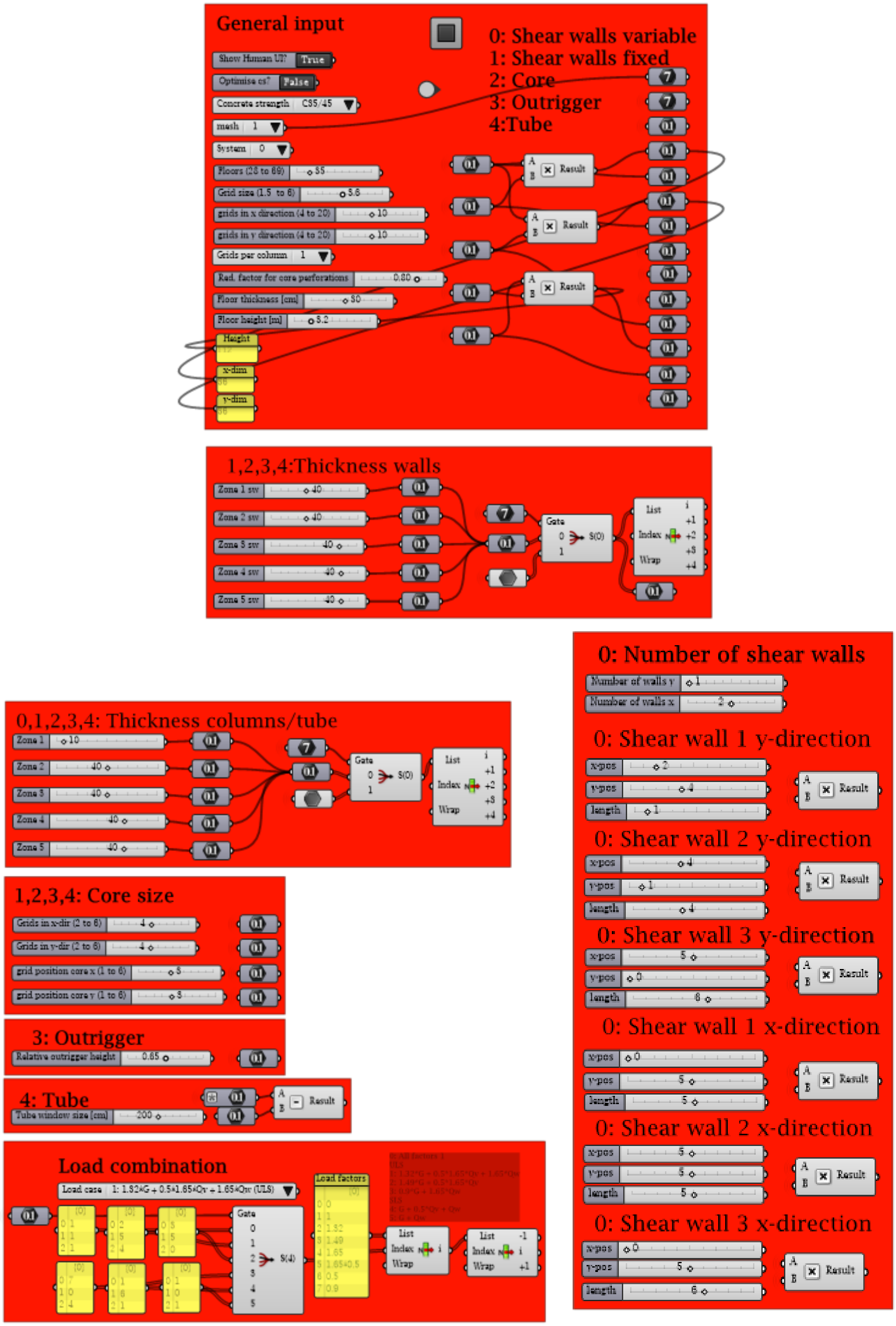


**Figure C.2** Complete model: Input

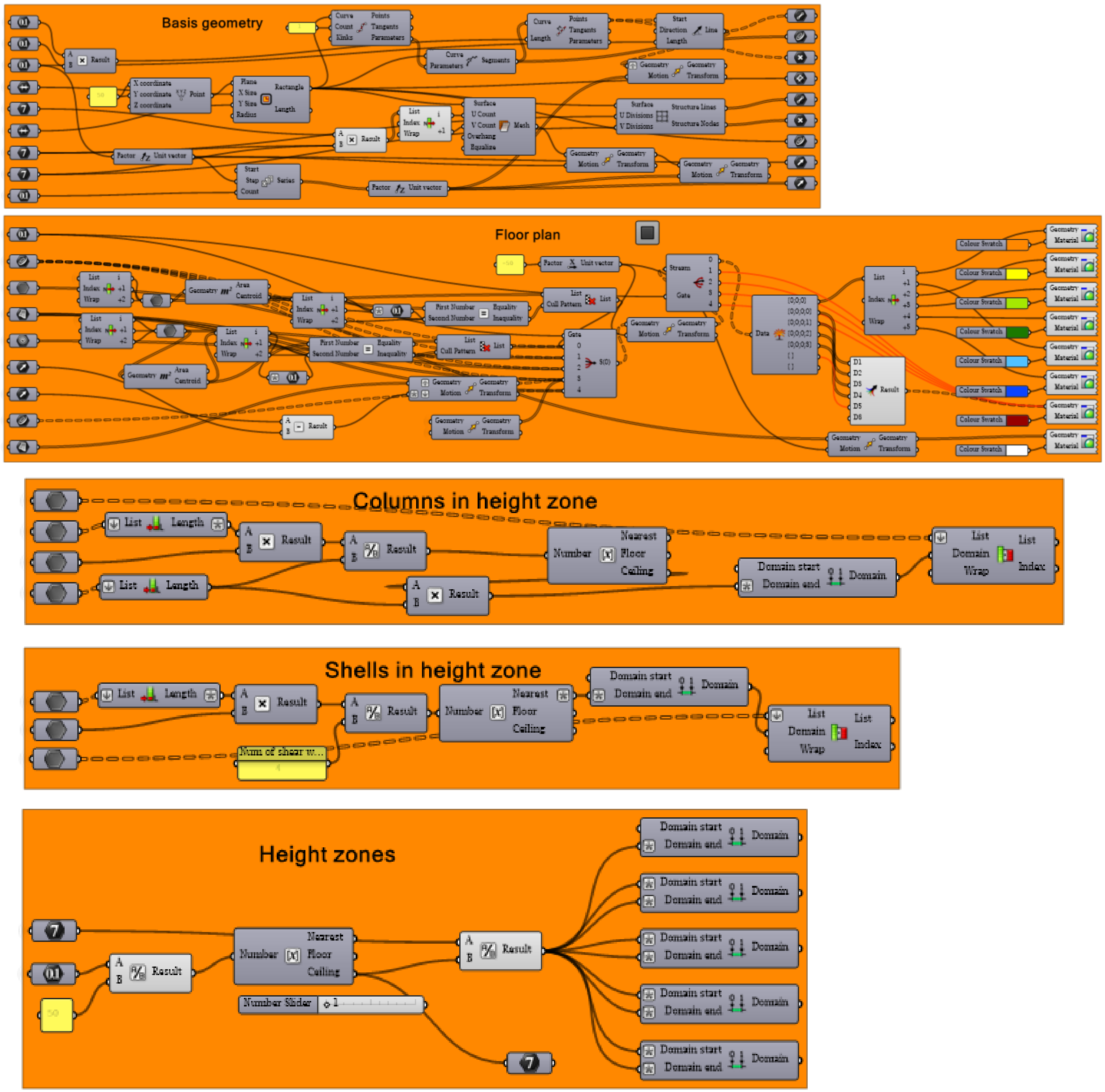


**Figure C.3** Complete model: Basis geometry

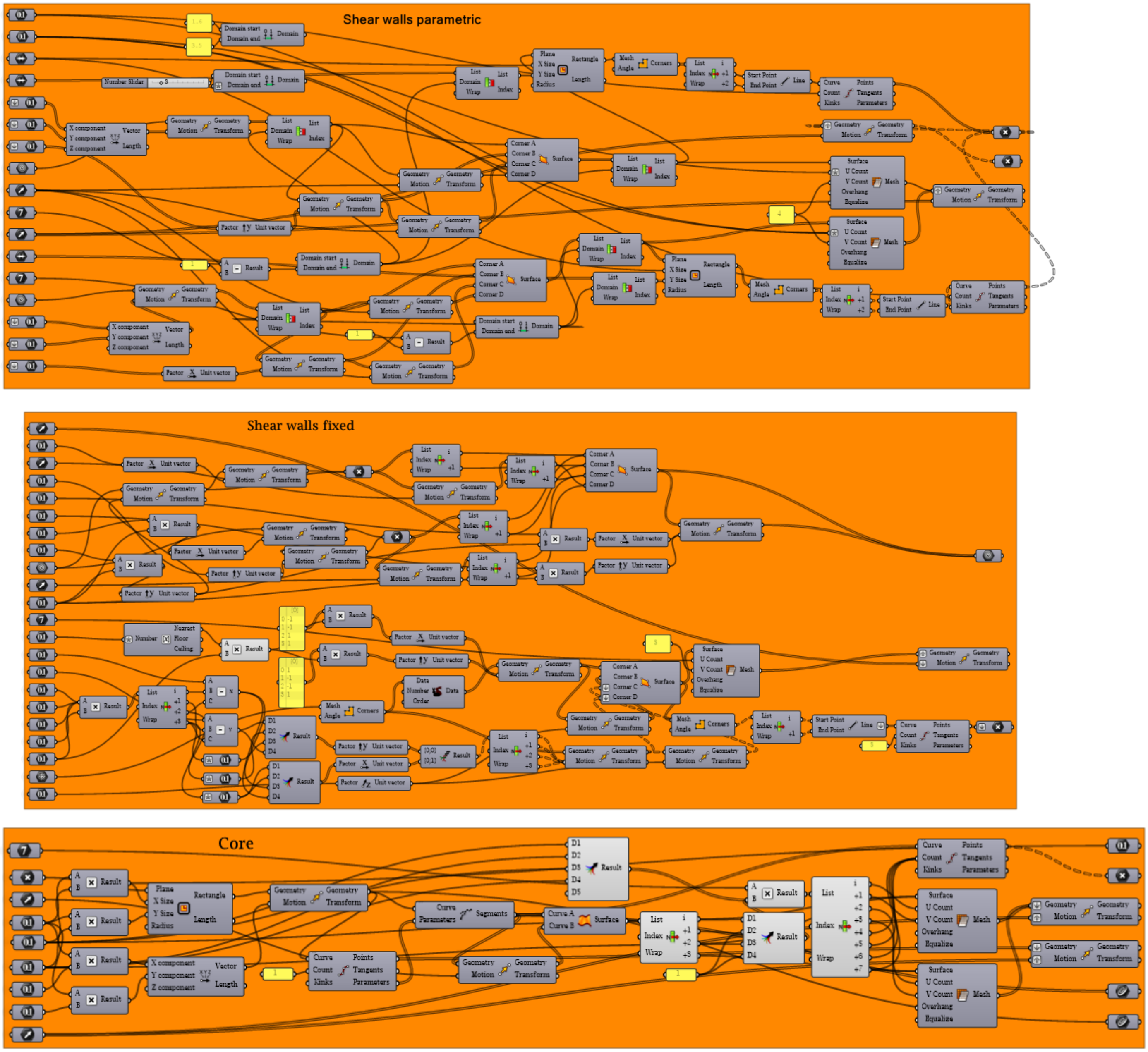


**Figure C.4** Complete model: Shear walls and core

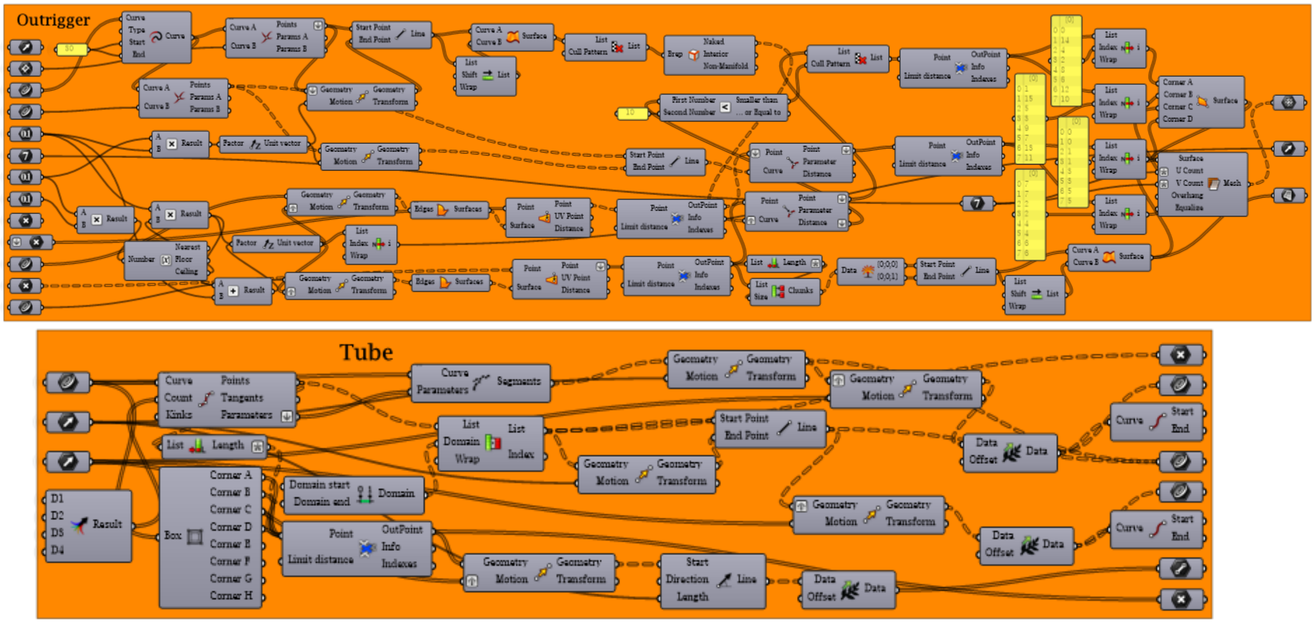


**Figure C.5** Complete model: Outrigger and tube

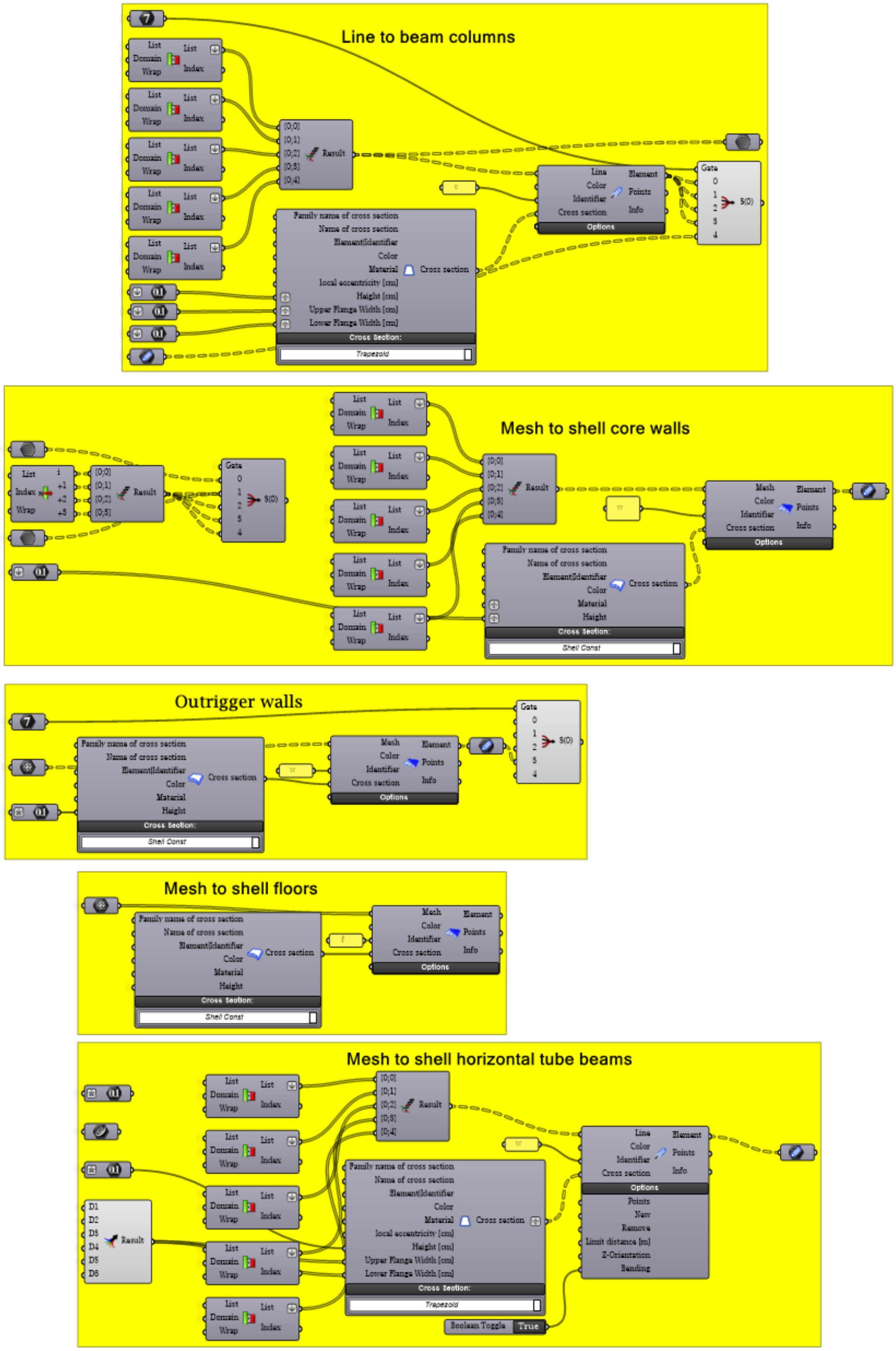


**Figure C.6** Complete model: Karamba input 1

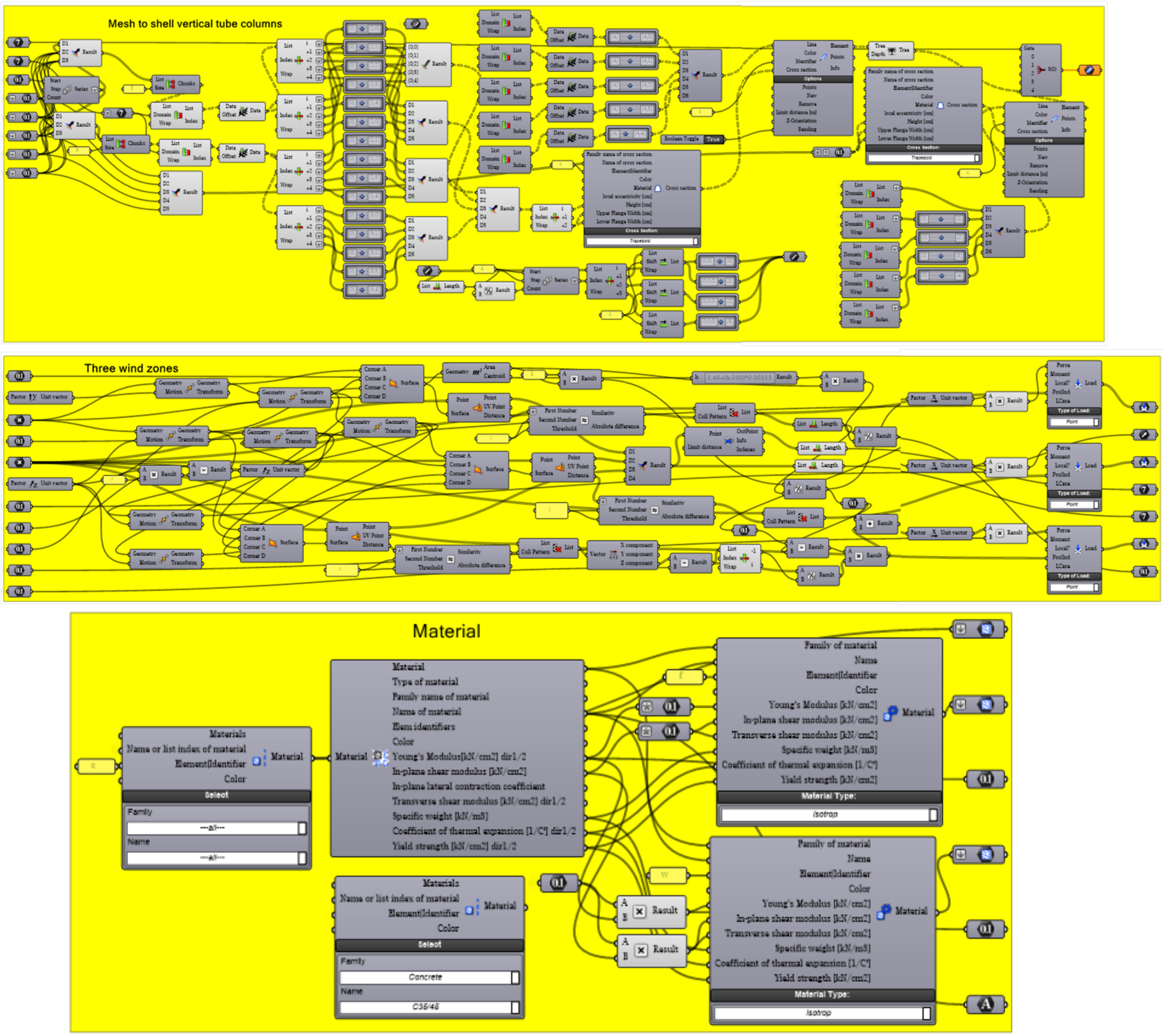


**Figure C.7** Complete model: Karamba input 2

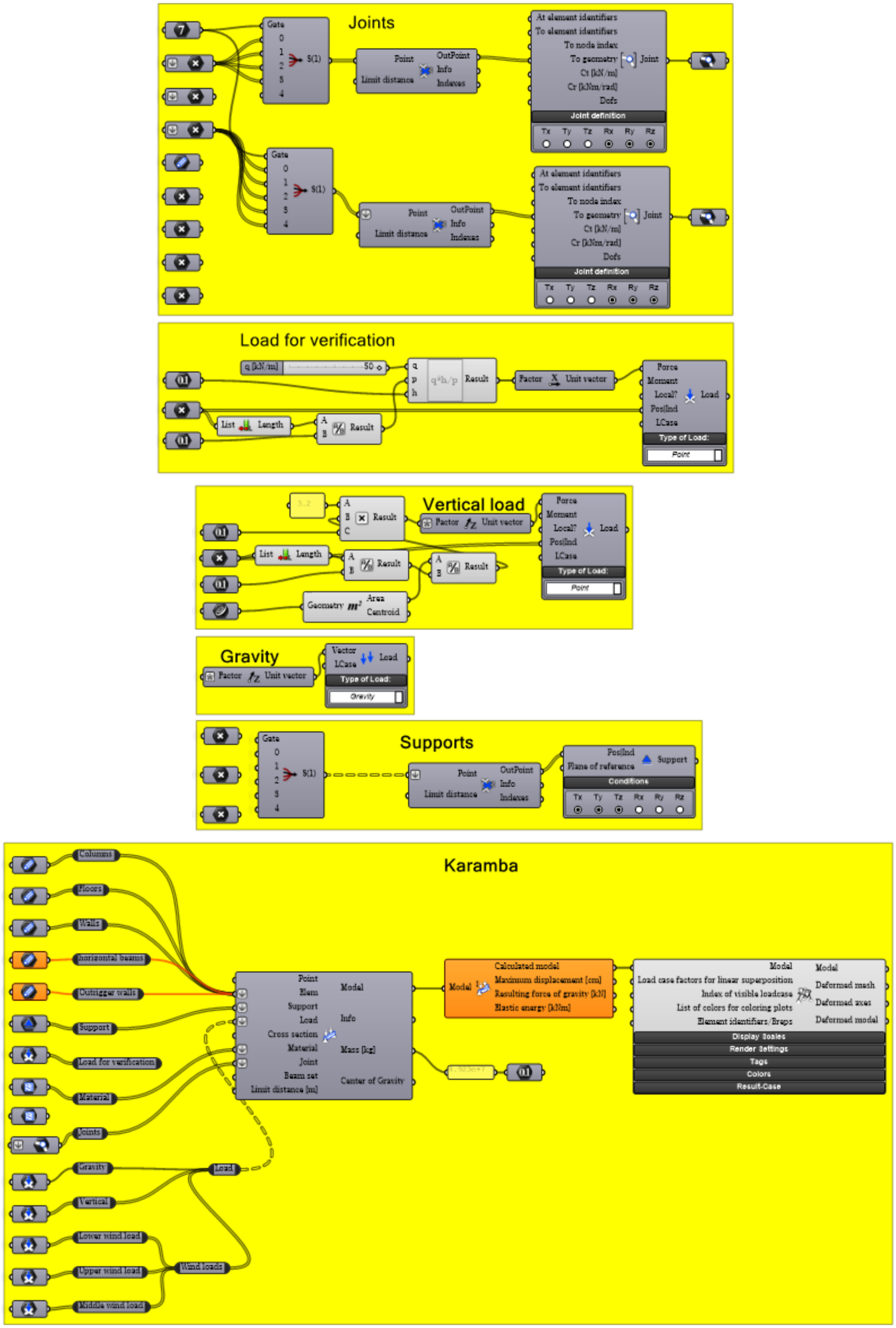


**Figure C.8** Complete model: Karamba input 3 and assembling

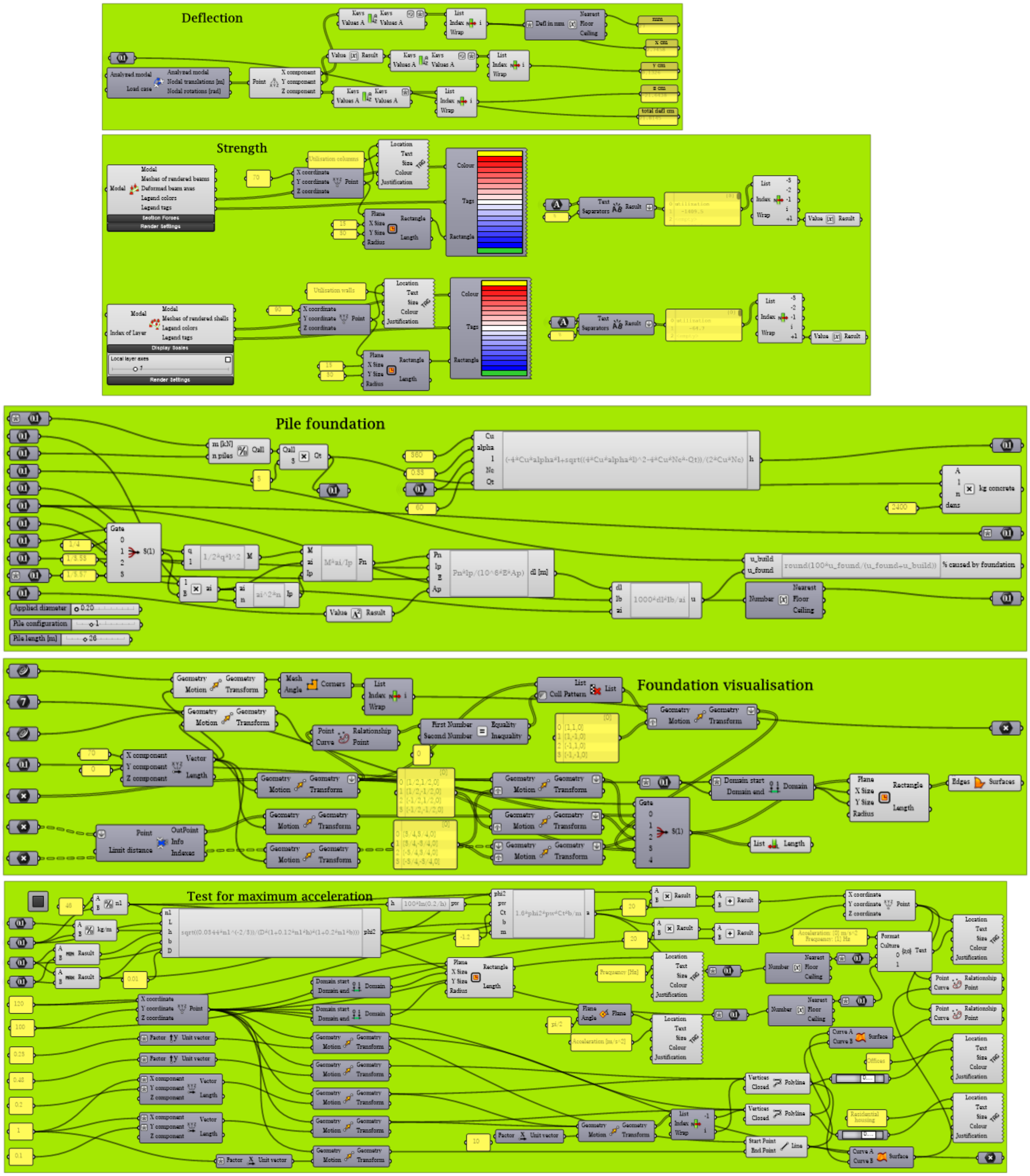


**Figure C.9** Complete model: Performance criteria

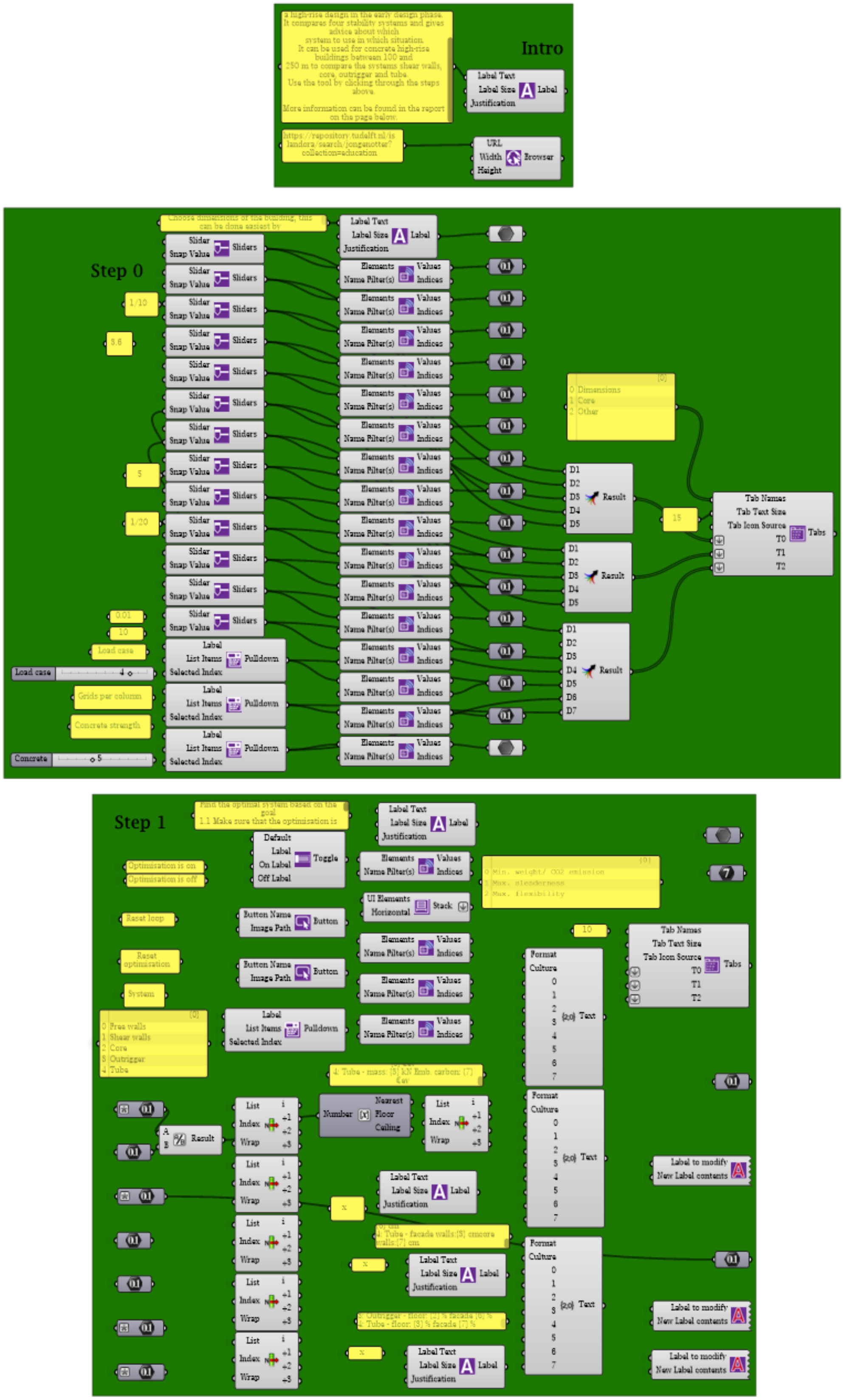

**Figure C.10** Complete model: Human UI intro, step 1 and 2

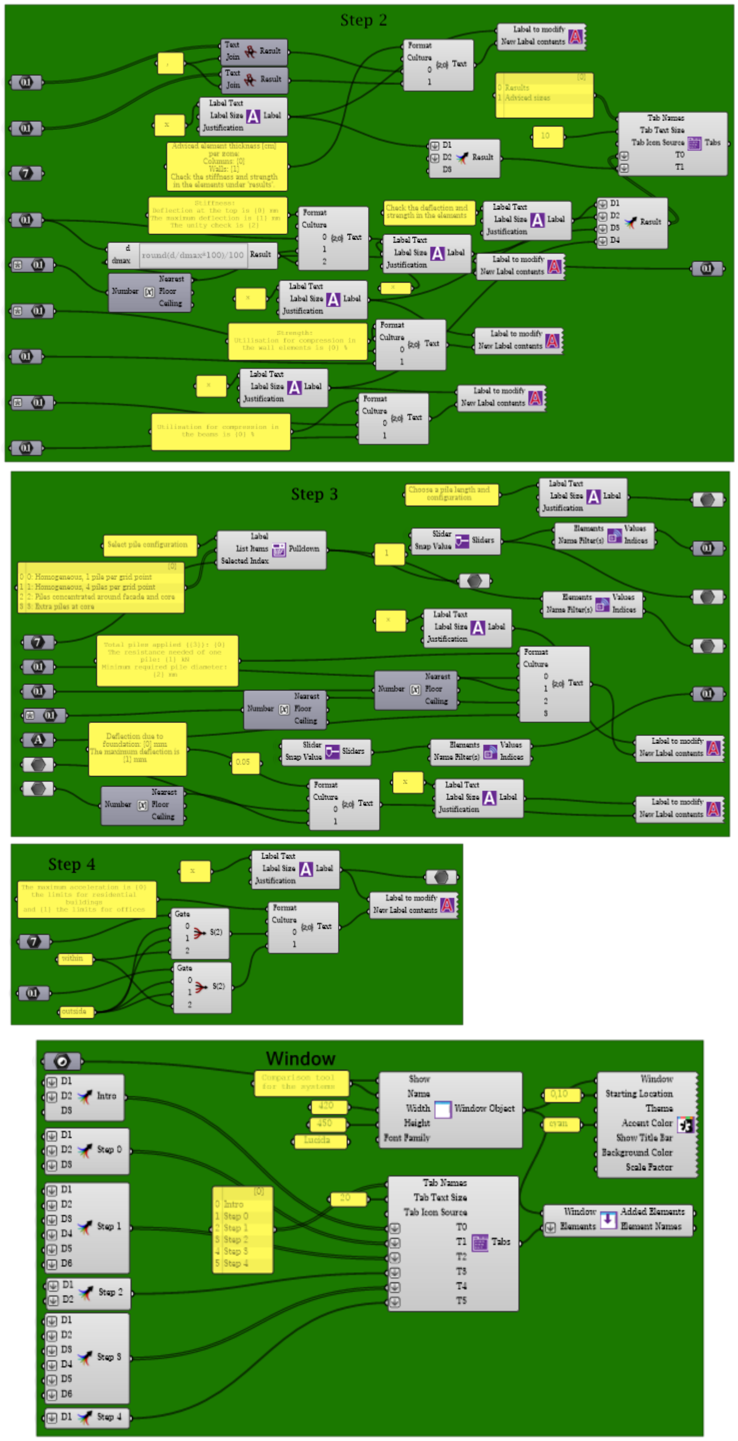


**Figure C.11** Complete model: Human UI step 2, 3, 4 and window

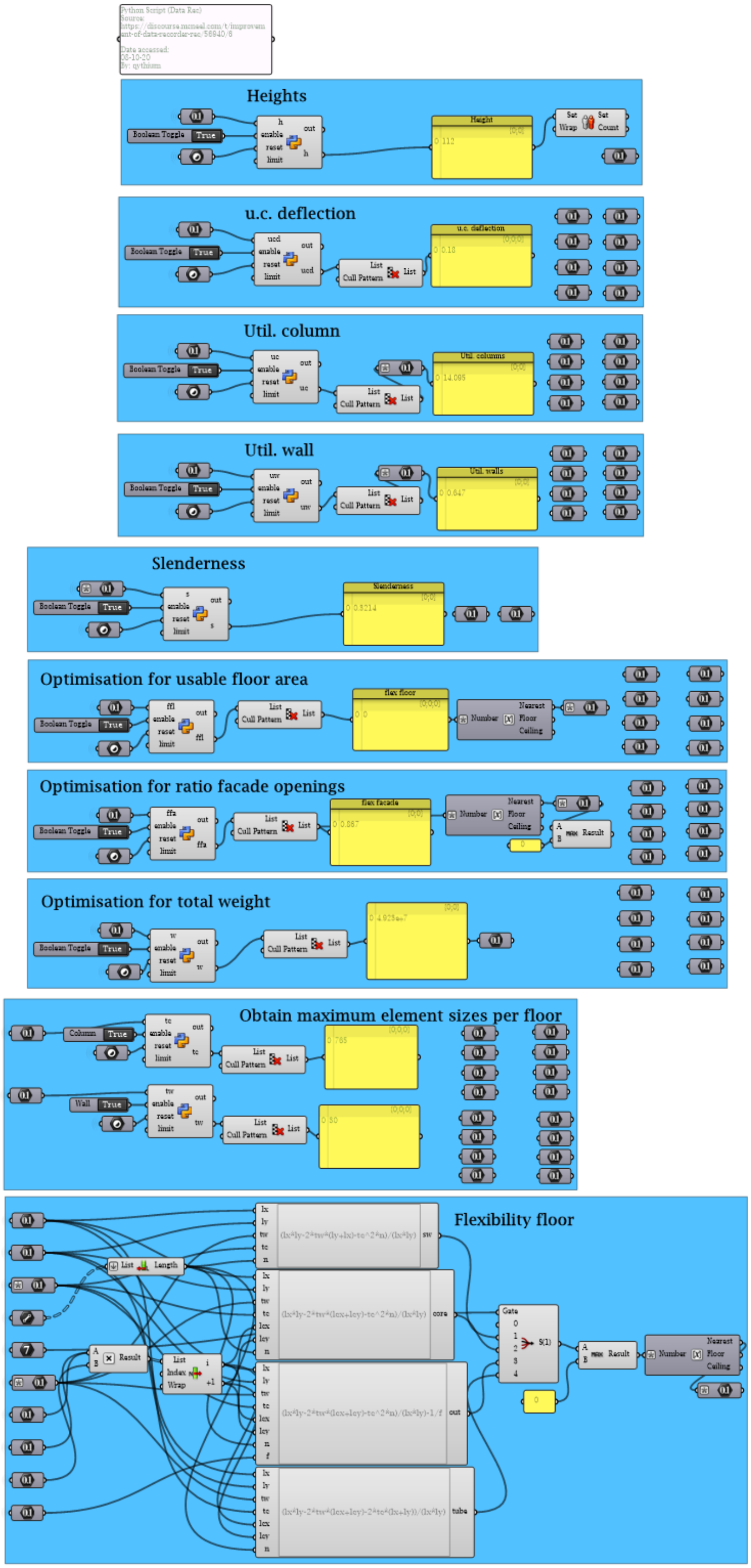


**Figure C.12** Complete model: Assembling optimisation results

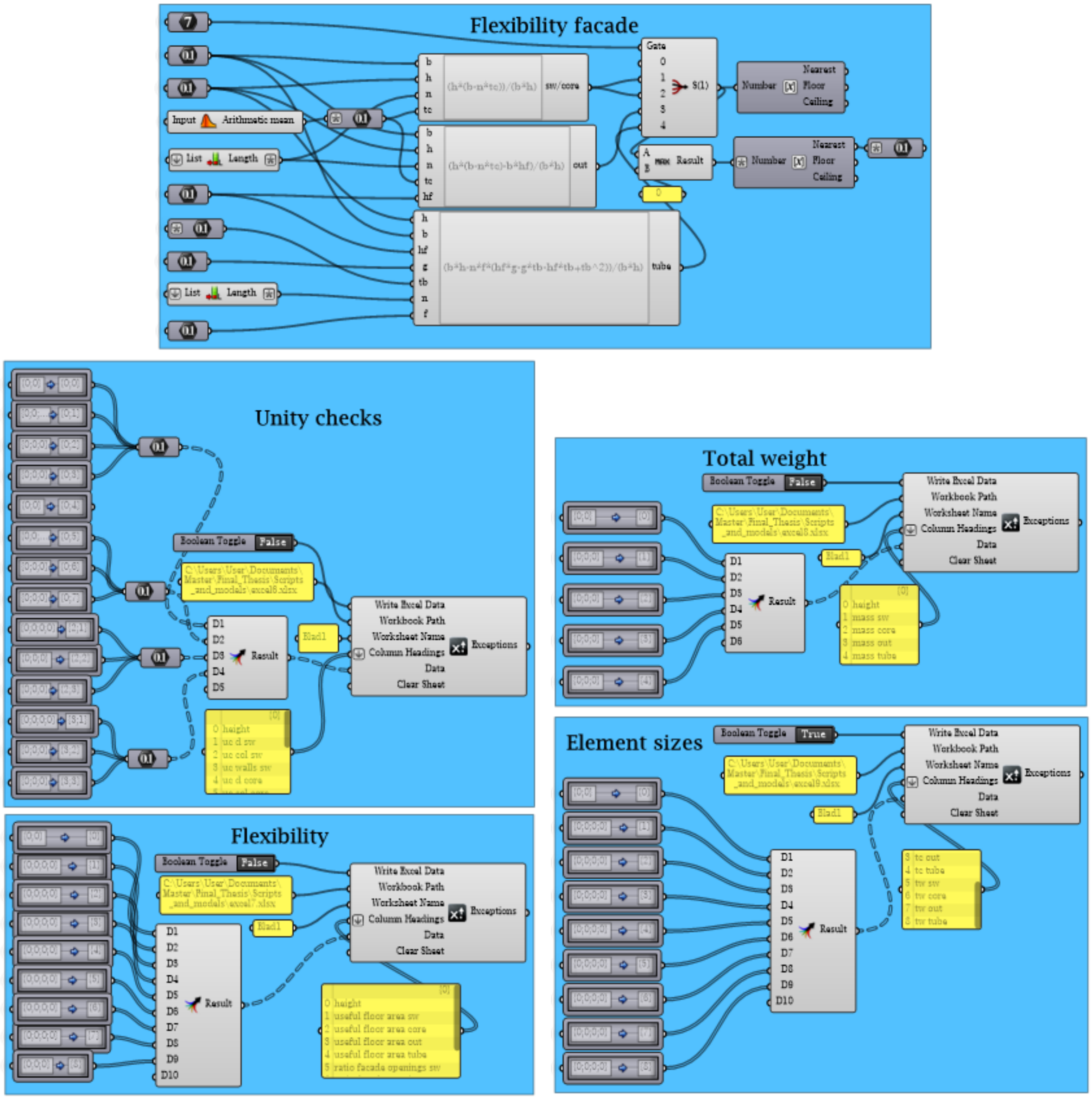


**Figure C.13** Complete model: Assembling optimisation results 2

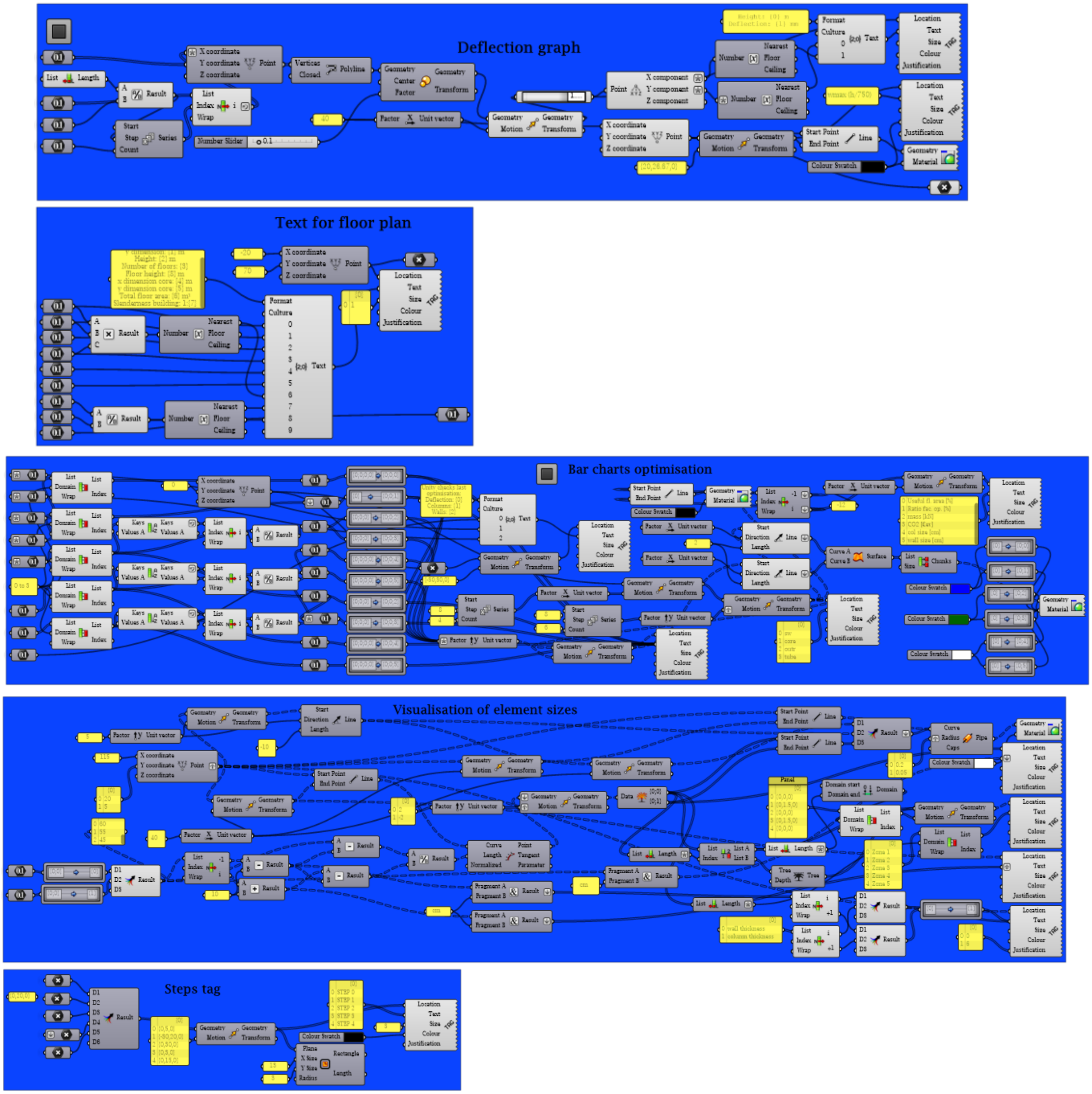


**Figure C.14** Complete model: Visualisation of steps in Human UI

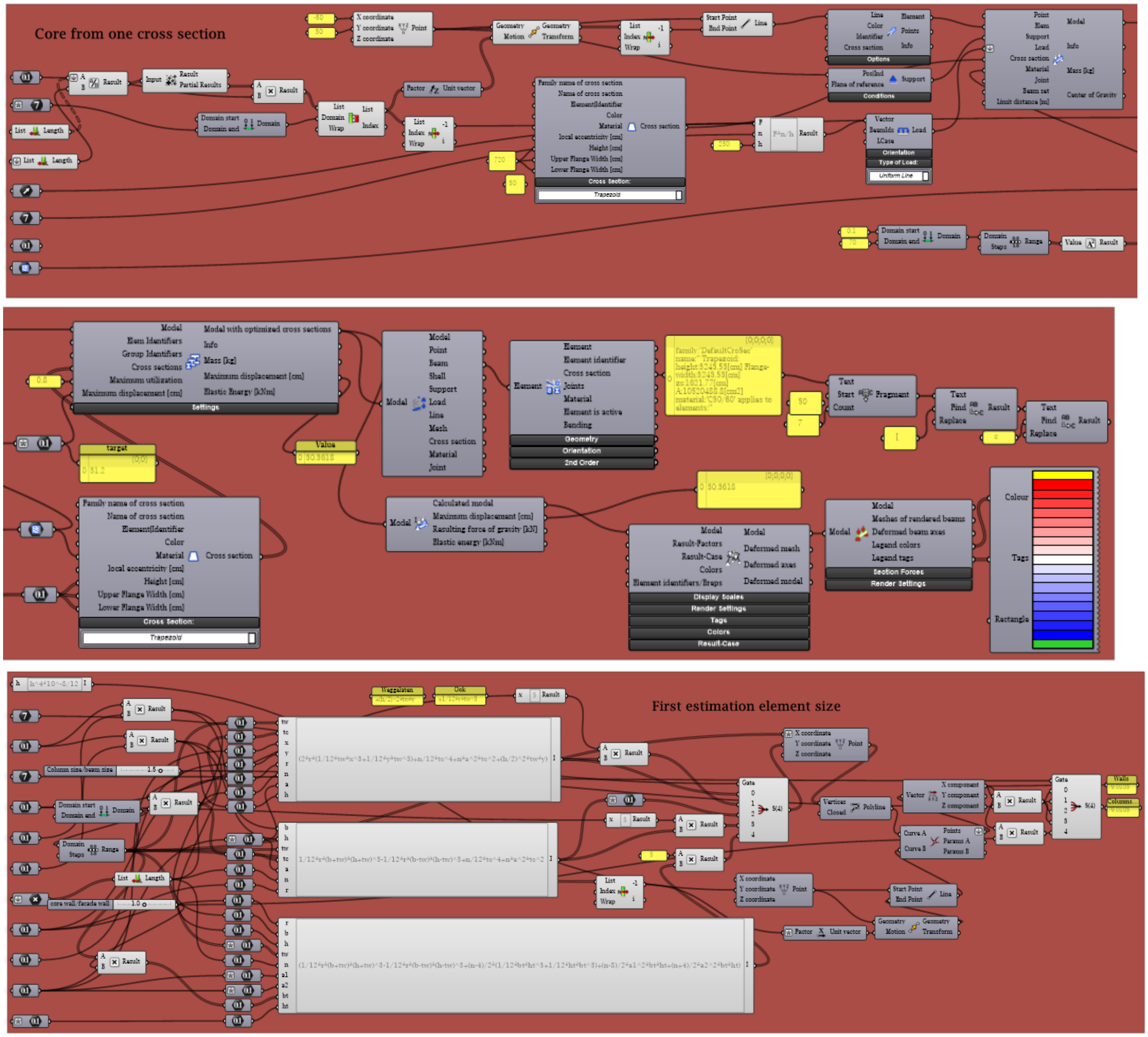


**Figure C.15** Complete model: Optimisation process 1

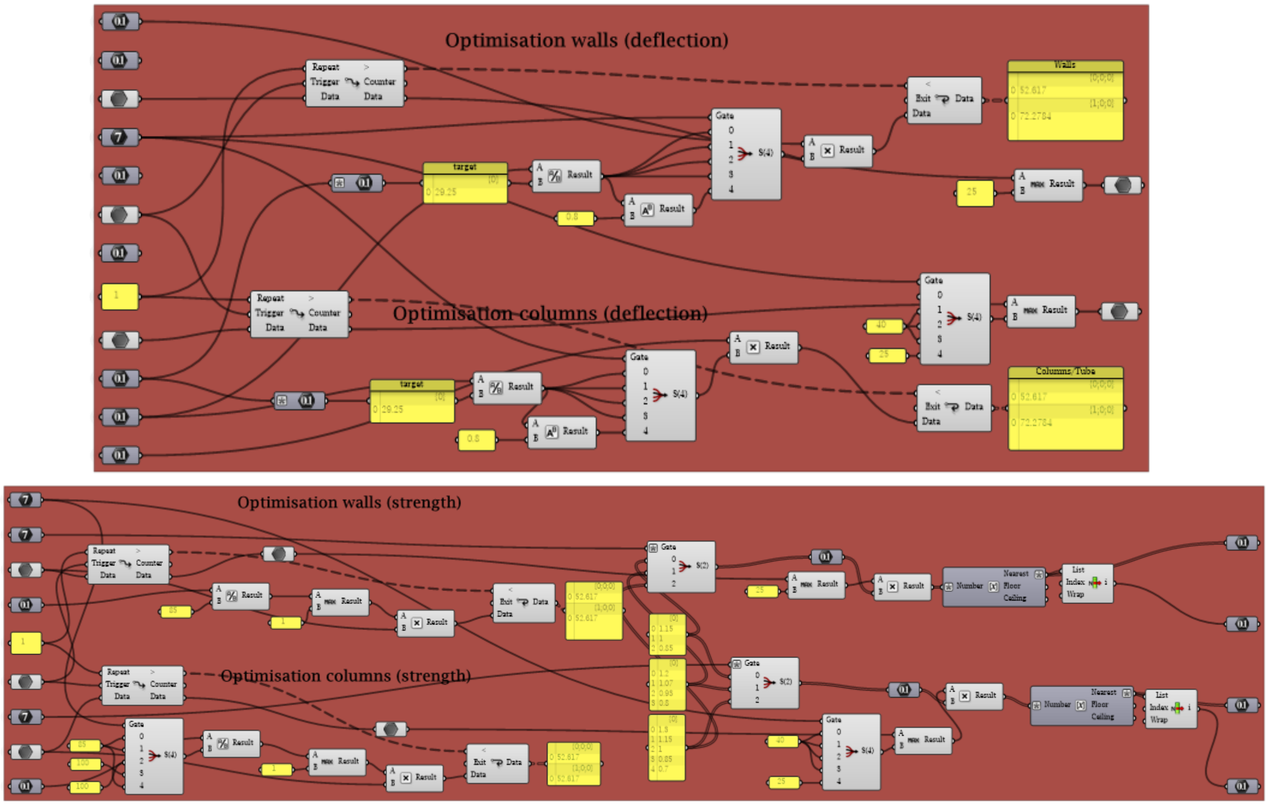


**Figure C.16** Complete model: Optimisation process 2

# Appendix D

# Results of optimisation

The next pages give an overview of the optimisation results from chapter 5.3. The graphs are presented as well as all values from the graphs. First the optimisation results of the unity checks are given, followed by the results for slenderness, total weight and carbon emission and flexibility.

## D.1 Optimisation results unity checks

| height | unity checks defl. sw | unity checks columns sw | unity checks walls sw | unity checks defl. core | unity checks columns core | unity checks walls core |
|---|---|---|---|---|---|---|
| 100,8 | 0,25 | 0,463 | 0,441 | 0,48 | 0,985 | 0,712 |
| 104,4 | 0,29 | 0,522 | 0,47 | 0,55 | 1,016 | 0,735 |
| 108 | 0,29 | 0,545 | 0,487 | 0,6 | 0,915 | 0,763 |
| 111,6 | 0,31 | 0,526 | 0,496 | 0,63 | 0,905 | 0,796 |
| 115,2 | 0,35 | 0,592 | 0,527 | 0,71 | 0,937 | 0,821 |
| 118,8 | 0,35 | 0,616 | 0,525 | 0,78 | 0,963 | 0,851 |
| 122,4 | 0,37 | 0,591 | 0,533 | 0,83 | 0,836 | 0,883 |
| 126 | 0,42 | 0,664 | 0,564 | 0,8 | 0,986 | 0,805 |
| 129,6 | 0,43 | 0,689 | 0,582 | 0,87 | 0,871 | 0,83 |
| 133,2 | 0,44 | 0,658 | 0,57 | 0,9 | 0,894 | 0,86 |
| 136,8 | 0,5 | 0,739 | 0,601 | 0,9 | 0,804 | 0,791 |
| 140,4 | 0,51 | 0,765 | 0,618 | 0,87 | 0,717 | 0,742 |
| 144 | 0,53 | 0,729 | 0,626 | 0,9 | 0,653 | 0,767 |
| 147,6 | 0,58 | 0,818 | 0,636 | 0,91 | 0,602 | 0,719 |
| 151,2 | 0,61 | 0,843 | 0,687 | 0,91 | 0,499 | 0,681 |
| 154,8 | 0,64 | 0,871 | 0,683 | 0,9 | 0,471 | 0,653 |
| 158,4 | 0,68 | 0,899 | 0,716 | 0,9 | 0,448 | 0,634 |
| 162 | 0,73 | 0,928 | 0,737 | 0,91 | 0,396 | 0,611 |
| 165,6 | 0,77 | 0,969 | 0,758 | 0,91 | 0,382 | 0,598 |
| 169,2 | 0,77 | 0,997 | 0,736 | 0,91 | 0,35 | 0,585 |
| 172,8 | 0,81 | 0,886 | 0,769 | 0,92 | 0,338 | 0,574 |
| 176,4 | 0,87 | 0,92 | 0,79 | 0,92 | 0,297 | 0,566 |
| 180 | 0,8 | 0,948 | 0,694 | 0,9 | 0,297 | 0,535 |
| 183,6 | 0,84 | 0,941 | 0,712 | 0,9 | 0,281 | 0,535 |
| 187,2 | 0,83 | 0,977 | 0,737 | 0,91 | 0,27 | 0,533 |
| 190,8 | 0,86 | 0,923 | 0,709 | 0,93 | 0,256 | 0,531 |
| 194,4 | 0,88 | 0,909 | 0,708 | 0,92 | 0,25 | 0,511 |
| 198 | 0,84 | 0,933 | 0,682 | 0,92 | 0,235 | 0,515 |
| 201,6 | 0,87 | 0,938 | 0,631 | 0,91 | 0,21 | 0,475 |
| 205,2 | 0,86 | 0,904 | 0,641 | 0,92 | 0,205 | 0,475 |
| 208,8 | 0,86 | 0,952 | 0,601 | 0,91 | 0,197 | 0,456 |
| 212,4 | 0,86 | 0,961 | 0,6 | 0,93 | 0,195 | 0,458 |
| 216 | 0,86 | 0,887 | 0,588 | 0,92 | 0,191 | 0,454 |
| 219,6 | 0,86 | 0,894 | 0,607 | 0,92 | 0,19 | 0,45 |
| 223,2 | 0,85 | 0,854 | 0,585 | 0,93 | 0,188 | 0,453 |
| 226,8 | 0,86 | 0,891 | 0,561 | 0,94 | 0,185 | 0,442 |
| 230,4 | 0,86 | 0,88 | 0,566 | 0,94 | 0,185 | 0,441 |
| 234 | 0,86 | 0,931 | 0,56 | 0,93 | 0,183 | 0,433 |
| 237,6 | 0,85 | 0,919 | 0,544 | 0,93 | 0,18 | 0,433 |
| 241,2 | 0,85 | 0,949 | 0,535 | 0,92 | 0,182 | 0,428 |
| 244,8 | 0,87 | 0,906 | 0,541 | 0,93 | 0,181 | 0,429 |
| 248,4 | 0,85 | 0,925 | 0,525 | 0,93 | 0,18 | 0,425 |

**Table D.1** Optimisation results for unity checks shear walls and core

| height | unity checks defl. outr. | unity checks columns outr. | unity checks walls outr. | unity checks defl. tube | unity checks columns tube | unity checks walls tube |
|---|---|---|---|---|---|---|
| **100,8** | 0,3 | 0,928 | 0,713 | 0,25 | 0,89 | 0,553 |
| **104,4** | 0,35 | 0,964 | 0,738 | 0,27 | 0,899 | 0,578 |
| **108** | 0,38 | 0,996 | 0,766 | 0,28 | 0,724 | 0,594 |
| **111,6** | 0,4 | 1,028 | 0,796 | 0,29 | 0,731 | 0,608 |
| **115,2** | 0,42 | 0,966 | 0,801 | 0,32 | 0,741 | 0,636 |
| **118,8** | 0,46 | 0,992 | 0,83 | 0,33 | 0,751 | 0,653 |
| **122,4** | 0,49 | 0,976 | 0,857 | 0,34 | 0,757 | 0,662 |
| **126** | 0,51 | 0,862 | 0,879 | 0,36 | 0,776 | 0,687 |
| **129,6** | 0,54 | 0,897 | 0,911 | 0,38 | 0,786 | 0,706 |
| **133,2** | 0,52 | 0,913 | 0,827 | 0,39 | 0,791 | 0,715 |
| **136,8** | 0,57 | 0,812 | 0,839 | 0,43 | 0,816 | 0,745 |
| **140,4** | 0,61 | 0,835 | 0,866 | 0,45 | 0,824 | 0,765 |
| **144** | 0,62 | 0,873 | 0,883 | 0,46 | 0,83 | 0,772 |
| **147,6** | 0,68 | 0,838 | 0,899 | 0,48 | 0,695 | 0,802 |
| **151,2** | 0,69 | 0,88 | 0,849 | 0,48 | 0,772 | 0,808 |
| **154,8** | 0,72 | 0,893 | 0,893 | 0,5 | 0,79 | 0,838 |
| **158,4** | 0,77 | 0,924 | 0,895 | 0,53 | 0,814 | 0,862 |
| **162** | 0,78 | 0,865 | 0,916 | 0,54 | 0,822 | 0,775 |
| **165,6** | 0,79 | 0,958 | 0,866 | 0,54 | 0,754 | 0,784 |
| **169,2** | 0,85 | 0,976 | 0,902 | 0,54 | 0,768 | 0,804 |
| **172,8** | 0,82 | 0,871 | 0,84 | 0,56 | 0,789 | 0,821 |
| **176,4** | 0,87 | 0,899 | 0,85 | 0,59 | 0,81 | 0,845 |
| **180** | 0,9 | 0,825 | 0,871 | 0,61 | 0,817 | 0,861 |
| **183,6** | 0,92 | 0,762 | 0,877 | 0,6 | 0,751 | 0,878 |
| **187,2** | 0,91 | 0,787 | 0,827 | 0,68 | 0,938 | 0,82 |
| **190,8** | 0,91 | 0,74 | 0,84 | 0,67 | 0,867 | 0,832 |
| **194,4** | 0,95 | 0,683 | 0,855 | 0,64 | 0,815 | 0,842 |
| **198** | 0,95 | 0,644 | 0,809 | 0,72 | 0,895 | 0,86 |
| **201,6** | 0,94 | 0,606 | 0,767 | 0,79 | 0,891 | 0,827 |
| **205,2** | 0,92 | 0,609 | 0,733 | 0,74 | 0,792 | 0,749 |
| **208,8** | 0,92 | 0,562 | 0,706 | 0,83 | 0,915 | 0,8 |
| **212,4** | 0,94 | 0,529 | 0,724 | 0,76 | 0,832 | 0,742 |
| **216** | 0,93 | 0,492 | 0,697 | 0,83 | 0,93 | 0,777 |
| **219,6** | 0,93 | 0,457 | 0,675 | 0,8 | 0,865 | 0,731 |
| **223,2** | 0,96 | 0,468 | 0,689 | 0,79 | 0,812 | 0,726 |
| **226,8** | 0,93 | 0,443 | 0,678 | 0,84 | 0,881 | 0,723 |
| **230,4** | 0,92 | 0,43 | 0,677 | 0,85 | 0,823 | 0,741 |
| **234** | 0,91 | 0,408 | 0,677 | 0,84 | 0,845 | 0,708 |
| **237,6** | 0,93 | 0,385 | 0,707 | 0,85 | 0,802 | 0,728 |
| **241,2** | 0,93 | 0,397 | 0,708 | 0,84 | 0,817 | 0,691 |
| **244,8** | 0,93 | 0,356 | 0,725 | 0,85 | 0,785 | 0,716 |
| **248,4** | 0,93 | 0,348 | 0,711 | 0,84 | 0,784 | 0,693 |

**Table D.2** Optimisation results unity checks outrigger and tube

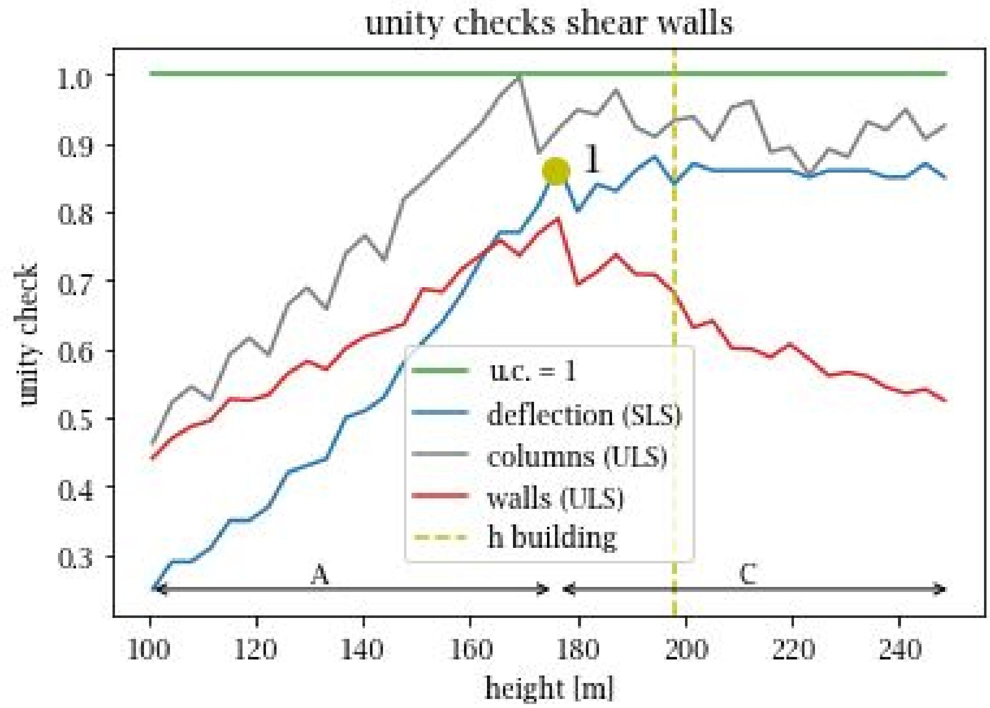
unity checks shear walls
unity check
height [m]
1.0
0.9
0.8
0.7
0.6
0.5
0.4
0.3
100
120
140
160
180
200
220
240
1
A
C
u.c. = 1
deflection (SLS)
columns (ULS)
walls (ULS)
h building

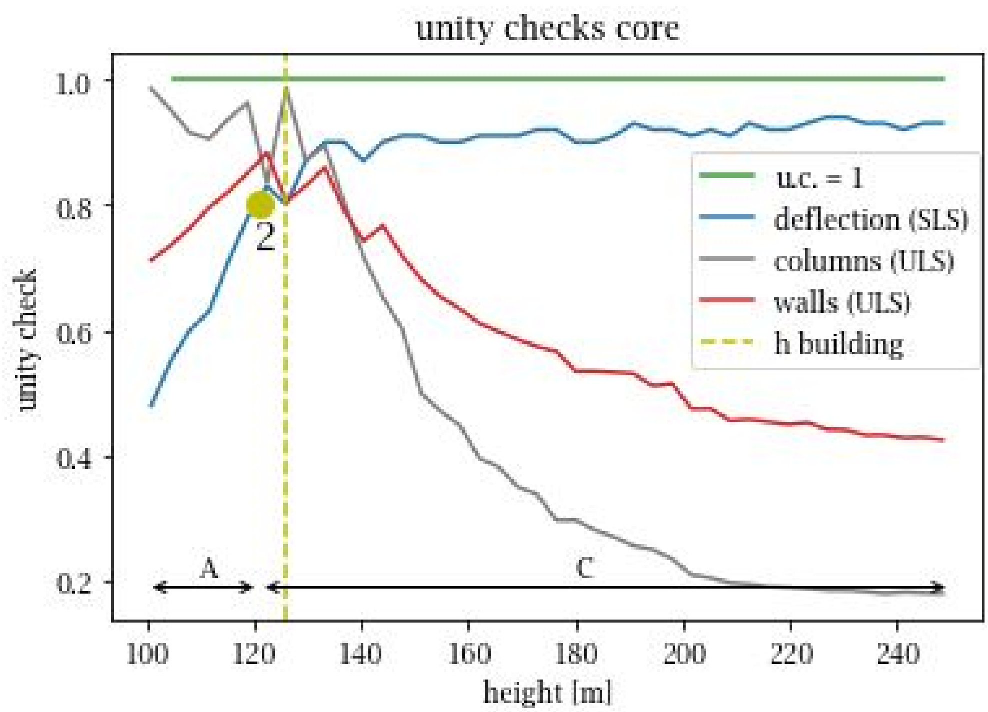
unity checks core
unity check
height [m]
1.0
0.8
0.6
0.4
0.2
100
120
140
160
180
200
220
240
2
A
C
u.c. = 1
deflection (SLS)
columns (ULS)
walls (ULS)
h building

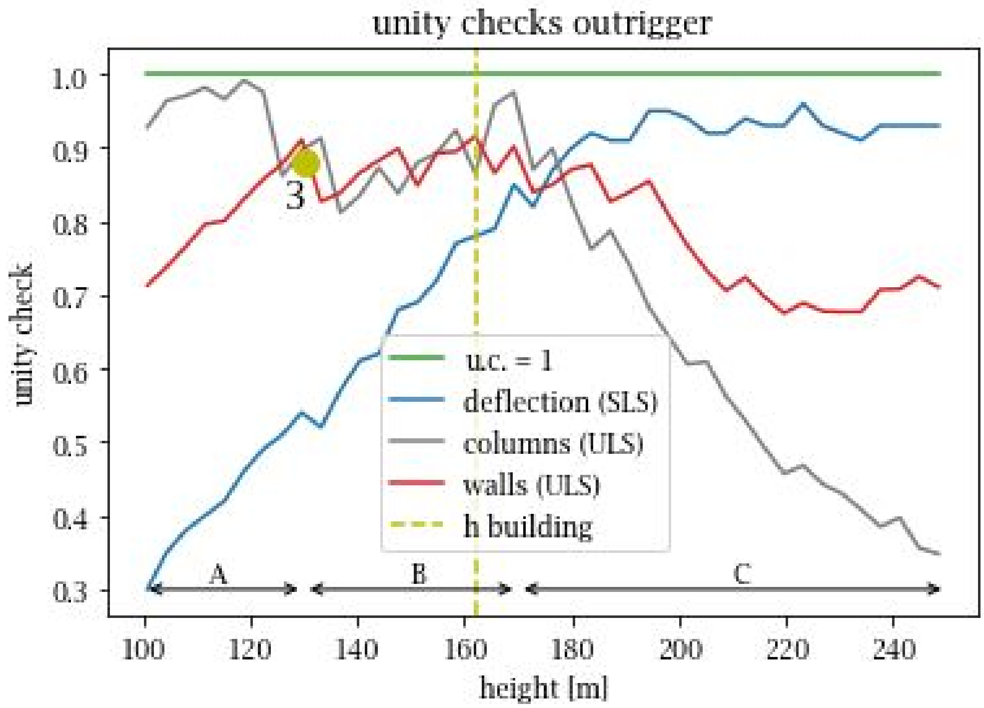
unity checks outrigger
unity check
height [m]
3
A
B
C
u.c. = 1
deflection (SLS)
columns (ULS)
walls (ULS)
h building

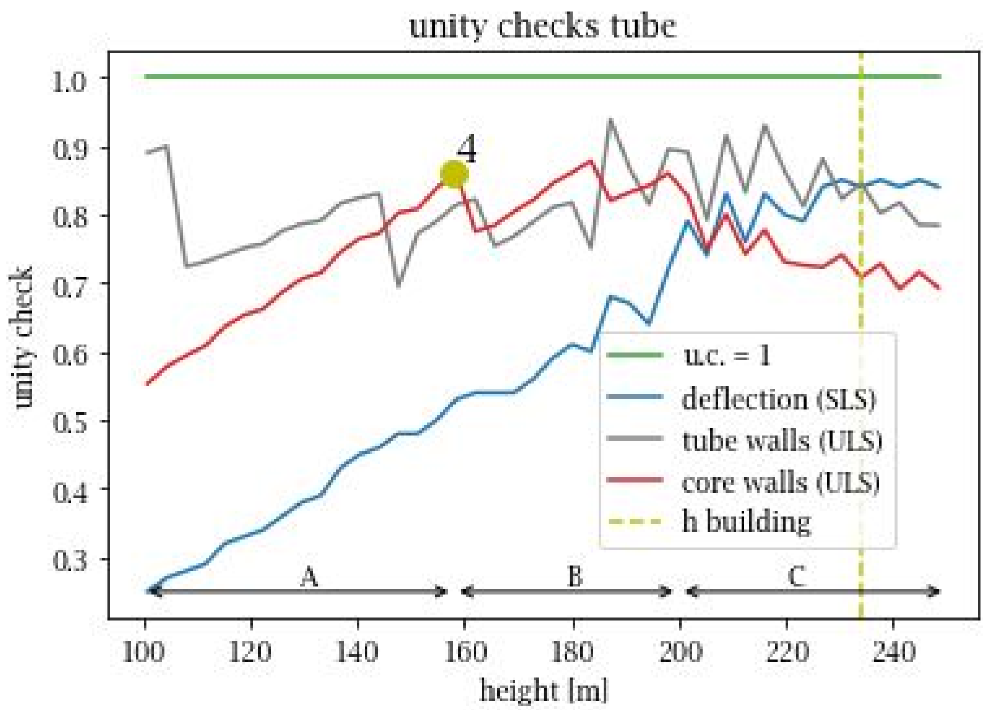
unity checks tube
unity check
height [m]
4
A
B
C
u.c. = 1
deflection (SLS)
tube walls (ULS)
core walls (ULS)
h building

## D.2 Optimisation results slenderness [cm]

| height | maximum column thickness shear wall | maximum column thickness core | maximum column thickness outrigger | maximum column thickness tube | maximum wall thickness shear wall | maximum wall thickness core | maximum wall thickness outrigger | maximum wall thickness tube |
|---|---|---|---|---|---|---|---|---|
| 100,8 | 45 | 45 | 45 | 30 | 30 | 30 | 30 | 30 |
| 104,4 | 45 | 45 | 45 | 30 | 30 | 30 | 30 | 30 |
| 108 | 45 | 50 | 45 | 30 | 30 | 30 | 30 | 30 |
| 111,6 | 45 | 50 | 45 | 30 | 30 | 30 | 30 | 30 |
| 115,2 | 45 | 50 | 50 | 30 | 30 | 30 | 30 | 30 |
| 118,8 | 50 | 50 | 50 | 30 | 30 | 30 | 30 | 30 |
| 122,4 | 50 | 55 | 50 | 30 | 30 | 30 | 30 | 30 |
| 126 | 50 | 50 | 55 | 30 | 30 | 35 | 30 | 30 |
| 129,6 | 50 | 55 | 55 | 35 | 30 | 35 | 30 | 30 |
| 133,2 | 55 | 55 | 55 | 35 | 30 | 35 | 35 | 30 |
| 136,8 | 55 | 60 | 60 | 35 | 30 | 40 | 35 | 30 |
| 140,4 | 55 | 65 | 60 | 35 | 30 | 45 | 35 | 30 |
| 144 | 55 | 70 | 60 | 35 | 30 | 45 | 35 | 30 |
| 147,6 | 60 | 75 | 65 | 35 | 30 | 50 | 35 | 30 |
| 151,2 | 50 | 85 | 65 | 45 | 30 | 55 | 40 | 30 |
| 154,8 | 55 | 90 | 65 | 45 | 30 | 60 | 40 | 30 |
| 158,4 | 55 | 95 | 60 | 45 | 30 | 65 | 40 | 30 |
| 162 | 55 | 105 | 65 | 45 | 30 | 70 | 40 | 35 |
| 165,6 | 55 | 110 | 65 | 50 | 30 | 75 | 45 | 35 |
| 169,2 | 60 | 120 | 60 | 50 | 30 | 80 | 45 | 35 |
| 172,8 | 60 | 125 | 65 | 50 | 30 | 85 | 50 | 35 |
| 176,4 | 60 | 140 | 65 | 50 | 30 | 90 | 50 | 35 |
| 180 | 65 | 145 | 65 | 50 | 35 | 100 | 50 | 35 |
| 183,6 | 65 | 155 | 75 | 55 | 35 | 105 | 50 | 35 |
| 187,2 | 70 | 165 | 75 | 50 | 35 | 110 | 55 | 40 |
| 190,8 | 65 | 175 | 80 | 50 | 40 | 115 | 55 | 40 |
| 194,4 | 70 | 185 | 85 | 55 | 40 | 125 | 55 | 40 |
| 198 | 65 | 200 | 90 | 50 | 45 | 130 | 60 | 40 |
| 201,6 | 70 | 215 | 100 | 55 | 50 | 145 | 65 | 45 |
| 205,2 | 75 | 225 | 100 | 60 | 50 | 150 | 70 | 50 |
| 208,8 | 80 | 245 | 110 | 55 | 55 | 165 | 75 | 50 |
| 212,4 | 85 | 255 | 115 | 65 | 55 | 170 | 75 | 55 |
| 216 | 90 | 270 | 120 | 60 | 60 | 180 | 80 | 55 |
| 219,6 | 95 | 285 | 130 | 65 | 60 | 190 | 85 | 60 |
| 223,2 | 100 | 295 | 130 | 70 | 65 | 195 | 85 | 60 |
| 226,8 | 100 | 315 | 140 | 65 | 70 | 210 | 95 | 65 |
| 230,4 | 105 | 330 | 150 | 65 | 70 | 220 | 100 | 65 |
| 234 | 115 | 350 | 155 | 70 | 75 | 235 | 105 | 70 |
| 237,6 | 120 | 370 | 160 | 70 | 80 | 245 | 105 | 70 |
| 241,2 | 125 | 380 | 165 | 75 | 85 | 255 | 110 | 75 |
| 244,8 | 130 | 405 | 175 | 75 | 85 | 270 | 115 | 75 |
| 248,4 | 135 | 425 | 180 | 80 | 90 | 285 | 120 | 80 |

**Table D.3** Optimisation results maximum element sizes

| height | minimum column thickness shear wall | minimum column thickness core | minimum column thickness outrigger | minimum column thickness tube | minimum wall thickness shear wall | minimum wall thickness core | minimum wall thickness outrigger | minimum wall thickness tube |
|---|---|---|---|---|---|---|---|---|
| 100,8 | 35 | 35 | 35 | 20 | 20 | 20 | 20 | 20 |
| 104,4 | 35 | 35 | 35 | 20 | 20 | 20 | 20 | 20 |
| 108 | 35 | 35 | 35 | 25 | 20 | 20 | 20 | 20 |
| 111,6 | 35 | 35 | 35 | 25 | 20 | 20 | 20 | 20 |
| 115,2 | 35 | 40 | 35 | 25 | 20 | 20 | 20 | 20 |
| 118,8 | 35 | 40 | 35 | 25 | 20 | 20 | 20 | 20 |
| 122,4 | 35 | 40 | 40 | 25 | 20 | 20 | 20 | 20 |
| 126 | 35 | 35 | 40 | 25 | 20 | 25 | 25 | 20 |
| 129,6 | 40 | 40 | 40 | 25 | 20 | 25 | 25 | 20 |
| 133,2 | 40 | 40 | 40 | 25 | 20 | 25 | 25 | 20 |
| 136,8 | 40 | 45 | 45 | 25 | 20 | 30 | 25 | 20 |
| 140,4 | 40 | 50 | 45 | 25 | 20 | 35 | 25 | 20 |
| 144 | 40 | 50 | 45 | 25 | 20 | 35 | 25 | 20 |
| 147,6 | 45 | 55 | 45 | 30 | 20 | 35 | 25 | 20 |
| 151,2 | 35 | 55 | 40 | 30 | 20 | 35 | 25 | 20 |
| 154,8 | 35 | 60 | 45 | 30 | 20 | 40 | 25 | 20 |
| 158,4 | 35 | 65 | 40 | 30 | 20 | 45 | 25 | 20 |
| 162 | 35 | 70 | 40 | 30 | 20 | 45 | 30 | 20 |
| 165,6 | 40 | 75 | 40 | 30 | 20 | 50 | 30 | 20 |
| 169,2 | 40 | 80 | 40 | 35 | 20 | 55 | 30 | 25 |
| 172,8 | 40 | 85 | 40 | 35 | 20 | 55 | 30 | 25 |
| 176,4 | 40 | 90 | 45 | 35 | 20 | 60 | 30 | 25 |
| 180 | 40 | 100 | 45 | 35 | 20 | 65 | 35 | 25 |
| 183,6 | 40 | 105 | 50 | 35 | 20 | 70 | 35 | 25 |
| 187,2 | 45 | 110 | 50 | 30 | 25 | 75 | 35 | 25 |
| 190,8 | 45 | 115 | 55 | 35 | 25 | 80 | 35 | 25 |
| 194,4 | 45 | 125 | 55 | 40 | 30 | 85 | 40 | 30 |
| 198 | 45 | 130 | 60 | 35 | 30 | 90 | 40 | 25 |
| 201,6 | 40 | 115 | 55 | 30 | 25 | 80 | 35 | 25 |
| 205,2 | 40 | 120 | 55 | 30 | 25 | 80 | 35 | 25 |
| 208,8 | 45 | 130 | 60 | 30 | 30 | 90 | 40 | 25 |
| 212,4 | 45 | 140 | 60 | 35 | 30 | 90 | 40 | 30 |
| 216 | 45 | 145 | 65 | 30 | 30 | 95 | 45 | 30 |
| 219,6 | 50 | 155 | 70 | 35 | 35 | 105 | 45 | 30 |
| 223,2 | 55 | 160 | 70 | 35 | 35 | 105 | 45 | 30 |
| 226,8 | 55 | 170 | 75 | 35 | 35 | 115 | 50 | 35 |
| 230,4 | 60 | 180 | 80 | 35 | 40 | 120 | 55 | 35 |
| 234 | 60 | 190 | 85 | 35 | 40 | 125 | 55 | 35 |
| 237,6 | 65 | 200 | 85 | 40 | 45 | 130 | 55 | 40 |
| 241,2 | 65 | 205 | 90 | 40 | 45 | 135 | 60 | 40 |
| 244,8 | 70 | 220 | 95 | 40 | 45 | 145 | 60 | 40 |
| 248,4 | 70 | 230 | 100 | 45 | 50 | 155 | 65 | 45 |

**Table D.4** Optimisation results minimum element sizes

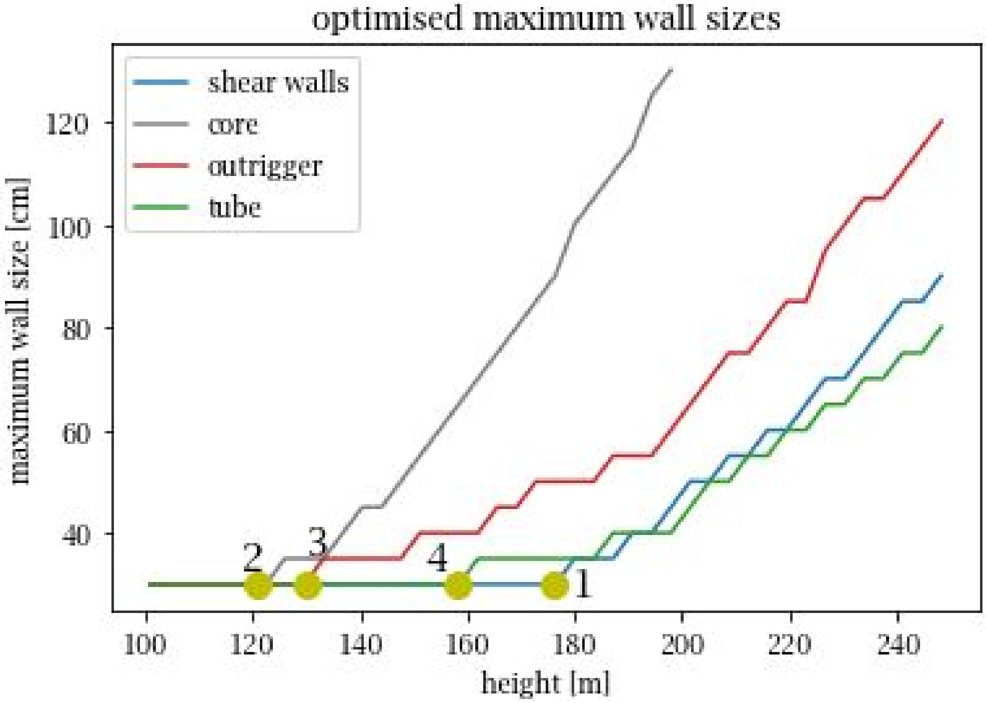
optimised maximum wall sizes
shear walls
core
outrigger
tube
maximum wall size [cm]
height [m]
1
2
3
4
40
60
80
100
120
100
120
140
160
180
200
220
240

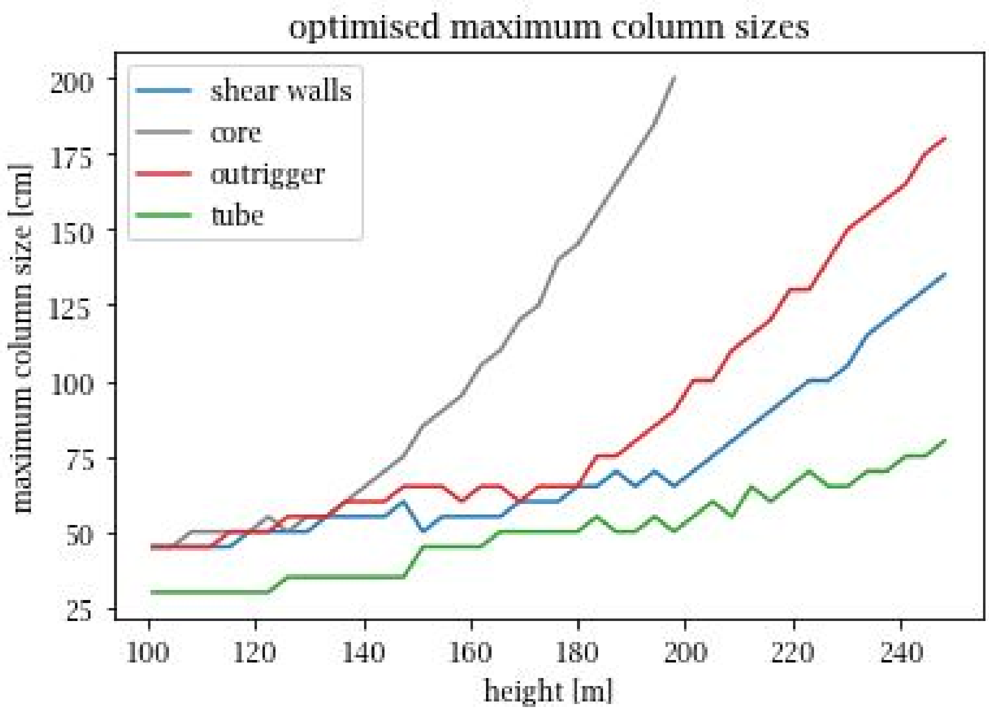
optimised maximum column sizes
shear walls
core
outrigger
tube
maximum column size [cm]
height [m]
25
50
75
100
125
150
175
200
100
120
140
160
180
200
220
240

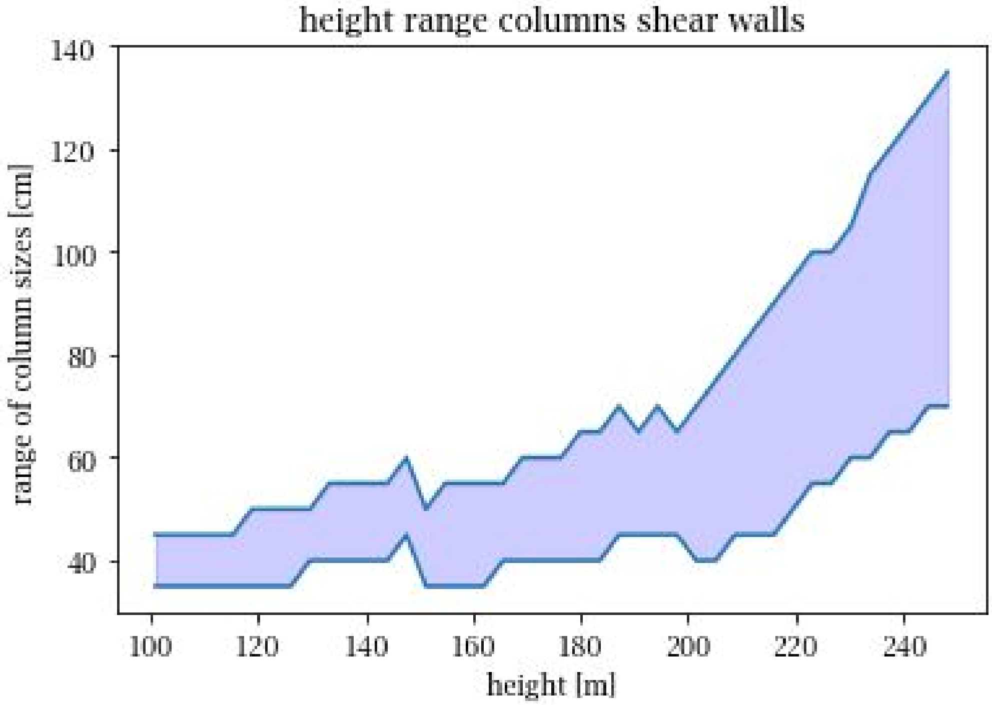
height range columns shear walls
range of column sizes [cm]
height [m]
140
120
100
80
60
40
100
120
140
160
180
200
220
240

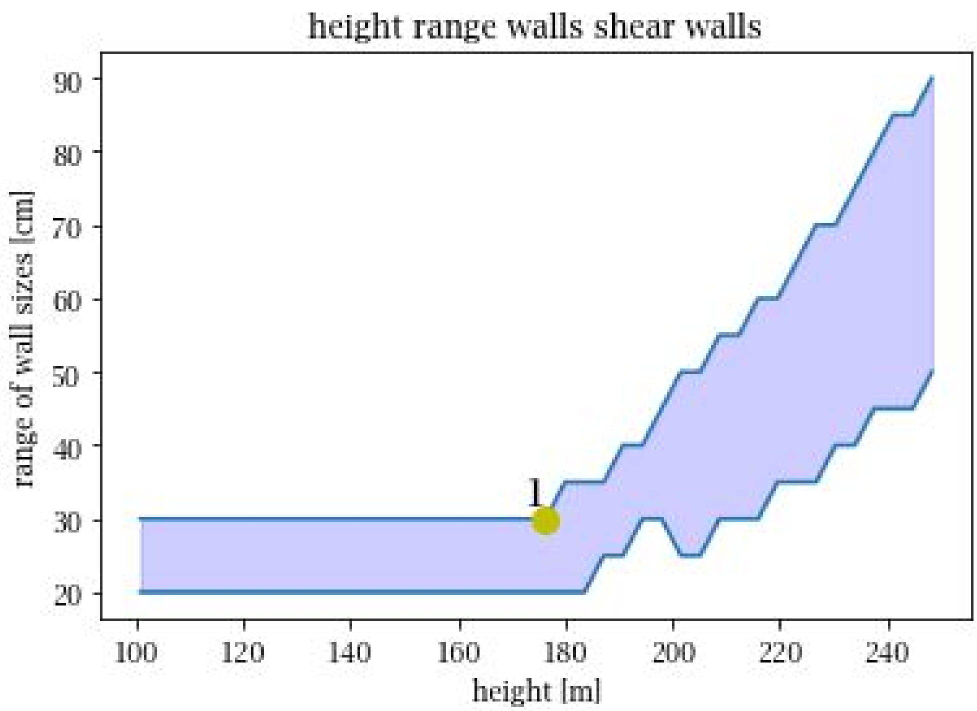
height range walls shear walls
range of wall sizes [cm]
height [m]
1
90
80
70
60
50
40
30
20
100
120
140
160
180
200
220
240

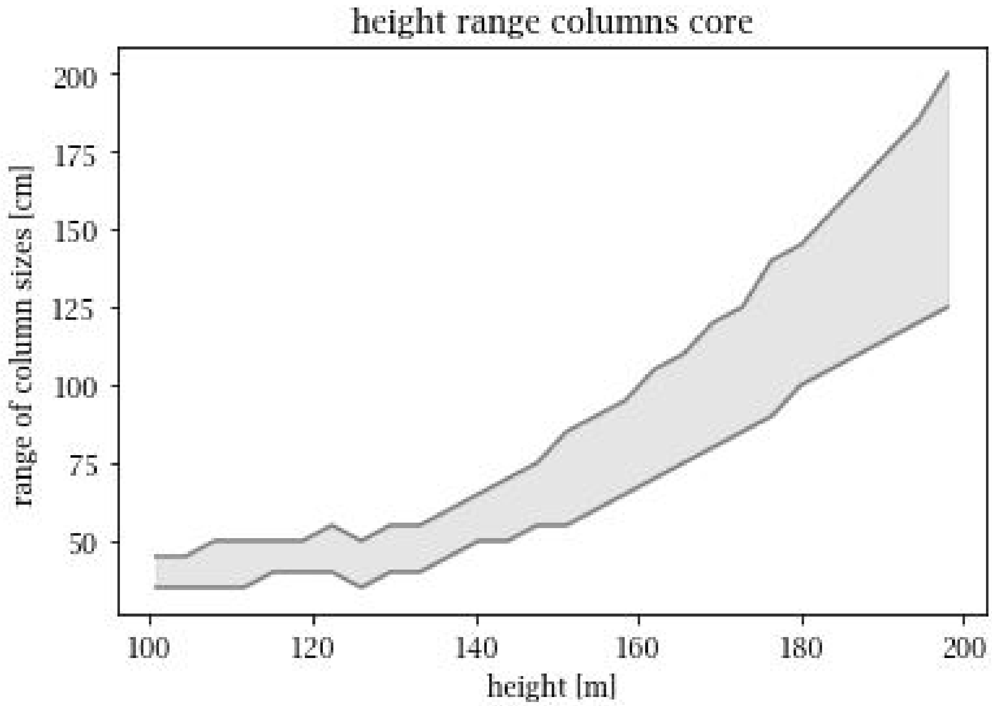
height range columns core
range of column sizes [cm]
200
175
150
125
100
75
50
100
120
140
160
180
200
height [m]

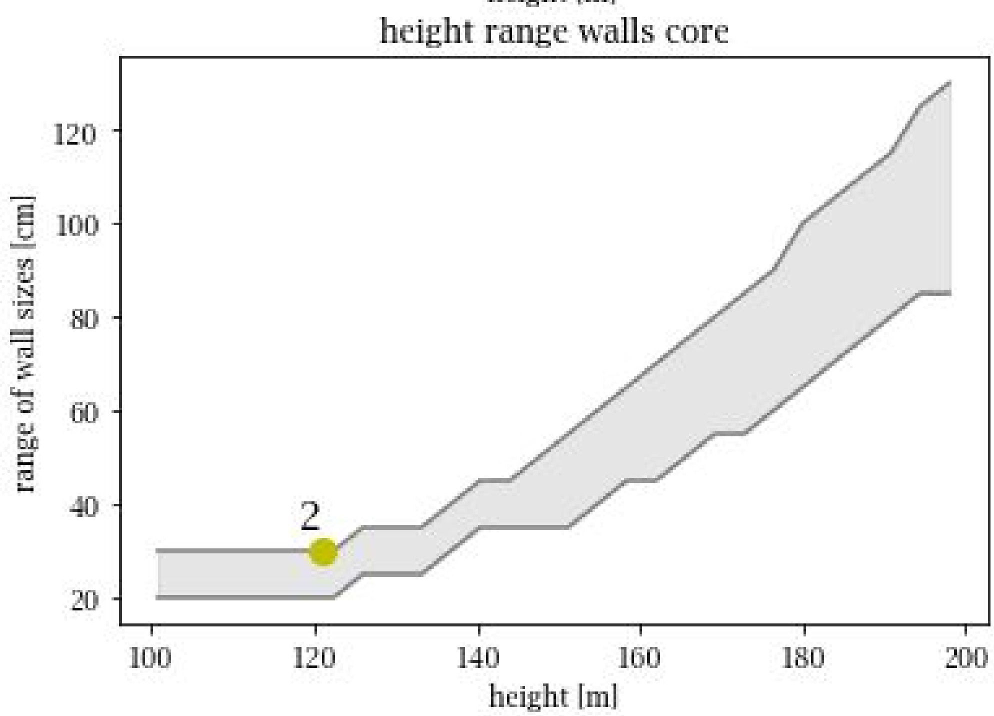
height range walls core
range of wall sizes [cm]
120
100
80
60
40
20
2
100
120
140
160
180
200
height [m]

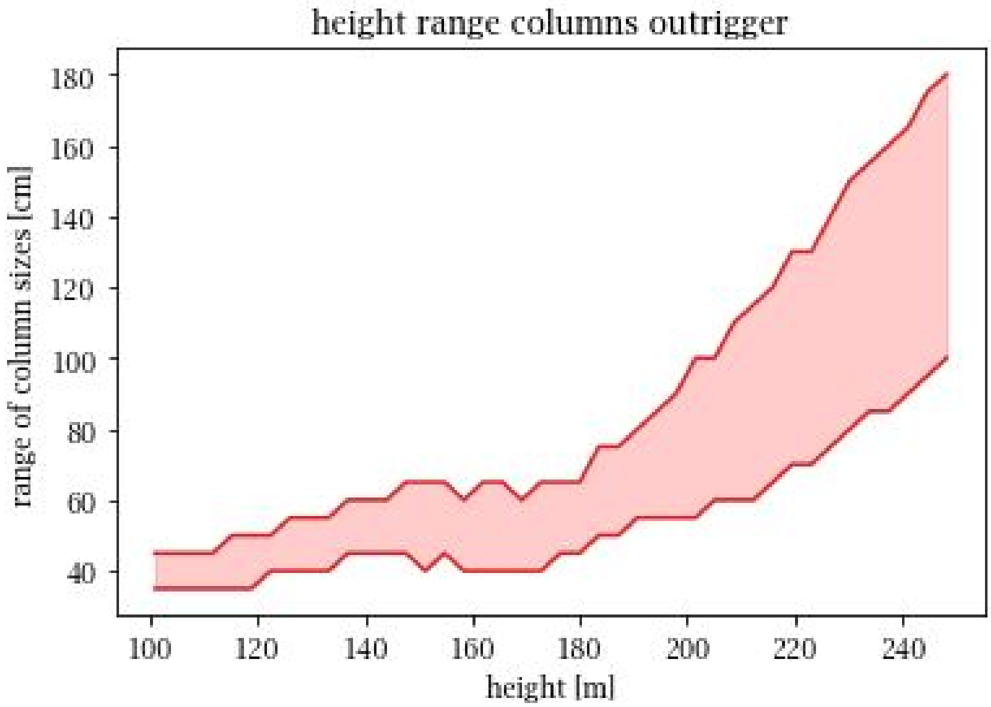
height range columns outrigger
range of column sizes [cm]
180
160
140
120
100
80
60
40
100
120
140
160
180
200
220
240
height [m]

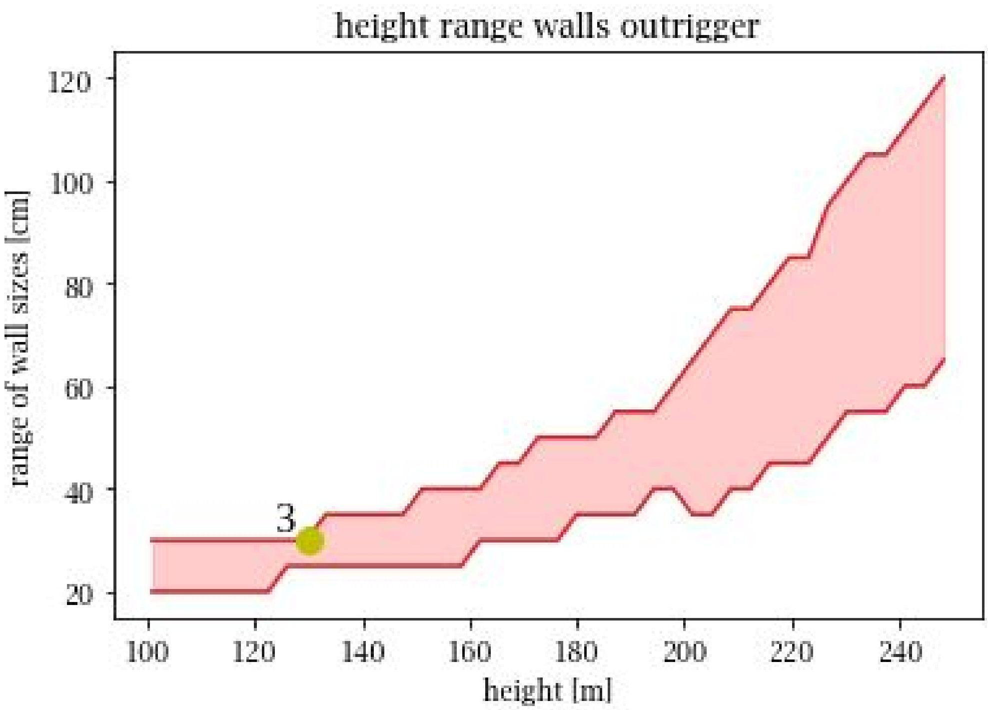
height range walls outrigger
range of wall sizes [cm]
120
100
80
60
40
20
3
100
120
140
160
180
200
220
240
height [m]

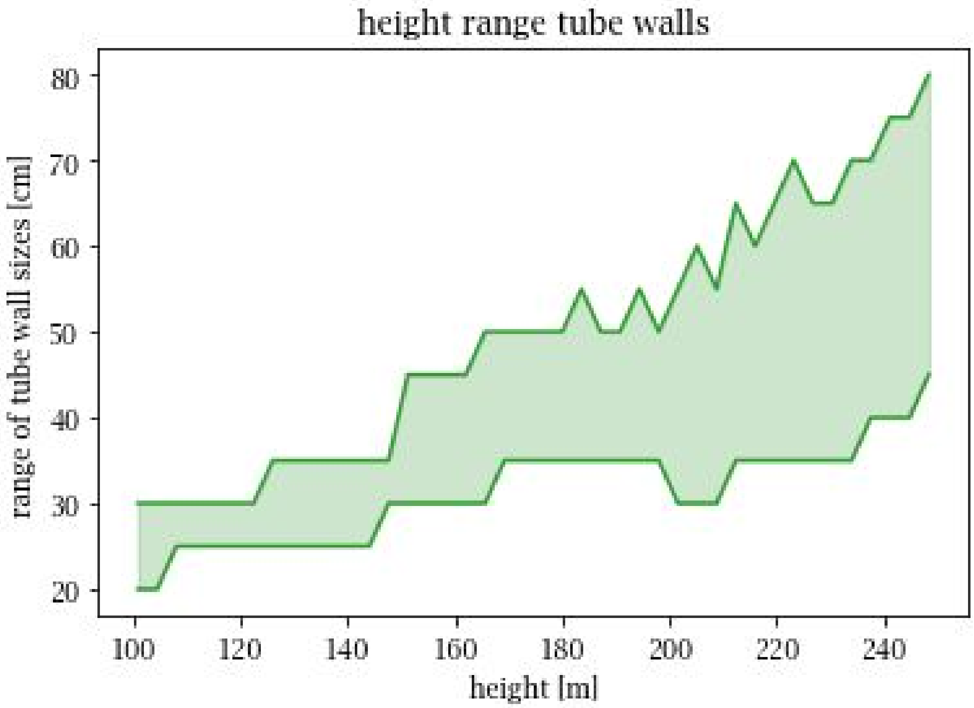
height range tube walls
range of tube wall sizes [cm]
height [m]
80
70
60
50
40
30
20
100
120
140
160
180
200
220
240

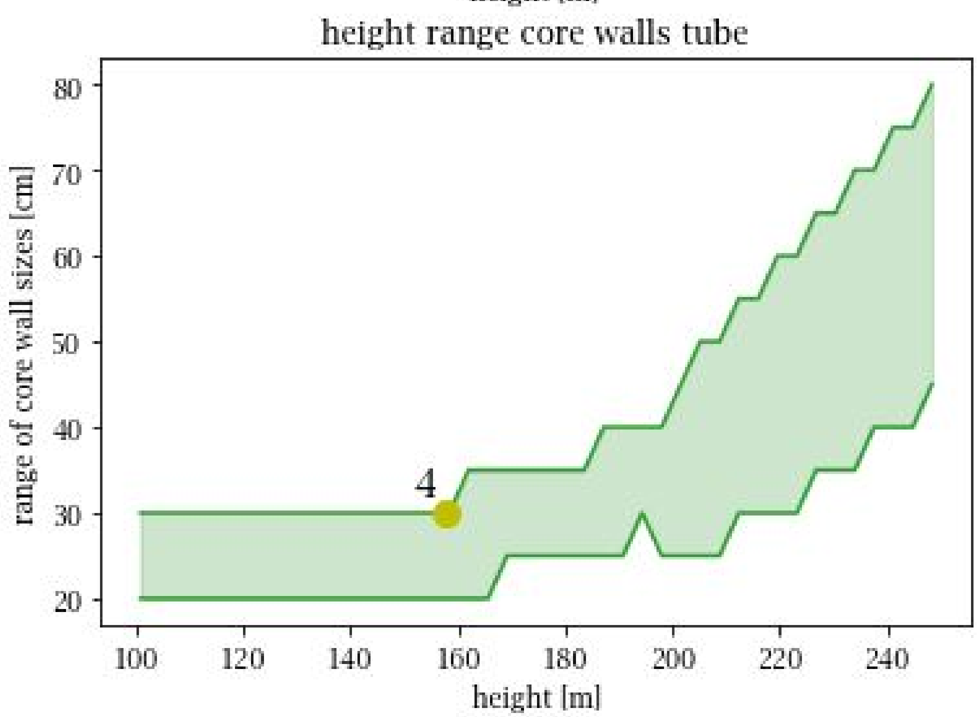
height range core walls tube
range of core wall sizes [cm]
height [m]
4
80
70
60
50
40
30
20
100
120
140
160
180
200
220
240

## D.3 Optimisation results total weight [kN] and carbon emission [€ev]

| height | total weight sw | total weight core | total weight outr. | total weight tube |
|---|---|---|---|---|
| 100,8 | 363000 | 326700 | 338300 | 396500 |
| 104,4 | 373400 | 336900 | 348900 | 408400 |
| 108 | 387400 | 350400 | 361000 | 427200 |
| 111,6 | 401900 | 365300 | 374600 | 443200 |
| 115,2 | 411500 | 376000 | 387800 | 454600 |
| 118,8 | 427400 | 387800 | 400000 | 476900 |
| 122,4 | 444700 | 404500 | 416300 | 494600 |
| 126 | 454200 | 417200 | 431400 | 513900 |
| 129,6 | 470000 | 435000 | 448800 | 529100 |
| 133,2 | 487000 | 448900 | 466500 | 545900 |
| 136,8 | 497800 | 478300 | 482000 | 558300 |
| 140,4 | 514200 | 506500 | 494700 | 573500 |
| 144 | 529000 | 528100 | 511900 | 590300 |
| 147,6 | 544800 | 555500 | 526200 | 608600 |
| 151,2 | 546600 | 586400 | 535900 | 622500 |
| 154,8 | 562500 | 620800 | 557200 | 639900 |
| 158,4 | 574800 | 656500 | 560600 | 653200 |
| 162 | 588600 | 698300 | 583700 | 670100 |
| 165,6 | 602700 | 740500 | 599800 | 697600 |
| 169,2 | 621700 | 796400 | 609100 | 728600 |
| 172,8 | 635800 | 837200 | 640600 | 743900 |
| 176,4 | 650100 | 908800 | 653000 | 761700 |
| 180 | 681500 | 974300 | 676000 | 779100 |
| 183,6 | 695800 | 1049000 | 701000 | 812800 |
| 187,2 | 736300 | 1131000 | 727700 | 799600 |
| 190,8 | 750700 | 1191000 | 755700 | 829800 |
| 194,4 | 780500 | 1289000 | 777100 | 875800 |
| 198 | 813100 | 1418000 | 816500 | 864300 |
| 201,6 | 817000 | 1445000 | 840600 | 844000 |
| 205,2 | 857100 | 1541000 | 872900 | 885200 |
| 208,8 | 892500 | 1722000 | 918500 | 883600 |
| 212,4 | 928600 | 1833000 | 959600 | 944800 |
| 216 | 964000 | 1997000 | 998200 | 945900 |
| 219,6 | 1015000 | 2185000 | 1057000 | 989900 |
| 223,2 | 1067000 | 2320000 | 1079000 | 1026000 |
| 226,8 | 1099000 | 2556000 | 1156000 | 1036000 |
| 230,4 | 1159000 | 2787000 | 1225000 | 1070000 |
| 234 | 1213000 | 3063000 | 1289000 | 1106000 |
| 237,6 | 1268000 | 3286000 | 1325000 | 1139000 |
| 241,2 | 1332000 | 3507000 | 1377000 | 1180000 |
| 244,8 | 1376000 | 3896000 | 1475000 | 1213000 |
| 248,4 | 1460000 | 4249000 | 1555000 | 1261000 |

**Table D.5** Optimisation results total weight

| height | carbon emission sw | carbon emission core | carbon emission outr. | carbon emission tube |
|---|---|---|---|---|
| 100,8 | 272250 | 245025 | 253725 | 297375 |
| 104,4 | 280050 | 252675 | 261675 | 306300 |
| 108 | 290550 | 262800 | 270750 | 320400 |
| 111,6 | 301425 | 273975 | 280950 | 332400 |
| 115,2 | 308625 | 282000 | 290850 | 340950 |
| 118,8 | 320550 | 290850 | 300000 | 357675 |
| 122,4 | 333525 | 303375 | 312225 | 370950 |
| 126 | 340650 | 312900 | 323550 | 385425 |
| 129,6 | 352500 | 326250 | 336600 | 396825 |
| 133,2 | 365250 | 336675 | 349875 | 409425 |
| 136,8 | 373350 | 358725 | 361500 | 418725 |
| 140,4 | 385650 | 379875 | 371025 | 430125 |
| 144 | 396750 | 396075 | 383925 | 442725 |
| 147,6 | 408600 | 416625 | 394650 | 456450 |
| 151,2 | 409950 | 439800 | 401925 | 466875 |
| 154,8 | 421875 | 465600 | 417900 | 479925 |
| 158,4 | 431100 | 492375 | 420450 | 489900 |
| 162 | 441450 | 523725 | 437775 | 502575 |
| 165,6 | 452025 | 555375 | 449850 | 523200 |
| 169,2 | 466275 | 597300 | 456825 | 546450 |
| 172,8 | 476850 | 627900 | 480450 | 557925 |
| 176,4 | 487575 | 681600 | 489750 | 571275 |
| 180 | 511125 | 730725 | 507000 | 584325 |
| 183,6 | 521850 | 786750 | 525750 | 609600 |
| 187,2 | 552225 | 848250 | 545775 | 599700 |
| 190,8 | 563025 | 893250 | 566775 | 622350 |
| 194,4 | 585375 | 966750 | 582825 | 656850 |
| 198 | 609825 | 1063500 | 612375 | 648225 |
| 201,6 | 612750 | 1083750 | 630450 | 633000 |
| 205,2 | 642825 | 1155750 | 654675 | 663900 |
| 208,8 | 669375 | 1291500 | 688875 | 662700 |
| 212,4 | 696450 | 1374750 | 719700 | 708600 |
| 216 | 723000 | 1497750 | 748650 | 709425 |
| 219,6 | 761250 | 1638750 | 792750 | 742425 |
| 223,2 | 800250 | 1740000 | 809250 | 769500 |
| 226,8 | 824250 | 1917000 | 867000 | 777000 |
| 230,4 | 869250 | 2090250 | 918750 | 802500 |
| 234 | 909750 | 2297250 | 966750 | 829500 |
| 237,6 | 951000 | 2464500 | 993750 | 854250 |
| 241,2 | 999000 | 2630250 | 1032750 | 885000 |
| 244,8 | 1032000 | 2922000 | 1106250 | 909750 |
| 248,4 | 1095000 | 3186750 | 1166250 | 945750 |

**Table D.6** Optimisation results carbon emission

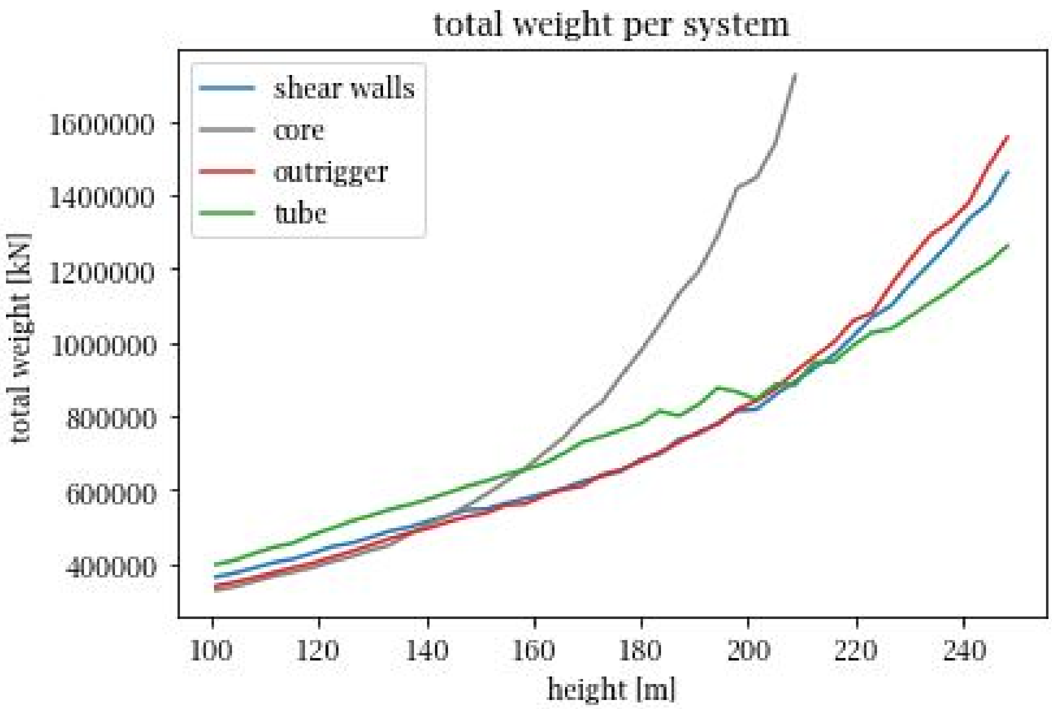
total weight per system
shear walls
core
outrigger
tube
total weight [kN]
1600000
1400000
1200000
1000000
800000
600000
400000
100
120
140
160
180
200
220
240
height [m]

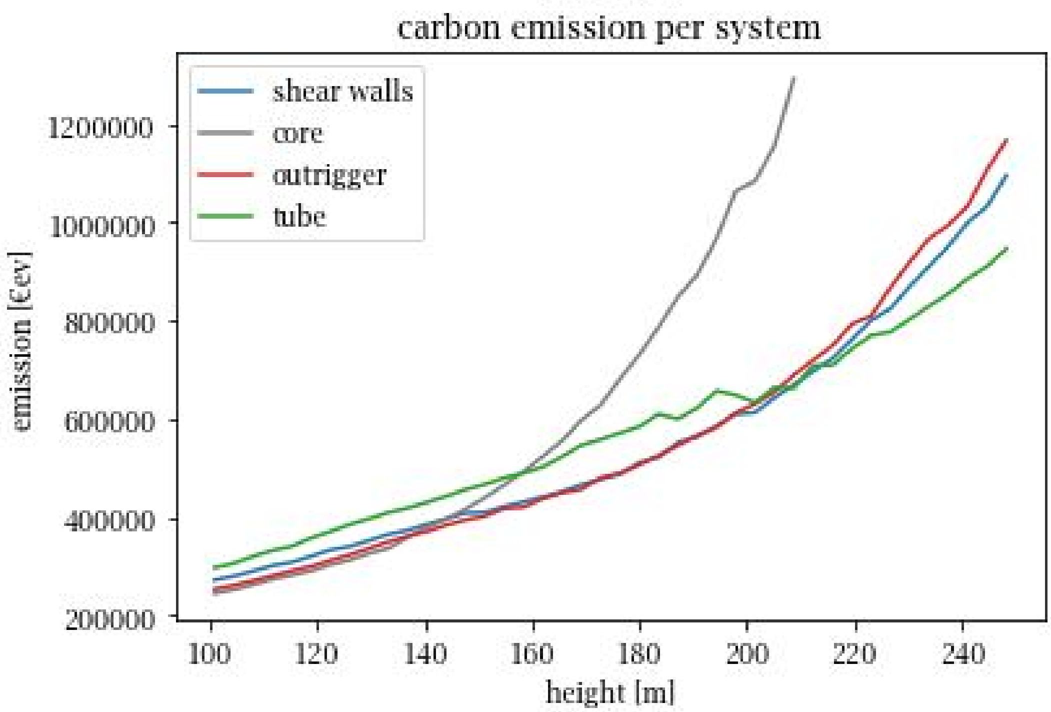
carbon emission per system
shear walls
core
outrigger
tube
emission [€ev]
1200000
1000000
800000
600000
400000
200000
100
120
140
160
180
200
220
240
height [m]

## D.4 Optimisation results flexibility [%]

| height | useful floor area sw | useful floor area core | useful floor area out | useful floor area tube | ratio facade openings sw | ratio facade openings core | ratio facade openings out | ratio facade openings tube |
|---|---|---|---|---|---|---|---|---|
| **100,8** | 96 | 98 | 94,4 | 95,3 | 91,7 | 91,7 | 88,1 | 66 |
| **104,4** | 96 | 98 | 94,5 | 95,3 | 91,7 | 91,7 | 88,2 | 66 |
| **108** | 96 | 97,8 | 94,6 | 95,3 | 91,7 | 91,7 | 88,3 | 66 |
| **111,6** | 96 | 97,8 | 94,8 | 95,3 | 91,7 | 91,7 | 88,4 | 66 |
| **115,2** | 96 | 97,8 | 94,7 | 95,3 | 91,7 | 91,7 | 88,5 | 66 |
| **118,8** | 95,8 | 97,8 | 94,8 | 95,3 | 91,7 | 91,7 | 88,6 | 66 |
| **122,4** | 95,8 | 97,6 | 94,9 | 95,3 | 91,7 | 91,7 | 88,7 | 66 |
| **126** | 95,8 | 97,6 | 94,8 | 94,8 | 91,7 | 90 | 88,3 | 66 |
| **129,6** | 95,8 | 97,4 | 94,9 | 94,8 | 91,7 | 90 | 87,8 | 66 |
| **133,2** | 95,6 | 97,4 | 94,7 | 94,8 | 91,7 | 90 | 87,3 | 66 |
| **136,8** | 95,6 | 97 | 94,6 | 94,8 | 91,7 | 88,3 | 87,4 | 66 |
| **140,4** | 95,6 | 96,6 | 94,7 | 94,8 | 91,7 | 86,7 | 87,4 | 66 |
| **144** | 95,6 | 96,3 | 94,7 | 94,8 | 91,7 | 86,7 | 87,5 | 66 |
| **147,6** | 95,4 | 95,9 | 94,6 | 94,8 | 91,7 | 85,6 | 87,6 | 66 |
| **151,2** | 95,8 | 95,1 | 94,6 | 93,7 | 91,7 | 84,6 | 86,8 | 66 |
| **154,8** | 95,6 | 94,6 | 94,7 | 93,7 | 91,7 | 83,3 | 85,6 | 66 |
| **158,4** | 95,6 | 94 | 94,7 | 93,7 | 91,7 | 81,7 | 86,9 | 66 |
| **162** | 95,6 | 93,1 | 94,6 | 93,4 | 91,7 | 80,8 | 86,1 | 66 |
| **165,6** | 95,6 | 92,6 | 94,6 | 92,9 | 91,7 | 79,2 | 85,3 | 66 |
| **169,2** | 95,4 | 91,6 | 94,7 | 92,9 | 91,7 | 77,9 | 85,4 | 66 |
| **172,8** | 95,4 | 90,9 | 94,3 | 92,9 | 91,7 | 76,7 | 84,2 | 66 |
| **176,4** | 95,4 | 89,3 | 94,3 | 92,9 | 91,7 | 75 | 84,6 | 66 |
| **180** | 94,7 | 88,4 | 94,1 | 92,9 | 90,8 | 72,9 | 83,8 | 66 |
| **183,6** | 94,7 | 87,2 | 93,9 | 92,3 | 90,8 | 70,8 | 83,9 | 66 |
| **187,2** | 94,4 | 85,9 | 93,7 | 92,7 | 89,6 | 69,2 | 83,1 | 66 |
| **190,8** | 94,1 | 84,5 | 93,5 | 92,7 | 89,2 | 67,5 | 82,7 | 66 |
| **194,4** | 93,9 | 82,8 | 93,3 | 92,1 | 88,8 | 65,4 | 82,3 | 66 |
| **198** | 93,6 | 80,6 | 92,8 | 92,7 | 87,5 | 62,9 | 81,5 | 66 |
| **201,6** | 92,8 | 77,9 | 91,9 | 91,9 | 88 | 62,7 | 81,2 | 66 |
| **205,2** | 92,5 | 76,1 | 91,4 | 91,1 | 87 | 61,7 | 80,6 | 66 |
| **208,8** | 91,7 | 72,3 | 90,8 | 91,7 | 86,3 | 58 | 79,3 | 66 |
| **212,4** | 91,4 | 70,4 | 90,5 | 90,3 | 86 | 56,7 | 78,6 | 66 |
| **216** | 90,6 | 67,3 | 89,9 | 90,9 | 85 | 53,7 | 77,7 | 66 |
| **219,6** | 90,3 | 64 | 88,8 | 90,1 | 84 | 51 | 76,7 | 66 |
| **223,2** | 89,4 | 61,8 | 88,9 | 89,6 | 83 | 49,7 | 76,7 | 66 |
| **226,8** | 88,8 | 57 | 87,5 | 89,9 | 82,7 | 46,3 | 74,4 | 66 |
| **230,4** | 88,5 | 53,3 | 86,4 | 89,9 | 81,7 | 43,3 | 72,8 | 66 |
| **234** | 87,2 | 48 | 85,6 | 89,1 | 80,7 | 40 | 71,8 | 66 |
| **237,6** | 86,2 | 42,6 | 85,1 | 89,1 | 79,7 | 37,3 | 71,2 | 66 |
| **241,2** | 85,3 | 39,6 | 84,4 | 88,3 | 78,3 | 35 | 70,5 | 66 |
| **244,8** | 84,8 | 32,3 | 83 | 88,3 | 78,3 | 30,7 | 68,5 | 66 |
| **248,4** | 83,8 | 26 | 81,6 | 87,6 | 76,7 | 27 | 67,2 | 66 |

**Table D.7** Optimisation results flexibility

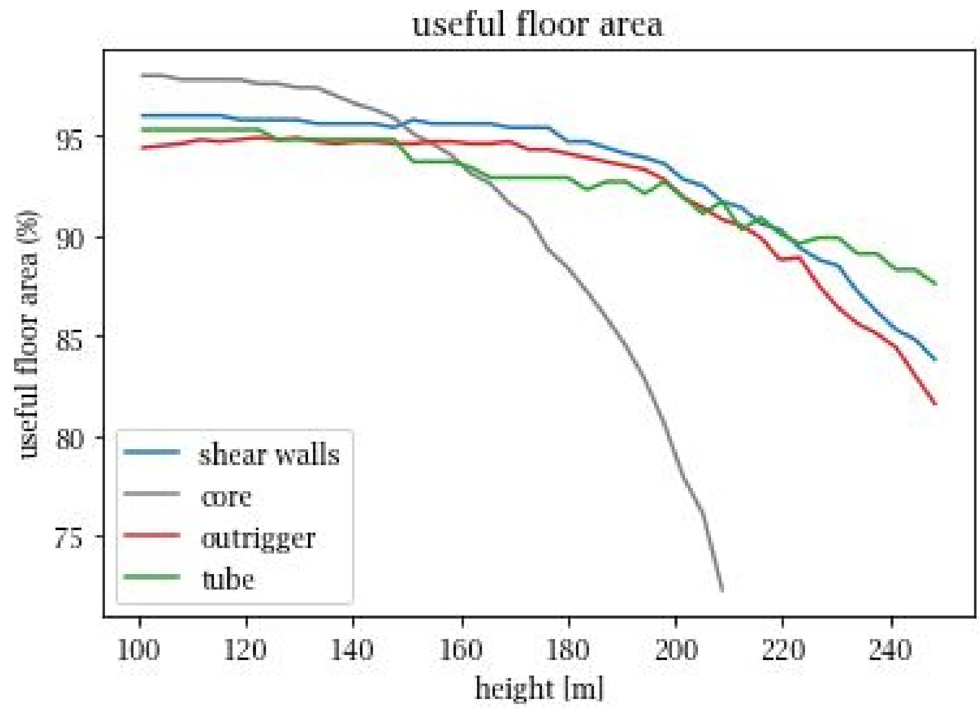
useful floor area
useful floor area (%)
95
90
85
80
75
100
120
140
160
180
200
220
240
height [m]
shear walls
core
outrigger
tube

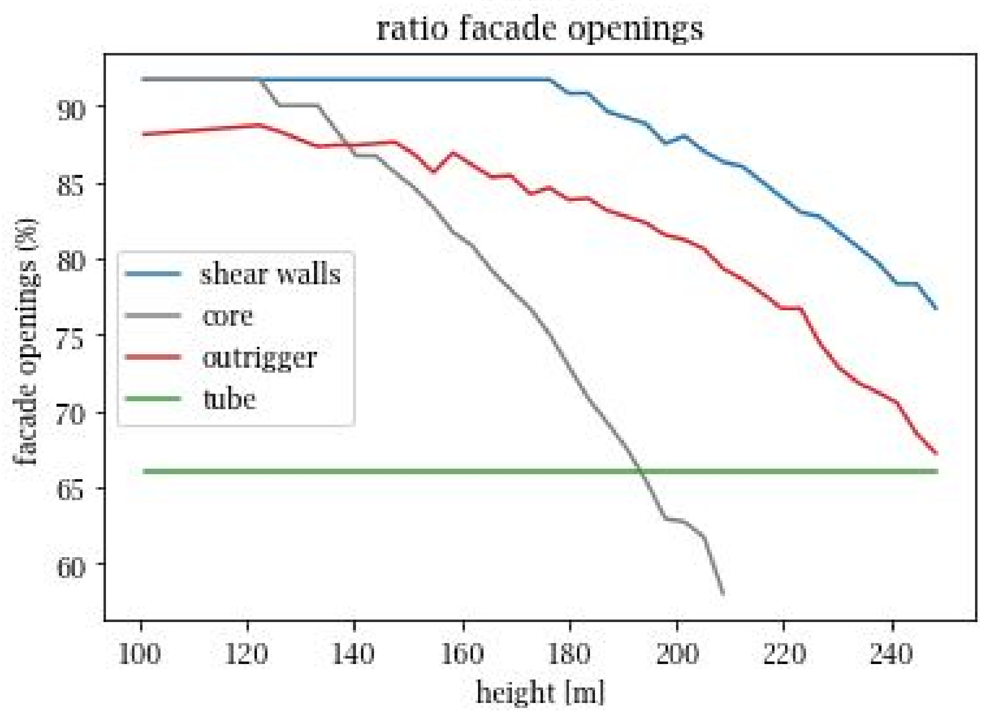
ratio facade openings
facade openings (%)
90
85
80
75
70
65
60
100
120
140
160
180
200
220
240
height [m]
shear walls
core
outrigger
tube